Surface forces in the presence of multivalent ions and polyelectrolytes

Moazzami Gudarzi, Mohsen

UNIVERSITÉ DE GENÈVE FACULTÉ DES SCIENCES

Section de chimie et biochimie
Département de chimie minérale et analytique Professeur Michal Borkovec

Surface Forces in the Presence of Multivalent Ions and Polyelectrolytes

THÈSE

présentée à la Faculté des sciences de l'Université de Genève

pour obtenir le grade de Docteur ès sciences, mention chimie

par

Mohsen Moazzami Gudarzi

De

Téhéran (Iran)

Thèse N^{o} 5100

GENÈVE
Atelier ReproMail
2017

UNIVERSITÉ
DE GENÈVE
FACULTÉ DES SCIENCES

DOCTORAT ÈS SCIENCES, MENTION CHIMIE

Thèse de Monsieur Mohsen MOAZZAMI GUDARZI

intitulée :

«Surface Forces in the Presence of Multivalent Ions and Polyelectrolytes»

La Faculté des sciences, sur le préavis de Monsieur M.BORKOVEC, professeur ordinaire et directeur de thèse (Département de chimie minérale et analytique), Monsieur T. BÜRGI, professeur ordinaire (Département de chimie physique), Monsieur C. LABBEZ, docteur (Laboratoire interdisciplinaire Carnot de Bourgogne, Université de Bourgogne Franche-Comté, Dijon, France) autorise l'impression de la présente thèse, sans exprimer d'opinion sur les propositions qui y sont énoncées.

Genève, le 13 juillet 2017

Thèse - 5100 -

Le Doyen

N.B. - La thèse doit porter la déclaration précédente et remplir les conditions énumérées dans les "Informations relatives aux thèses de doctorat à l'Université de Genève".

Contents

Abstract 5

Résumé 7

1- Introduction 9

1.1- Electrical double layer forces 11

Double layer structure: 11

Double layer forces 16

Regulation parameter 20

Effect of multivalent ions: 23

Polyelectrolytes 25

1.2- van der Waals forces 27

Intermolecular interactions: 27

Pair-wise additivity: Hamaker approach 29

Beyond additivity: Lifshitz theory 34

1.3- The Derjaguin approximation 37

1.4- DLVO theory 38

1.5- Non-DLVO forces 40

Hydrophobic forces 41

Depletion forces 42

1.6- Colloidal probe AFM 47

1.7- Outline of thesis 54

1.8- References 58

2- Forces between negatively charged interfaces in the presence of cationic multivalent oligoamines measured with the atomic force microscope 65

3- Nanometer-ranged attraction induced by multivalent ions between similar and dissimilar surfaces probed by the atomic force microscope (AFM) 77

4- Long-ranged and soft interactions between charged colloidal particles induced by multivalent coions 93

5- Interplay between depletion and double layer forces acting between charged particles in solutions of like-charged polyelectrolytes.....105
6- Depletion and double layer forces acting between charged particles in solutions of like-charged polyelectrolytes and monovalent salt 113
7- Conclusion.....127
Acknowledgement.....131

Abstract

Colloids and interfaces interacting through polar media such as water often carry electric charges and thus Columbic forces play a dominant role in these systems. Presence of the ions carrying multiple charges strongly modifies these forces and the overall behavior of the colloidal dispersions. This thesis focuses on the surface forces between charged interfaces in the presence of the multivalent ions and polyelectrolytes. This is done through comprehensive force measurements by means of Atomic Force Microscopy (AFM). Specifically, colloidal probe AFM is used to study the impact of organic multivalent ions and polyelectrolytes on surface forces between different charged colloidal particles.

The thesis is prefaced with an introduction to surface forces and colloidal stability theory. A theoretical background of various types of surface forces involving in this work is presented. It is discussed how interplay of repulsive and attractive forces controls the stability of the colloidal dispersions. A brief overview of the AFM and colloidal probe technique is also given in this part.

Second chapter reports direct force measurements between negatively charged particles, sulfate latex (SL), in the presence of linear aliphatic oligoamines of different valences up to +4. In solutions containing mono and divalent ions, forces can be well described with Derjaguin, Landau, Verwey, and Overbeek (DLVO) theory. However, at short distances additional attractive non-DLVO forces are detected which is ascribed to hydrophobic interactions. It is also shown that counter-ions of higher valences have high tendency to adsorb to the interface and eventually reverse the charge. These multivalent counter-ions also induce additional attractive forces but with a range much larger than the one for monovalent counterpart.

A comprehensive study of surface forces between similar and dissimilar charged latex particles in solutions containing multivalent cationic aliphatic hexamines (N6) and in simple monovalent KCl solutions is presented in chapter three. DLVO theory can describe the surface forces at large distances provided that the double layer forces are rationalized by Poisson-Boltzmann (PB) equation and charge regulation effect is taken into account. Short ranged non-DLVO attractive forces are detected between latex particles in both similar and dissimilar cases. The non-DLVO forces can be modeled with an exponential force profiles, however with different ranges and magnitudes. In KCl solutions, the range of these attractive forces is about 0.3 nm. However, in solutions containing N6, the range of these forces varies depending on the type of the particles. An experimental mixing rule is proposed to predict the range and magnitude of these forces between dissimilar particles from studies of similar particles.

Above studied revealed that accurate prediction of the double layer forces in the presence of the multivalent ions requires consideration of PB equation in complete form and linear approximation of this equation fails to provide a correct calculation. This is especially crucial where the multivalent ions act as co-ions, *i.e.* possess similar charge as interface. Chapter four

studies this matter in full details and shows this is a generic feature for multivalent co-ions. Depletion of highly charged co-ions from the interspace of two interacting charged interfaces is found to be the origin of non-linearity of the double layer forces.

In chapter five, applicability of PB equation to explain the double layer forces extends to polyelectrolyte solutions. Polyelectrolyte molecules are expelled from the vicinity of like-charged interfaces and it is the remaining counter-ions which controls the double layer forces. The PB equation predicts highly non-exponential force profiles in such situations which indeed match with experimental force curves provided that polyelectrolytes are considered as highly asymmetric electrolytes. At larger distance, however, structuring of the polyelectrolytes leads to appearance of oscillatory depletion forces. The interplay of depletion and double layer forces rationalizes the experimental forces. The measured effective valence of polyelectrolytes is always smaller than nominal charges of polyelectrolytes due to the counter-ion condensation on polymer backbone.

In mixtures of polyelectrolytes and monovalent salt above picture still holds and surface forces are composed of depletion and double layer forces. This is the subject of chapter six. Double layer forces are modeled with PB theory for mixture of monovalent salt and highly asymmetric multivalent ions representing like-charge polyelectrolytes. It is proved electrostatic repulsion acting on polyelectrolyte molecules forces them to expel from the interspace of interacting particles which in turn determines the thickness of depletion layer near to the interface. This argument is used to predict the phase of oscillatory depletion forces which matches well with experimental data. However, this account fails at high salt and polymer concentration where the electrostatic repulsion is not strong enough to prevent polymer molecules from the adsorption. Therefore, polyelectrolytes adsorb to like-charged interfaces at this regime.

Résumé

Les colloïdes et les interfaces interagissant à travers un environnement polaire tel que l'eau possèdent généralement des charges électriques et par conséquent les forces de Coulomb jouent un rôle prédominant dans ces systèmes. La présence d'ions portant de multiples charges modifie ces forces et le comportement général de la suspension colloïdale. Cette thèse se focalise sur les forces de surface entre des interfaces chargées en présence d'ions multivalents et de polyélectrolytes. Pour étudier ces forces, des mesures de force ont été effectuées par microscopie à force atomique (AFM). Plus précisément, une sonde colloïdale a été utilisée afin d'étudier l'impact d'ions organique multivalents et de polyélectrolytes sur les forces de surface entre différentes particules colloïdales chargées.

Cette thèse introduit d'abord les motions de forces de surface ainsi que la théorie de stabilité colloïdale. Une introduction sur les divers types de forces de surface est également présentée dans ce travail. Par ailleurs, il sera traité du contrôle de la stabilité colloïdale des dispersions en présence de forces répulsive et attractive. Une brève introduction sur l'AFM ainsi que sur la technique de la sonde colloïdale est donnée dans cette partie.

Le second chapitre traite des mesures de forces entre des particules de latex sulfaté (SL) chargées négativement, en présence oligoamines aliphatiques linéaire de différentes valences (jusqu'à une valence de +4). Dans des solutions contenant des ions mono- et di-valents, les forces en présence peuvent être décrites par la théorie de Derjaguin, Landau, Verwey, and Overbeek (DLVO). Cependant à de courtes distances, des forces additionnelles d'origines non-DLVO peuvent être détectées et elles sont attribuées aux interactions hydrophobes. De plus, il est montré que les contre-ions de hautes valences ont fortement tendances à s'adsorber sur la surface et à inverser la charge de celle-ci. Ces contre-ions multivalents induisent aussi une force attractive additionnelle mais d'une portée plus importante que celle des contre-ions monovalents.

Une étude approfondie sur les forces de surface en solution entre des particules similaires ou différentes de latex chargées en présence d'hexamines aliphatiques cationiques multivalentes (N6) ou d'un sel monovalent, le KCl, est présentée dans le chapitre trois. La théorie de DLVO permet de décrire les forces de surface pour de grandes distances à condition que les forces de double couche soient normalisées par l'équation de Poisson-Boltzmann (PB) et que l'effet a régulation de charges soit prise en compte. Des forces attractives d'origine non-DLVO pour de petites distances ont été détectées entre des particules de latex indépendamment du cas où celles-ci sont similaires ou différentes. Les forces non-DLVO peuvent être modélisées par un profil de force exponentiel, cependant avec des portées et amplitudes différentes. Dans les solutions de KCl, la portée de ces forces attractives est d'environ 0.3 nm. Cependant dans des solutions contenant des N6, la portée de ces forces varie et dépendent du type de particules. Une règle empirique est proposée pour prédire la portée et l'amplitude des ces forces entre des particules différentes basée sur les études des particules similaires.

Les études précédentes ont révélé que la prédiction exacte des forces de double couche en présence d'ions multivalents nécessite la forme complète de l'équation de PB et que l'approximation linéaire de cette équation échoue à aboutir à des résultats cohérents. Cela est d'autant plus vrai lorsque les ions multivalents agissent comme des co-ions, c'est-à-dire que les co-ions possèdent une charge similaire à celle de l'interface. Le chapitre quatre étudie cette problématique en détail et montre que c'est une caractéristique générale pour les co-ions multivalents. L'épuisement des co-ions hautement chargés dans la zone entre deux interfaces interagissant est à l'origine de la non-linéarité des forces de double couche.

Dans le chapitre cinq, la validité de l'équation de PB pour expliquer les forces de double couches est étendue aux solutions contenant des polyélectrolytes. Les polyélectrolytes sont expulsés du voisinage des interfaces de charges similaires et ce sont les contre-ions en solution qui contrôlent les forces de double couche. L'équation de PB prédit des forces de profil non-exponentielle dans de telle situation ce qui en effet coïncide avec les courbes de mesures de forces si on considère que les polyélectrolytes sont des ions asymétriques hautement chargées avec une valence effective. Pour de plus grandes distance, cependant, l'organisation des polyélectrolytes conduit à l'apparition de forces d'épuisement oscillatoires. La combinaison des forces d'épuisement et de double couche permet d'expliquer les forces expérimentales. La mesure de la valence effective des polyélectrolytes est toujours plus petite que celle de sa charge nominale due à l'adsorption des contre-ions sur la chaine de celles-ci.

Dans les mélanges de polyélectrolytes et de sel monovalent, les résultats des chapitres précédents sont toujours valides et les forces de surface sont composées des forces d'épuisement et de double couche. Ceci est l'objet du chapitre six. Les forces de double couche sont modélisées par la théorie de PB pour un mélange de sel monovalent et d'ions multivalents hautement asymétriques représentés par les polyélectrolytes. Il a été démontré que les répulsions électrostatiques entre les polyélectrolytes conduisent à leur expulsion de la zone d'interaction entre les particules ce qui permet de déterminer l'épaisseur de la couche d'épuisement proche de l'interface. Cet argument est utilisé pour prédire la période des forces oscillatoire d'épuisement dont les résultats concordent avec les données expérimentales. Cependant, cette démarche ne peut être utilisée pour de fortes concentrations en sel et de polymère due au fait que les répulsions électrostatiques ne sont pas assez fortes pour empêcher les polymères de s'adsorber sur la surface. Par conséquent, les polyélectrolytes s'adsorbent sur des surfaces de charges similaires dans ce régime.

CHAPTER 1

1- **Introduction**

The concept of '*attractive*' and '*repulsive*' forces dates back to the ancient Greek notion of '*the four elements*' which were believed to create matter when combined with the two divine powers—'*love*' (attraction) and '*strife*' (repulsion).[1,2] Two millennia later, contrary to the general attractive gravitational forces, Newton proposed that the Boyle's gas law required the existence of repulsive forces among gas '*particles*'.[2] Even though this account was proved not to reflect the underlying physics of the ideal gas law, it coined the notion that the counterbalance of attractive and repulsive forces controls the functioning and properties of materials.

Colloids are ubiquitous in nature and also technologically important in many industries such as the pharmaceutical industry, cosmetics, oil refinery, food processing, paint and ink manufacturing and electronics. Colloidal dispersions are heterogeneous systems consisting of nano or micro particles dispersed in a continuum medium. Surface forces play a key role in controlling the behavior of colloidal dispersions because these systems are associated with interfaces. Despite the fact that production of some common products based on colloids such as inks, cosmetics and (processed) foods dates back to early civilizations, the understanding of the physics behind colloidal properties formed only in the 20th century.[2-4] Advances in thermodynamics, quantum physics and the invention of powerful microscopes provided a platform for chemists and physicists to delve into the so-called "*attractive and repulsive*" forces.

In the early 20th century, it was well-established that colloidal particles dispersed in polar media were charged and repelled each other due to the overlapping of the electrical double layer that formed at the interface.[3] However, many experimental observations including the aggregation of colloidal particles, suggested the existence of attractive forces as well. When J. D. van der Waals devised the equation of state of gases, he identified an attractive force between gas molecules. He stated in his Nobel Lecture that this "*attraction only has an appreciable value at distance close to the size of the molecules*".[5] Indeed, F. London proved it, and showed this attractive interaction energy scales with the intermolecular distance by the power of *-6* ($W_{vdW} \sim d^{-6}$).[6] This brought doubt to the origin of the attraction between the colloidal particles as van der Waals (vdW) forces because these forces are short-ranged and weak for molecular systems. Nonetheless, in 1932 Kallmann and Willstaetter (who collaborated with F. London) proposed that the range and magnitude of these forces would be large enough to explain a series of phenomena in colloidal systems provided vdW interactions were *additive*.[7] H. C. Hamaker later extended this idea to derive his expression for vdW interactions between macroscopic objects.[8] However, these calculations were based on disputable assumptions. Indeed, as noted by I. Langmuir "*These calculations ... are based on the very improbable assumption that these forces involve a kind of 'action at a distance' and are not influenced through which they are transmitted.*"[9] Despite this controversy, force laws based on this approach could still successfully explain the aggregation behavior of many colloidal systems.[10] Research eventually led to the establishment of the colloidal stability theory in the 1940s.[11-13] Interestingly, in the 1950s E. Lifshitz derived force laws for vdW interactions from the first principles which supported the force laws based on the '*additive*' approach.[14,15]

The cornerstone of colloidal stability theories is the counterbalance of attractive and repulsive forces. Taking into account vdW and double-layer forces explained many observations regarding the stability of colloids.[3,11-13] However, these studies did not give direct information about the range, magnitude, and the shape of the surface forces. Moreover, they did not account for forces other than vdW and double-layer forces.[2] Therefore, direct measurements of the surface forces became a crucial objective in colloid and interface science.[16-19] Different techniques such as surface force apparatus,[19,20] atomic force microscopy,[21,22] and total internal reflection microscopy[23] developed to study the interactions between the interfaces directly. Studies using these techniques revealed new types of surface forces and reinforced our understanding of surface forces and colloidal interactions.[24]

1.1- Electrical double layer forces

Double layer structure:

When a surface is exposed to a polar media such as water, the interface will get charged due to ionization of surface groups and/or ion adsorption. This charged interface generates an electric field in the media which causes accumulation of counter-ions (the oppositely charged ions) at proximity of the interface and depletion of the co-ions (similarly charged ions). For the sake of electro-neutrality of the system equal net amount of counter-ion should form an ion structure close to the surface (in salt-free case). This phenomenon was first modeled by considering a compact layer of counter-ions with equal amount of charge at the surface which are immobilized by electrostatic attraction, forming an '*electric double layer*' (EDL). This model is known as Helmholtz model (Figure 1a).[2] Later, this representation was modified and it was proposed that the formation of EDL is product of interplay of ionic diffusion and electrostatic interactions. Therefore, the ions form a '*diffuse*' layer close to the surface where the concentration of counter-

ions gradually decreases to the bulk concentration (Figure 1b). (Gouy-Chapman model) The commonly used model is combination of both of these pictures. It is suggested that part of counter-ions are closely bound to the interface forming a compact layer known as '*Stern*' or '*Helmholtz*' layer while the rest of counter-ions form a diffuse layer (Figure 1c). The response and behavior of EDL strongly depend on the distribution of '*cloud*' of ions next to the surface.

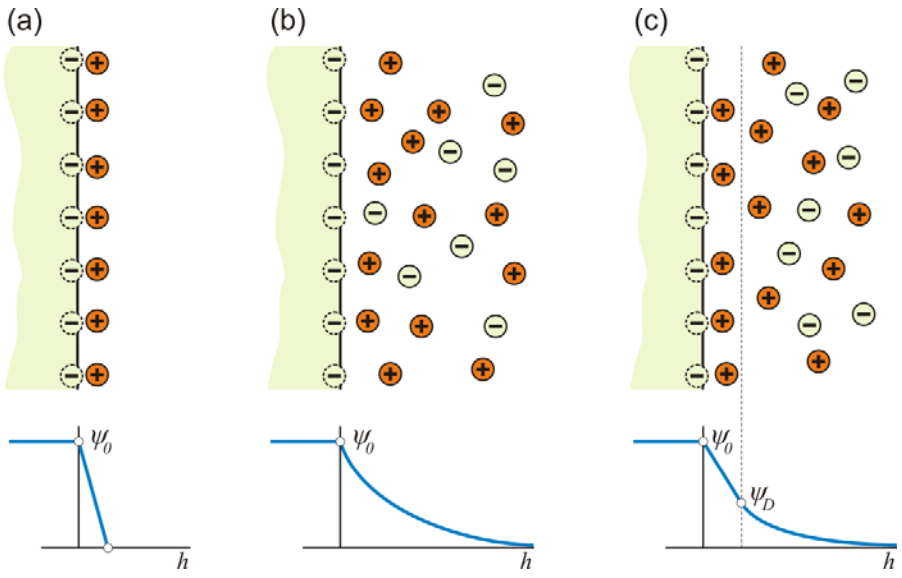

Figure 1. Structure of the electrical double layer: (upper row) the schematic of ion distribution in (a) Helmholtz (b) Gouy-Chapman and (c) basic Stern models. (Bottom row) Electrostatic potential profiles in the corresponding models. The dotted line in (c) indicates the onset of the Stern layer.

In Gouy-Chapman model, the interplay of electrostatic interaction and ionic diffusion due to thermal motion leads to formation of the diffused layer. To this end, let's consider chemical potential, μ, of a point charge ions, i, with valence of Z_i :[2]

$$\mu_i = Z_i q\psi + kT \ln c_i + \mu_{0i} \qquad (1.1)$$

Where μ_{0i} represents the standard chemical potential, q the elementary charge, ψ the electrostatic potential, k the Boltzmann constant, T temperature and c the number concentration. Given $\psi_{Bulk} = 0$ and $c_{i\,Bulk} = c_{0i}$, equation (1.1) gives a Boltzmann distribution of ions:

$$c_i = c_{0i} e^{-\frac{Z_i q \psi}{kT}} \tag{1.2}$$

The electrostatic potential is related to electric field, E, through the Poisson equation:

$$\frac{dE}{dx} = \frac{\rho}{\varepsilon_0 \varepsilon} \tag{1.3}$$

Where ρ stands for the total electric charge per unit volume, ε_0 the vacuum permittivity and ε the dielectric constant of medium. Given that:

$$E = -\frac{d\psi}{dx} \tag{1.4}$$

We arrive to:

$$\frac{d^2\psi}{dx^2} = -\frac{\rho}{\varepsilon_0 \varepsilon} \tag{1.5}$$

The total electric charge per unit volume is given by:

$$\rho = q \sum_i Z_i c_i \tag{1.6}$$

When equation (1.2) and (1.6) inserted to equation (1.5), we obtain the celebrated Poisson-Boltzmann (PB) equation:

$$\frac{d^2\psi}{dx^2} = -\frac{q}{\varepsilon_0 \varepsilon} \sum_i Z_i c_{0i} e^{-\frac{Z_i q \psi}{kT}} \tag{1.7}$$

The PB equation is non-linear differential equation and does not have a general analytical solution. However, at low electrostatic potential, the exponential terms in summation can be estimated using Taylor expansion. Therefore, if:

$$\psi \ll \frac{kT}{Z_i q} \tag{1.8}$$

The equation (1.7) can be approximated as:

$$\frac{d^2\psi}{dx^2} = -\frac{q}{\varepsilon_0 \varepsilon} \left[\sum_i Z_i c_{0i} - \sum_i \frac{Z_i^2 c_{0i} q \psi}{kT} \right] \tag{1.9}$$

Electro-neutrality of the solution requires that the first term in bracket becomes zero and as result we get:

$$\frac{d^2\psi}{dx^2} = \left[\sum_i \frac{Z_i^2 q^2 c_{0i}}{\varepsilon_0 \varepsilon kT} \right] \psi = \kappa^2 \psi \tag{1.10}$$

The constant κ has unit of inverse of length. A characteristic length scale is now defined as:

$$\kappa^{-1} = \left[\frac{\varepsilon_0 \varepsilon kT}{\sum_i Z_i^2 q^2 c_{0i}} \right]^{\frac{1}{2}} \tag{1.11}$$

And is known as the '*Debye length*'.

We now deal with linear equation (1.10) which has general analytical solution of:

$$\psi = C_1 e^{-\kappa x} + C_2 e^{\kappa x} \tag{1.12}$$

The constants C_1 and C_2 are defined by boundary conditions. Given that distances far from the interface the potential vanishes, $C_2 = 0$. At the interface, *x = 0*, the potential is equal to the surface potential, ψ_0, thus $C_1 = \psi_0$ and:

$$\psi = \psi_0 e^{-\kappa x} \tag{1.13}$$

Therefore, electrostatic potential decays exponentially with respect to distance from the interface. This linear form of PB equation is known as Debye-Hückel (DH) approximation. This estimation is valid as far as the equation (1.8) satisfied. Therefore, for highly charged interfaces and/or systems involving multivalent ions, this approximation fails to predict the structure of the EDL and associated forces.

The equation (1.13) implies that the smaller the Debye length (κ^{-1}) is, the faster electrostatic potential decays. To provide a lucid physical picture of the Debye length, let's apply the Gauss's law at the interface:

$$E_{x=0} = -\frac{\sigma}{\varepsilon_0 \varepsilon} \tag{1.14}$$

Where σ is the surface charge density. From equations (1.4), (1.13) and (1.14), we arrive to:

$$\sigma = \varepsilon_0 \varepsilon \kappa \psi_0 \tag{1.15}$$

Now, if the diffuse layer is seen as a plate capacitor, then the capacity is defined as:

$$C_D = \frac{\sigma}{\psi_0} = \frac{\varepsilon_0 \varepsilon}{\kappa^{-1}} \tag{1.16}$$

This equation suggests that the Debye length is in fact the '*effective*' thickness of the so-called diffuse layer capacitor. In the case of 1:1 electrolytes and at room temperature, the equation (1.11) gives:

$$\kappa^{-1} = \frac{0.304}{\sqrt{c}} \tag{1.17}$$

Where c is the electrolyte concentration in unit of molar and the Debye length's unit is in nanometer. Thus, in water the Debye length cannot exceed 1 μm, at electrolyte concentration of 160 mM (close to ionic strength of blood plasma) is less than 8 Å and at 700 mM of electrolyte (sea water) is about 3.6 Å. This implies the EDL forces are in nanometer length scale in aquatic systems. One should keep in mind that the DH approximation fails in highly charged systems and solutions containing multivalent ions.[25] Hence, the above argument needs to be revisited in those systems.

Double layer forces

The above analysis is made for one interface. However, when another charged surface approaches to this interface, it perturbs the equilibrium of the system once the double layers '*touch*' each other.[26,27] Here, the case for two identical interfaces will be discussed.

As mentioned in previous part, the counter-ions concentration close to the charged interface is higher than bulk. Therefore, when two equally charged surfaces approach each other, the so-called '*clouds*' of ions overlap and local concentration of counter-ions increases. This generates an osmotic pressure and provides repulsive forces.[2] The induced pressure to the surfaces is

related to changes in chemical potentials of ions and can be modeled using Gibbs-Duhem relation:[2]

$$\sum_i N_i d\mu_i = -SdT + VdP \tag{1.18}$$

Where N represents the number of species, S the entropy, T the Temperature, V the volume and P the pressure. Given that the system is considered isothermal, the first term on the right hand side is zero. From equation (1.1) we arrive to:

$$d\mu_i = Z_i q d\psi + kT\frac{dc_i}{c_i} \tag{1.19}$$

The number concentrations of ions are defined as:

$$c_i = \frac{N_i}{V} \tag{1.20}$$

Therefore, from equations (1.18) to (1.20) one finds:

$$d\Pi = \sum_i \left[kTdc_i + Z_i c_i q d\psi\right] \tag{1.21}$$

Where Π is the osmotic pressure. From equations (1.5) and (1.6), we have:

$$d\Pi = kT\sum_i dc_i - \varepsilon_0 \varepsilon \frac{d^2\psi}{dx^2} d\psi \tag{1.22}$$

This equation can now be integrated from infinite separation of the interfaces to the actual one considering that $2\frac{d^2\psi}{dx^2}d\psi = d(\frac{d\psi}{dx})^2$ and from equation (1.2) one gets:

$$\Pi = kT\sum_i c_i\left[e^{-\frac{Z_i q\psi}{kT}} - 1\right] - \frac{\varepsilon_0\varepsilon}{2}\left(\frac{d\psi}{dx}\right)^2 \tag{1.23}$$

Let's choose the origin of the system, $x = 0$, at midplane and therefore the surfaces are located at $x = \pm\frac{h}{2}$, where h is the separation distance. (Figure 2) As the surfaces are identical, one finds by symmetry $\frac{d\psi}{dx} = 0$. Thus, the second term in equation (1.23) can be omitted for the symmetric cases. Now, let's consider the case for a symmetric *Z:Z* electrolytes. Given that $\cosh(x) = \frac{e^x + e^{-x}}{2}$, the equation (1.23) is simplified to:

$$\Pi = 2kTc_0\left[(\cosh(\frac{Zq\psi}{kT}) - 1)\right]_{h=0} \tag{1.24}$$

Expanding the hyperbolic cosine using Taylor series, $\cosh(x) = 1 + \frac{x^2}{2!} + \ldots$, one finds:

$$\Pi = \frac{Z^2 q^2 c_0}{kT}\psi^2 \tag{1.25}$$

To calculate the pressure from the above equation, one needs to derive the electrostatic potential at the midplane. From the previous section, we learnt that the potential decays exponentially (in DH limit) and is given by equation (1.13). However, for two interacting surfaces the potential is higher and one can assume at the midplane, it is twice the value for the isolated surface at a distance $x = \frac{h}{2}$. (Figure 2) This is a '*superposition*' approximation and is valid at large distances. (Figure 2) Following this approximation and inserting equations (1.11) and (1.13) into equation (1.25), one finds:

$$\Pi = \frac{\varepsilon_0 \varepsilon}{2} \kappa^2 \psi_{h=0}^2 \tag{1.26}$$

And

$$\Pi = 2\varepsilon_0 \varepsilon \kappa^2 \psi_0^2 e^{-\kappa x} \tag{1.27}$$

From the relation of surface pressure to surface energy, W:[11]

$$W(h) = \int_h^\infty \Pi(x')dx' \tag{1.28}$$

One can derive the interaction energy between two equally charged surfaces as follow:

$$W(h) = 2\varepsilon_0 \varepsilon \kappa \psi_0^2 e^{-\kappa h} \tag{1.29}$$

This relation can be rewritten using equation (1.15) as a function of surface charge density, again in DH limit, as follow:

$$W(h) = \frac{2\sigma^2}{\varepsilon_0 \varepsilon \kappa} e^{-\kappa h} \tag{1.30}$$

The above relation states the magnitude of double layer forces strongly depends on the surface charge density whereas the range of the forces is dictated by number density of ions in the solution. In fact, no matter how charged the interface is, screening the double layer forces by electrolytes in solution makes these forces short ranged and eventually other surface forces dominate the system. Once again, it is importance to note that the validity of above relation is limited to low charged systems, where $\psi \ll \frac{Z_i q}{kT}$, and at large distances, $h > \kappa^{-1}$. The breakdown

of this approximation at small distances originates from the fact that charging properties of interfaces alter as two surfaces approach to each other.[26,27]

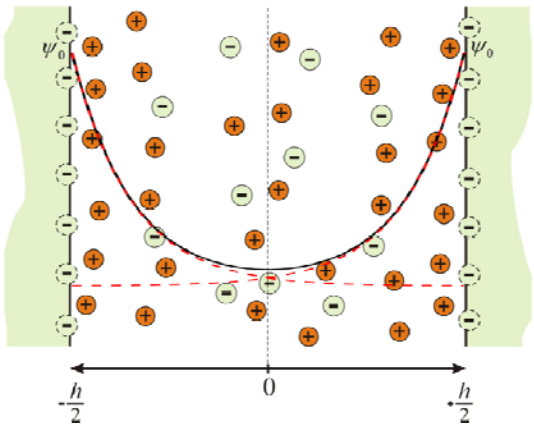

Figure 2. *Superposition approximation: the electrostatic potential at the midplane of two interacting charged plates is twice as the one for the isolated plate.*

Regulation parameter

The bottom line of above derivation for double layer forces is the superposition approximation. This approximation implies the electrostatic potential between two plates is twice as the isolated plate. Therefore, at contact, the electrostatic potential is two times higher than the surface potential of an isolated interface, *e.g.* $\psi_0\big|_{h=0} = 2\times\psi_0\big|_{h\to\infty}$. On the other hand, the equation (1.2) tells us the concentration of ionic species close the surface scales the electrostatic potential exponentially. Moreover, the double layer forces directly related to concentration distribution of ions due to the osmotic nature of these forces. Therefore, assuming that surface electrostatic potential increases upon decreasing the separation distance entails increase of local concentration of ions close to the surface compare to the case where the surface potential stays constant. This means higher double layer forces. Thus, depending on how two electrical double layers interact

with each other, different magnitudes of forces should appear.[28] Superposition approximation is just one way of modeling the interaction of the charged interfaces.

From the Gauss's law, equation (1.14), and definition of electrostatic potential one finds:

$$\frac{\sigma}{\varepsilon_0 \varepsilon} = -\left.\frac{d\psi}{dx}\right|_{x=\pm\frac{h}{2}} \tag{1.31}$$

If ψ stays constant (*constant potential, CP*) as two interfaces approach each other, above equation implies the surface charge density decreases and eventually the interfaces discharge completely ($\sigma \to 0$). On other hand, if σ stays the same as the one for isolated interface (*constant charge, CC*), ψ continuously increases as two interfaces get closer. This behavior of the interface is in fact connected to how chemical equilibrium of dissociation-association of charged groups responds to variation of the electric field at the interface.[29] In fact, discharging the interface in the case of CP condition can be seen as induced counter-ion binding.[28-30]

In reality most of the charged interfaces behave neither in CC regime nor in CP regime.[29] Indeed, as the separation distance decreases both ψ and σ regulate in a way that is dictated by the ion adsorbtion equilibrium and PB equation. In these situations the PB equation must be solved self-consistently in order to satisfy the dissociation equilibrium. This, however, demands for knowledge of dissociation constants which is not available for many interfaces. Moreover, for those interfaces with well-defined dissociation constants, *e.g.* silica, the experimental data does not always satisfactory match with this approach.[29,31,32]

A common approach that takes into account the charge regulation effect is to model the electrical double layer with *basic Stern model*.[28] (Figure 1c) The model considers a compact layer, *i.e.* Stern layer, of ions with certain thickness (d_S) where potential drops from the surface potential

(ψ_0) to diffused layer potential (ψ_D). The thickness of Stern layer is connected to finite size of ions.[33] This model for the structure of electrical double layer can be seen as two parallel capacitors where the capacitance of the Stern layer follows:[29]

$$C_S = \frac{\sigma}{\psi_0 - \psi_D} = \frac{\varepsilon_0 \varepsilon}{d_S} \tag{1.32}$$

The potential drop in the Stern layer and its magnitude compare to the one in the diffused layer is directly related to charge regulation properties of the interface. This has been quantified by introducing the '*regulation parameter*' (p) as:[29]

$$p = \frac{C_D}{C_S + C_D} \tag{1.33}$$

This parameter usually varies between 1 and 0. When $p = 0$ the diffuse layer potential remains constant and CP condition satisfies. When $p = 1$, the situation corresponds to the CC condition. However, for many experimentally relevant cases, this parameter takes a value in between which corresponds to '*constant regulation*' (CR) condition.[27] This parameter provides information on how an interface regulates itself upon interaction with other interfaces. It is a property of the surface and intimately connected to ion adsorbtion kinetics of the surface.[32] Double layer forces at short distances strongly depend on this parameter.[2,34] (Figure 3)

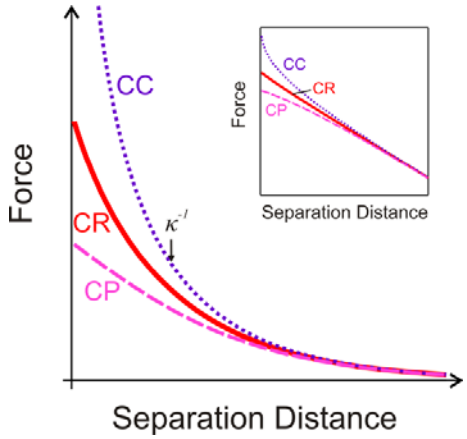

Figure 3. *Double layer forces in monovalent salt calculated using PB theory. Depending on the charge regulation property of the surface, the double layer forces usually sit between two boundaries, i.e. constant charge (CC) and constant potential (CP). At the constant regulation (CR) limit, the magnitude of the force at short distances ($h < \kappa^{-1}$) depend on the regulation parameter. Inset shows the same forces but in semi-logarithm scale. At large distances the forces are linear in this way of presentation.*

Effect of multivalent ions:

The Coulomb's law states the electrostatic force between ions is directly related to the valence of the ions. Consequently, the electric potential energy acting on a multivalent ion is larger compare to the monovalent counterpart. Therefore, in competition between thermal and electrostatic energy acting on ions, multivalent ions tend to be less diffusive and accumulate more at proximity of the interface.[35,36] This can be quantitatively seen in Boltzmann relation for distribution of ions next to a charged interface, equation (1.2). The high affinity of multivalent counter-ions to accumulate at the interface and as a result decline of surface charge of the interface, strongly manipulates the double layer forces.[25] In addition, equation (1.11) states multivalent ions are more efficient in terms of screening of the double layer forces; and for the same concentration of salts the Debye length is shorter for higher valences of ions.

Early studies on stability of colloidal dispersions by Schulze and Hardy more than a century ago showed the '*coagulative power*' of salts mainly depends on the valence of the counter-ions.[37,38] Later, it was established that multivalent ions are also able to tune the surface charge of colloids and '*charge reversal*' phenomenon observed in many systems.[39] In such cases, addition of the counter-ions leads to charge neutralization at certain concentration and after adding more of these ions the interface gains the same charge as the multivalent counter-ions.[25,31] This leads to re-entrant stabilization of colloids in the presence of some multivalent ions, where colloidal particles first coagulate at charge neutralization point and then form a stable dispersion upon increase of ion concentration.[40] Despite common feature of this phenomenon, quantifying this process is not straightforward. From the DH approximation we have $\psi_0 = \frac{\sigma}{\varepsilon_0 \varepsilon} \kappa^{-1}$. Therefore for an interface with surface charge density of σ, the surface potential just decreases in magnitude by addition of salt and charge reversal is not seen in this model.[36] Neglecting the finite size of ions and the interaction between ions themselves and the interfaces in the PB theory are named as the main reasons for failure of this model to predict the proper trend for surface potential and forces.[35,36,41]

The shortcomings associated with the mean-field PB theory for the systems involving multivalent ions initiated new line of research to derive proper force laws for electrical double forces in the presence of multivalent ions.[41-43] The major outcome of these theoretical studies is that the PB theory overestimates the repulsive double layer forces and the forces should be more attractive particularly at shorter distances. The evidence of the presence of such attraction became possible by the advent of force measurement techniques. These measurements directly provide evidences for the presence short-ranged attractive forces which could not be justified by van der Waals forces.[44-46] Even though the origin of these attractive interactions is still matter of debate, both

theoretical and experimental work indicates that the PB theory cannot capture the whole picture of double layer forces especially at short distances.

Research on surface forces in the presence of multivalent ions is now focus on learning more about the origin of deviation from the mean-field PB theory and deriving general force laws for the so-called additional attractive forces. Different types of interactions such as ion–ion correlations,[36,41] surface charge heterogeneities,[47] hydrophobic forces,[48] charge fluctuations,[49] or electrolyte depletion[50] have been proposed as the possible additional forces involving in these systems. On the other hand, understanding how ions interact with and adsorb to (or desorb from) the interface will help to provide clear picture of charge reversal physics and also resolve 150-years old mystery of ion-specific effects.[51]

Polyelectrolytes

Polyelectrolytes (PEs) are macromolecules bearing ionizable groups. Under appropriate conditions, the functional groups in PEs dissociate and leave charged groups on polymer chain and release counter-ions into the media.[52] This class of polymers covers a wide range of natural biopolymers and synthetic polymers. The highly charged nature of PEs leads to strong interaction of these molecules with the interface.[52] In addition, unlike the neutral polymers, PEs are greatly responsive to the changes in ionic properties of environments such as pH, ionic strength and valences of counter-ions.[53] These properties originated from Coulombic inter- and intra- forces between polymer segments and the interfaces. Strong affinity of PEs to adsorb on oppositely charged interfaces make them popular candidates for tuning the surface forces and designing new materials.[52,54,55] The adsorbtion of PEs to planar oppositely charged interfaces has been intensively studied both experimentally and theoretically. The adsorbtion behavior of PEs

resembles the one for charged particles and the adsorbtion level depends on ionic strength and size of PEs.[56]

The impact of oppositely charged PEs on the double layer forces between the charged interfaces is similar to multivalent counter-ions. At very low dose of PEs, the polymer molecules neutralize the surface charges and at a certain dose the surface potential becomes zero.[57] Addition of more PEs leads to the overcharging the interfaces and the double layer forces revive. Finally the interface saturates and the surface potential reaches to a plateau. The adsorbed PE layer is usually very compact and the adsorbtion process is typically irreversible.[52]

The above feature is generic for oppositely charged systems. The saturation of the interfaces with PEs happens at concentrations of few tens milligram per liter (at low salt level).[52,57] At the high concentration of PEs the interface attains the same charge as the PEs and polymer molecules is expected to repel from the interface due to the electrostatic forces. Therefore, the like-charged regime, where PEs and the interface have the same charge, is present at high concentration of PEs. In the cases where the intrinsic charges of the surface and PEs molecules are the same, the like-charged regime exists at any dose of the PEs. Despite the ubiquitously of this regime, little is known about the double layer forces in these circumstances. In these situations, most of the counter-ions in the medium are originated from the dissociation of the ionic groups of PEs.[58] Attempts related addressing this matter were mainly centered on DH limit and introducing an '*effective*' Debye length for double layer forces.[59] The central assumption in this approach is that only monovalent ions, whether from background solution or counter-ions of PEs, contribute to screening of the double layer forces.[59] This assumption violates the key hypothesis in derivation of DH approximation where equation (1.10) derived from equation (1.9), which was based on electroneutrality. If one argues that PEs molecules can be assumed as multivalent co-ions in this

derivation, then the validity of DH approximation will be limited to the situation where $\psi \ll \frac{kT}{Z_i q}$ holds, which is irrelevant for the cases of PEs due to the very high valence of them. Resolving this ambiguity is however the subject of Chapter 5 and 6 of this thesis.

1.2- van der Waals forces

Intermolecular interactions:

The celebrated van der Waals' equation of state implies the failure of ideal gas law is caused by finite size of gas molecules (or particles; as at that time existence of atoms were doubted!) and attractive interaction between the molecules.[5] These attractive forces are ubiquitous and as J. D. van der Waals stated; '*matter will always display attraction*'.[60] This insight by van der Waals inspired the work of liquefaction of helium.[60] However, the physics behind this universal attractive forces had not been clarified till the advent of quantum mechanics.[2]

Understanding the origin of vdW attraction initiated a series of research by different researchers to quantify these intermolecular forces from the first principles. W. H. Keesom regarded the '*dipole moment*' as the most important constant for the forces between molecules, which is present in polar molecules.[6] By averaging all possible position and orientation for dipole moments, he derived the interaction energy as follow:

$$W(h)_{Keesom} = -\frac{2}{3}\frac{\mu_1^2 \mu_2^2}{(4\pi\varepsilon_0)^2 kT}\frac{1}{h^6} \tag{1.34}$$

Where μ_i is the dipole moment and h the intermolecular distance. This equation represents an attractive interaction and is very short-ranged compared to Coulomb's law. This interaction is known as Keesom or *orientation* or dipole-dipole interaction.

The above relation entails that this interaction should vanish at elevated temperatures, which was not consistent with experimental observations.[6] As a result, P. Debye concluded that there should be other interactions acting between molecules independent of the temperature. The charge distribution of a molecule will be affected by the electric field, *E*, and this electric field might be induced from the neighboring molecules with a dipole moment. This influence on molecules appears in the form an '*induced*' moment, M , and is defined by '*polarisability*', α , as follow:

$$M = \alpha \cdot E \tag{1.35}$$

If molecule *1* generates an electric filed due to the dipole moment of μ_1 close to the molecule *2* with polarisability α_2, an attractive interaction between two molecules appears and follows:

$$W(h)_{Debye} = -\frac{\mu_1^2 \alpha_2}{(4\pi\varepsilon_0)^2}\frac{1}{h^6} \tag{1.36}$$

This interaction is also called *induction* or dipole-induced dipole interaction.

The problem associated with above interaction was that these types of forces should be absence in symmetrical molecules such as rare gases.[6] In addition, both Keesom and Debye interactions should largely diminished due to cancellation of these forces when many molecules are interacting with each other. Therefore, van der Waals equation of state could not be fully described by these two interactions.[6]

In 1930's, F. London presented a comprehensive picture of vdW forces based on the quantum mechanics.[6] The quantum mechanics state all particles possess the zero-point motion even at absolute zero temperature. These fluctuations instantaneously generate fluctuating dipole in any molecules, including a neutral atom. The generated dipole subsequently induces a fluctuating

electromagnetic dipole field which in turn induces a fluctuating dipole on the nearby molecules.[61] These transient dipoles in average produce an attractive interaction. One can derive the force law as:

$$W(h)_{London} = -\frac{3}{2}\frac{\alpha_1\alpha_2}{(4\pi\varepsilon_0)^2}\frac{h_p\nu_1\nu_2}{(\nu_1+\nu_2)}\frac{1}{h^6} \tag{1.37}$$

Where h_p is the Planck constant and ν_i the orbiting frequency of electrons. If one takes the statistic distribution of charges, no influence is not expected between the atoms. Therefore, this type of interaction originates from the vibration and movement of electrons at finite speed. The resonance frequency of the induced dipoles is caused as result by quantum fluctuation of electric field which is also the physical foundation of the adsorption spectrum that underlies the dispersion of white light into the spectrum of a rainbow.[62] That is why London named this type of interaction as '*dispersion*' forces. In his groundbreaking work, London also showed the experimental van der Waals constant for many non-polar gases can be well predicted by this expression. He also verified that the contribution of dispersion forces to vdW interaction in non-polar molecules is superior to other two forces.[6]

Pair-wise additivity: Hamaker approach

The intriguing feature of three aforementioned forces is that they all scale the intermolecular distance in the same way. Therefore, they can be united in general form for vdW interaction as:

$$W(h)_{vdW} = -\frac{C_{Keesom}+C_{Debye}+C_{London}}{h^6} = -\frac{C}{h^6} \tag{1.38}$$

Where C is scaling factor in power law equations of (1.34), (1.36) and (1.37).

As mentioned in the introduction part, the shortcoming of the above expression to justify the attractive forces between the colloidal particles is fast decay of attraction as a function of the separation distance. The above relation however is valid for molecular systems and for collection of the molecules, *e.g.* colloidal particles, one deal with a many-body problem. If additivity is applicable for the vdW interactions, then a pair-wise additive approximation gives the total vdW interaction between macroscopic bodies.[62] The additivity of vdW forces was first addressed by London himself where he stated '*one may imagine that the simultaneous interaction of many molecules can simply be built up as an additive superposition of single forces between pairs.*'[6] This approximation was examined by many researchers.[7,8,10-13] The exciting aspect of these works is the vdW interactions become long-ranged and quite strong at relevant separation distances for colloidal particles.[11]

The pair-wise additive approximation for vdW interaction between two macroscopic bodies can be written as:[63]

$$W(h)_{vdW} = -\int_{V1}\int_{V2} \rho_1 \rho_2 \frac{C}{h^6} dV_1 dV_2 \tag{1.39}$$

Where ρ_i is the position distribution function of atoms in macroscopic bodies. Above equation usually gives a power law relation but the scaling factor and power law number depends on the geometry of the interacting bodies. (Figure 4) For two flat surfaces with homogenous distribution of atoms one finds the vdW interaction energy per unit area as:

$$W(h)_{vdW} = -\frac{\pi \rho_1 \rho_2 C}{12 h^2} \tag{1.40}$$

H. C. Hamaker applied this approach for several geometries and obtained the same.[8] He argued that the vdW potential obeys a general form of $W(h)_{vdW} = -A \cdot g(h)$, where *g(h)* is just function of geometry. (Figure 4) However, constant *A* appears which has the unit of energy. This constant named after him and known as '*Hamaker constant*' and defined as:

$$A = \pi^2 \rho_1 \rho_2 C \tag{1.41}$$

The reason that pre-factor of π^2 appears in the formula is apparently the fact that he first solved the equation (1.39) for two spheres which gives the following potential:[8]

$$W(h)_{vdW} = -\frac{\pi^2 \rho_1 \rho_2 C}{6h}\left(\frac{R_1 R_2}{R_1 + R_2}\right) = -\frac{A}{6h}\left(\frac{R_1 R_2}{R_1 + R_2}\right) \tag{1.42}$$

R_i is the spheres' radius. To estimate the magnitude of vdW interactions, one needs to have values for ρ_i and *C*. For most of liquids and solids, ρ_i is about $1\text{-}10\times10^{28}$ atom.m^{-3}. The constant *C* can vary within the range of 1×10^{-79} to 400×10^{-79} J.m^6. Based on this approximations, Hamaker proposed a range of 0.7×10^{-21} to 300×10^{-21} J for this constant in vacuum.[8] This indeed concurs with more rigorous calculations. From equation (1.42) for two spheres with diameter of 100 nm, the vdW energy at separation distance of 10 nm can be in the range of 0.14 to 60 *kT*. Therefore, the vdW forces are strong enough to overcome other repulsive forces such as double layer forces and induce aggregation.[11]

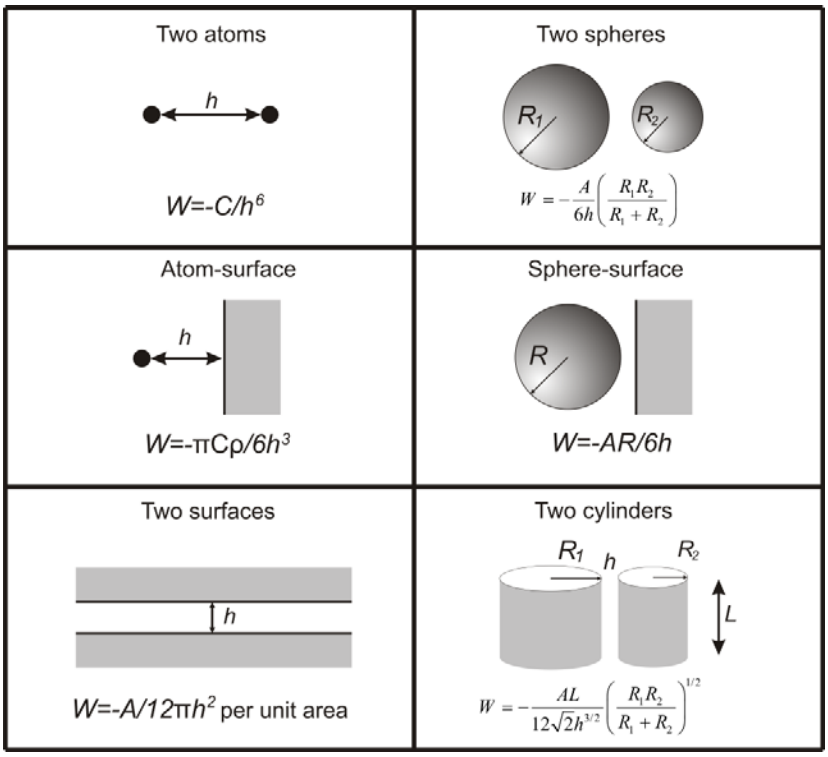

Figure 4. *van der Waals interaction energy between bodies of different geometries. Pair-wise approach indicates that vdW interaction scales the separation distance as* $W(h)_{vdW} = -A \cdot g(h)$ *and g(h) depends on the geometry.*[2]

Above estimation is however valid in vacuum. The impact of medium was also discussed by Hamaker.[8] If the interaction of one particle with the surrounding medium is un-affected by the presence or absence of the other particle(s), the Hamaker constant between particle *1* and *2* through medium *0* (A_{102}) will be:

$$A_{102} = A_{12} + A_{00} - A_{10} - A_{20} \tag{1.43}$$

Where A_{ij} is the Hamaker constant between materials *i* and *j* interacting through vacuum. Inserting equation (1.41) in above equation one finds:

$$A_{102} = \pi^2 \left(\rho_1 \rho_2 C_{12} + \rho_0^2 C_{00} - \rho_0 \rho_1 C_{01} - \rho_0 \rho_2 C_{02} \right) \tag{1.44}$$

Where C_{ij} is the scaling factor between material *i* and *j*, equation (1.38). Given that the main contribution of the vdW interaction originates from the dispersion forces, we can assume from equation (1.37):

$$C_{ij} = K\alpha_i\alpha_j \frac{\nu_i\nu_j}{(\nu_i + \nu_j)} \tag{1.45}$$

K is a constant. Inserting equation (1.45) in (1.44) and considering $\gamma_i = \alpha_i\rho_i\nu_i$, we arrive to:

$$A_{102} = K\pi^2 \left(\frac{\gamma_1\gamma_2}{\nu_1 + \nu_2} + \frac{\gamma_0^2}{2\nu_0} - \frac{\gamma_0\gamma_1}{\nu_0 + \nu_1} - \frac{\gamma_0\gamma_2}{\nu_0 + \nu_2} \right) \tag{1.46}$$

For two identical materials above equation becomes:

$$A_{101} = K\pi^2 \left(\frac{\nu_0\nu_1(\gamma_0 - \gamma_1)^2 + (\nu_1\gamma_0 - \nu_0\gamma_1)^2}{2\nu_0\nu_1(\nu_0 + \nu_1)} \right) \tag{1.47}$$

Given $\nu_i > 0$, this equation implies that the vdW interaction between similar materials is always attractive, regardless of the medium they are interacting through. In addition, if $\nu_0 = \nu_1 = \nu$, then we have:

$$A_{101} = \frac{K\pi^2}{2} \frac{(\gamma_0 - \gamma_1)^2}{\nu} \tag{1.48}$$

As for vacuum $\gamma = 0$, the Hamaker constant across any medium is always smaller than the one across the vacuum. Therefore, the vdW forces are *screened* by medium. Extend of this screening, according to equation (1.48), depends on the difference between γ of medium and interacting bodies. γ is the product of polarisability, molar density and adsorbtion frequency of the materials

which in principle depends on the optical properties.[62] If the optical properties of interacting bodies and medium are identical, there are no dispersion forces between them.

Another interesting feature of equation (1.46) is that under certain circumstances the Hamaker constant can be negative, suggesting a *repulsive* vdW forces. This only happens when the interacting bodies are dissimilar and interacting through a dense medium.[8] Again, if $\nu_0 = \nu_1 = \nu_2 = \nu$, then from equation (1.46) one finds:

$$A_{102} = \frac{K\pi^2}{2}\frac{(\gamma_1 - \gamma_0)(\gamma_2 - \gamma_0)}{\nu} \tag{1.49}$$

Therefore, dispersion forces become repulsive if $\gamma_2 < \gamma_0 < \gamma_1$, which again signifies the role of optical properties of the materials not only on the magnitude of the dispersion forces but also on the sign of the interaction.

The pair-wise additive approximation, despite of its simplicity and doubtful assumptions, revealed many interesting aspects of vdW interactions, which matched very well with observations of colloid chemists.[11-13] It clarified how extremely weak and short-ranged vdW forces among molecules can cumulate and provide interactions as large as several *kT* at relevant separation distances. It also qualitatively showed why the strength of these interactions is strongly material-dependent. However, calculation of Hamaker constants from macroscopic properties of materials remained ambiguous and normally this parameter was used as fitting parameter in aggregation studies of colloidal particles.[2,11]

Beyond additivity: Lifshitz theory

The works by F. London showed the ever-present dispersion forces arise from the fluctuation of electromagnetic field.[6] This inspired the approaches based on the quantum mechanics.[64] The

approach was taken by Lifshitz and his colleagues to calculate vdW interaction between macroscopic bodies also had purely quantum character.[14,15] They approached the problem from purely macroscopic point of view and made the calculation directly for interacting bodies. They treated the bodies as continuous media with known response to electromagnetic fields. Understanding the original derivation of the Lifshitz formula requires thorough knowledge of the quantum filed theory, which is beyond the scope of this text. However, these studies showed the scaling powers for different geometries stay valid (Figure 4), and one just needs to replace Hamaker constant with a Hamaker *function*. The general form for Hamaker function for a material *1* interacting with material *2* through media *0* is presented as:[62]

$$A_{102}(h) = \frac{3kT}{2} \sum_{\substack{sampling \\ frequencies}} \left(\frac{\varepsilon_1 - \varepsilon_0}{\varepsilon_1 + \varepsilon_0}\right)\left(\frac{\varepsilon_2 - \varepsilon_0}{\varepsilon_2 + \varepsilon_0}\right) R(h) \tag{1.50}$$

Where ε_i is the dielectric function and $R(h)$ gives the effects of '*retardation*'. The retardation effect occurs due to the facts that the interactions have electromagnetic origin and the finite velocity of light restricts the response of the materials.[64] This effect becomes important at separation distances close to the corresponding sampling frequencies which are mainly located at UV region (at room temperature). The sampling frequencies come from the quantum field theory and are those whose corresponding photon energies are proportional to thermal energy.[62] The contribution of frequencies at visible and UV region are usually the most important due to high sampling in this region and appreciable magnitude for dielectric value.[2,62] This fact simplifies the calculation of Hamaker constant if one considers main adsorption frequencies of materials which are accessible from optical spectrum of materials.[62]

An interesting feature of equation (1.50) is the appearance of the dielectric function of the materials in calculation of dispersion forces. This can be understood better if one thinks of '*electric susceptibility*', χ_e, instead of dielectric function. These two are related and $\chi_e=\varepsilon-1$. The electric susceptibility expresses the tendency of a dielectric material for polarization in response to an applied electric field.[62] This bears a resemblance to the origin of the dispersion forces as discussed in pervious part. The dielectric function is measurable in wide ranges frequency for most of the materials and thus Hamaker function can be calculated from the microscopic properties and based on the first principles.

The full spectrum optical properties of the many materials are mostly not available. In addition, original calculation of Hamaker constant based on Lifshitz theory is not straightforward and is a heavy mathematical task. Therefore, simplified versions of the Lifshitz theory were introduced by simulating optical response of materials with simple models. Using single harmonic oscillator to mimic the response of dielectric materials resulted in following expression for Hamaker constant:[2]

$$A_{132} = \frac{3kT}{4}\left(\frac{\varepsilon_1' - \varepsilon_0'}{\varepsilon_1' + \varepsilon_0'}\right)\left(\frac{\varepsilon_2' - \varepsilon_0'}{\varepsilon_2' + \varepsilon_0'}\right) + \frac{3h_p\nu_e}{8\sqrt{2}}\frac{(n_1^2 - n_0^2)(n_2^2 - n_0^2)}{(n_1^2 + n_0^2)^{0.5}(n_2^2 + n_0^2)^{0.5}\left\{(n_1^2 + n_0^2)^{0.5} + (n_2^2 + n_0^2)^{0.5}\right\}} \quad (1.51)$$

Where ε_i' is the static dielectric constant (dielectric value at zero frequency), n_i the index of refraction and ν_e the main adsorption frequency. This relation predicts screening the vdW interactions with medium and possibility of existence of repulsive vdW forces, as well. The first term in above equation is known as zero-frequency term and is shown to represent the Keesom and Debye interaction.[65] The second term represents the dispersion forces. The first term cannot exceed *0.75kT* and is negligible in most of the cases (in vacuum). However, for bodies interacting

through a medium having similar refractive index but different dielectric constant, the contribution of zero-frequency term can be dominant, for instant in the case of lipid bilayers interacting through water.[66] The derivation of above equations and more details about the Lifshitz theory can be found elsewhere.[62,65]

1.3- The Derjaguin approximation

The derivation of the surface force two flat interfaces is more straightforward compared to arbitrary objects. Boris Derjaguin proposed a practical way to calculate the surface forces between arbitrary objects from the surface energy between two flat interfaces.[2] The Derjaguin approximation states the total force acts between two surfaces is sum of forces among the surface elements. This can be written as:

$$F(h) = \int \Pi(x) dA \tag{1.52}$$

Where Π is the surface pressure between the surface elements with surface area of dA. This approximation is schematically illustrated for a sphere and a planar wall in Figure 5. In this case, the surface area of each element is $dA = 2\pi r dr$. r and the height of the elements are related through Pythagorean Theorem:

$$x = h + R - \sqrt{R^2 - r^2} \rightarrow r dr = dx\sqrt{R^2 - r^2} \tag{1.53}$$

If $R >> r$, then $dA = 2\pi R dx$. Therefore, one finds:

$$F(h) = 2\pi R \int \Pi(x) dx = 2\pi R W(h) \tag{1.54}$$

The above relation can be extended to other geometries and one will find:

$$F(h) = 2\pi R_{eff} W(h) \tag{1.55}$$

R_{eff} is the effective length scale for a given geometry. For the two spheres one gets:

$$R_{eff}^{-1} = R_1^{-1} + R_2^{-1} \tag{1.56}$$

This approximation is however valid for the separation distances much smaller than the size of the interacting bodies.

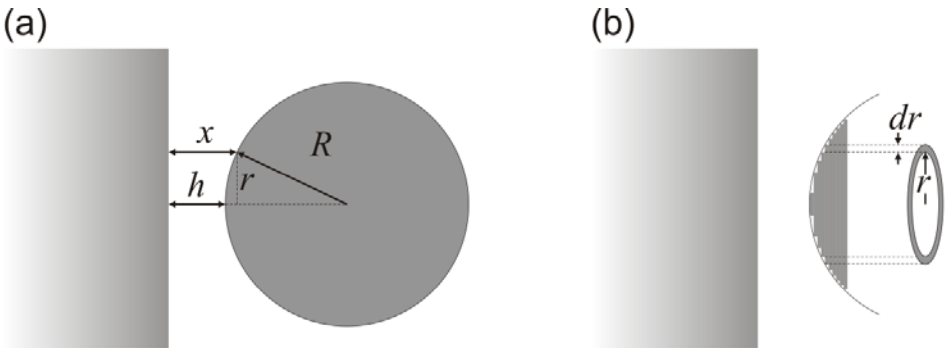

Figure 5. *Derjagiun approximation which relates the surface forces, F(h), (a) between a sphere and planar wall to surface energy, W(h), between two planar walls. (b) This is done through disintegrating the interacting surface into disk-like elements.*

1.4- DLVO theory

The long-standing question of how a colloidal system stays stable against aggregation was solved and addressed independently by two groups of scientists: *B. Derjaguin, L. Landau and E. Verwey, T. Overbeek* (DLVO).[11-13] The idea that one needs to formulate a potential energy between the interacting colloidal particles to comprehend their aggregation behaviour however was known for a while and was examined by other researchers as well.[7,9,10,67] However, DLVO managed to describe many experimental observation in colloidal dispersions by evaluating the interaction energy potential between interfaces.[11,13]

Colloidal particles move due to the Brownian motion. Therefore, they collide with each other. Whether the colliding particles stick together or not depends on the inter-particle interactions.[65] Finding the probability of aggregation is thus a diffusion problem.[11] It was first addressed by Von Smoluchowski for rapid coagulation case, where there is attraction between the particles.[11,68] These studies find in the absence of the repulsive forces the colloidal particles aggregates in time scale of seconds at relevant particle concentrations. However, when there is repulsive energy barrier of E for particles to pass, the probability of successful sticking modifies by Boltzmann factor, $e^{-\frac{E}{kT}}$. This implies the energy barrier of few tens of kT is enough to increase the aggregation time scale into years and makes the dispersion stable.[11] The DLVO theory addressed the energy potential between the particles and also the factors controlling that. It made many aspects of particle aggregation clear by evaluating the inter-particle energy potential.[11,65]

The DLVO theory states the interaction energy between the interfaces combines attractive vdW and repulsive double layer forces:

$$W_{DLVO} = W_{vdW} + W_{EDL} \tag{1.57}$$

As the vdW interactions between the particles in usually independent of ion concentration of the solution, it is the changes in the range and magnitude the double layer forces that control the aggregation. Generally, at low ionic strength the double layer forces are long ranged and easily overcome the attractive vdW forces.[65] This provides an energy barrier which can be in order of few tens of kT. However, if the range or magnitude of the double layer interactions decreases, at the certain point the vdW interactions overcome the double layer interactions and no barrier form. (Figure 6) At this point the aggregation of the particle follows the diffusion limit fast aggregation. This is known as *critical coagulation concentration (CCC)*.[56] (Figure 6a) This turning point in

aggregation behaviour of colloid was experimentally detected for many colloidal systems and DLVO theory provides a basis for its existence. To predict the *CCC* of a colloidal system DLVO needed to assign a certain Hamaker constant to the colloids which turned out to be close to Hamaker's prediction. This agreement convinced them that the attractive forces behind the colloidal aggregation are indeed vdW forces.[11]

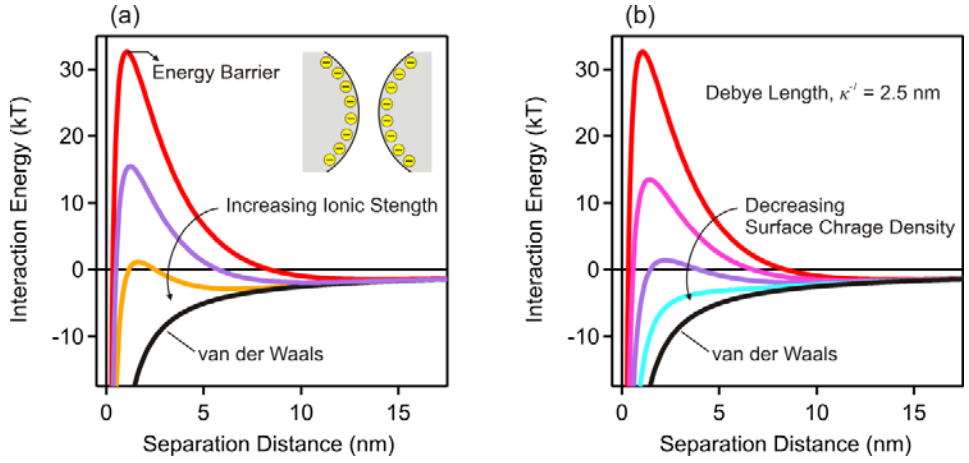

Figure 6. *Interaction energy between two identical spherical particles based on the DLVO theory: The calculations were performed for two particles with radius of 250 nm and Hamaker constant of 5×10^{-21} J. Equation (1.42) was used to estimate vdW interactions. Double layer forces were calculated at DH limit and applying The Derjaguin approximation. (a) Surface charge density was kept constant at 5 $mC.m^{-2}$ and the interaction energy was calculated at different ionic strength. The sticking energy barrier diminishes at certain ionic strength which corresponds to CCC (see text). (b) The interaction energy potential at fixed ionic strength of 15 mM and different surface charge density. Decreasing the surface charge density lowers the energy barrier and eventually leads to fast aggregation regime.*

1.5- Non-DLVO forces

DLVO theory assumes the total interaction between the interfaces is controlled by two forces, *i.e.* van der Waals and electrical double layer forces. Both of these interactions are derived based on the mean-field theories. This picture often breakdowns in realistic systems, especially at

separation distances close to the molecular sizes. The failure of the DLVO theory is due to the inaccuracy of the mean-field theories and/or presence of other intermolecular forces. These forces are also known as non-DLVO forces.[2]

These additional non-DLVO forces could have different origins. The nature of the surface, presence of macromolecules or multivalent ions or surface active agents can cause different types of the non-DLVO forces with different magnitude and ranges.[24] These forces can be monotonically repulsive or attractive, or have oscillatory nature. Different sorts of these forces have been indentified and studied, mostly using direct force measurements, such as hydrophobic attraction,[22] hydration repulsion,[48] patch-charge attraction[69] or polymer induced forces.[65] The detailed representation of these forces is beyond the scope of this text. Following, just two types of non-DLVO forces which relevant to this thesis is presented, *i.e.* hydrophobic interactions and depletion forces.

Hydrophobic forces

The hydrophobic interaction was first conceptualized in study of association of non-polar species in water such as micelle formation.[70] The strong temperature dependence of these phenomenons revealed the entropic origin of these interactions. However, the type of the interaction between the macroscopic hydrophobic interfaces is shown to be different than the hydrophobic molecules.[70] Between two hydrophobic interfaces, at the certain distance, the liquid water film confined in between becomes thermodynamically unstable and a first-order transition from liquid state to gas is expected.[71] This transition applies significant attractive forces to the interfaces and normally leads to the collapse of the interfaces into the contact. This explanation however is not always consistent with experimental data.

In early 80's, force measurement between large hydrophobic surfaces (~ 1 cm) revealed long ranged attractive forces which was stronger than vdW forces.[72] These forces decay exponential with respect to the separation distance with decay length in order of one nanometer.[48,69,72] However, the subsequent measurements were not consistent with this picture. Especially the range of the forces varies from a nanometer to tens of nanometer. In some cases, the measured forces were erratic and non-monotonic.[73] Later investigations showed that in many of those cases the surfaces that used for force measurement whether were heterogeneously charged or contaminated with surface nano-bubbles.[74] Therefore, the measured forces were combination of hydrophobic interaction and patch charge interaction or capillary collapse of surface bubbles.

In the cases where the surface was homogeneously charged and bubble-free, the range of the measured so-called hydrophobic forces was smaller than the previous reports and went into sub-nanometer regime.[48,70,74] The origin of these forces is still debated and not clear. The simple thermodynamic model based the thermodynamic instability of the water thin film between the interfaces predicts much larger ranges for the hydrophobic interaction.[71] It is on the other hand proposed that the water thin film experience meta-stable forms between two hydrophobic surfaces and breakage of the water thin film and subsequent collapse happen at much smaller separation distances.[75,76] This ambiguous underlying origin of hydrophobic interaction prohibits devising a force law from the first principles. However, most of the experimental data can be fitted and justified with exponential form with decay length between 10 and 3 Å.[48]

Depletion forces

A solute distributes homogenously throughout the media for the sake of minimizing the free energy of the system. However, if for any reason the solute '*depletes*' from a region in the system, an osmotic pressure builds up. Recalling the equation (1.21) to (1.23) and assuming the

electrostatic potential is constant, one finds the osmotic pressure in the depletion zone follows the gas law:

$$\Pi_{osmotic} = -c_{bulk} kT \tag{1.58}$$

The origin of the depletion of the solute from a particular zone can be different. For two interacting interfaces in media containing hard-sphere solutes with radius of *r*, the center of the solutes cannot occupy a space adjacent to the interfaces known as excluded volume. (Figure 7) When the separation distance of the two interfaces become smaller than *2r*, all the solutes expel from the gallery and a negative osmotic pressure builds up. This leads to an attraction between the two interfaces. The attractive energy at $h \geq 2r$ is zero and reaches to its maximum value at the contact. From the relation of surface pressure to surface energy one finds:[2]

$$W_{depletion}(h) = \int_{h}^{2r} \Pi_{osmotic} dh = -c_{bulk} kT(2r - h) \tag{1.59}$$

The depletion force between two large spheres with radius of *R*, $R >> r$, can be then obtained from the Derjaguin approximation as follow:

$$F(h) = \pi R W_{depletion}(h) = -\pi c_{bulk} kTR(2r - h) \tag{1.60}$$

This relation states that the depletion forces scale the separation distance linearly and reach to a maximum value of $2\pi rR \times \Pi_{osmotic}$ at contact.

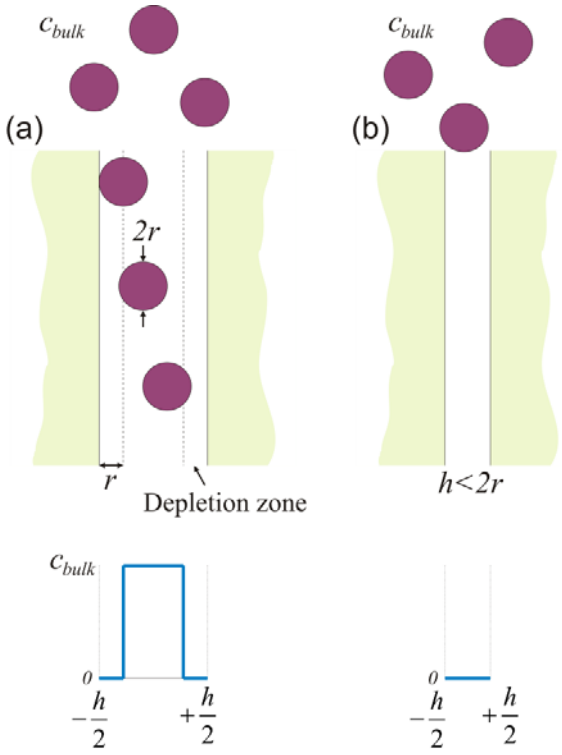

Figure 7. *Depletion attraction: presence of non-adsorbing particles, i.e. hard-sphere depletant, in solution induces an attractive force between interfaces. (a) The center of the depletant cannot explore the depletion zone where the concentration of the depletant is zero (bottom). (b) When separation distance becomes smaller than the diameter of the depletant, h<2r, the concentration of the depletant drops to zero (bottom) and an osmotic pressure builds up which leads to an attractive force.*

Above argument was first made by Asakura and Oosawa.[77] It was proposed that in a mixture of colloidal particles and non-adsorbing polymers (depletant), there is attractive depletion forces acting between the particles. For a neutral polymer, the size of the polymer coil can be approximated with radius of gyration, R_g. Therefore, the *range* of the depletion forces is dominated by the size of polymers and as a result molecular mass. However, the *magnitude* of the depletion forces is the product of the size and osmotic pressure of the polymer solution. For dilute polymer solutions $\Pi_{osmotic} \sim M_n^{-1}$ and as $R_g \sim M_n^{0.5}$ for theta solvent, then $F_{depletion} \sim M_n^{-0.5}$.[65]

Therefore, increasing the range of the depletion forces is at the expense of weakening them.[2] So, depletion forces in the case of neutral polymers whether are short-ranged and interfere with other forces such as vdW or long-ranged but weak and irrelevant.

The above formulation is valid for the case where the interaction between the depletant and the interface follows hard-core interaction. However, when the interfaces and depletant are similarly charged the double layer forces significantly increase the depletion range. This situation is very common in solutions containing polyelectrolytes, micelles and nanoparticles.[78] Indeed, when two charged interfaces approach, the like-charged species in solution are expelled from the interspace due to the double layer repulsion. The length scale, at which the exclusion of the charged species occurs, depends very much on the range of the electrostatic forces.[79] Therefore, the range of depletion forces in these cases can be much larger than the depletants' size. In addition, as charged depletants carry ionic groups, their exclusion from the interspace also imposes an enhanced osmotic pressure due to the imbalance of counter and co-ions in- and outside of the depletion zone. Therefore, both range and magnitude of depletion forces in these systems are larger compared to the systems involving neutral interfaces and depletants. This facilitates the detection of depletion forces in these systems using direct force measurements. Furthermore, both range and magnitude of the depletion forces is sensitive to the presence of salt.

If one considers the hard-sphere case again (Figure 7), then the local concentration of the spheres are related to probability of finding the center of the sphere at the given position. Next to the interfaces, the concentration is zero due to the impermeability of the hard-sphere and the interface, *i.e.* hard-core interaction. Above arguments imply that the concentration reaches to the bulk concentration beyond the depletion zone. However, the spheres themselves also interact through hard-core interaction and at high concentration of the spheres the concentration gradient

does not follow a simple step function.[79] If the sphere concentration is close to dense packing condition, at the distance *r* from the interface the concentration should peak and then decrease and again peak at distance *3r*.(Figure 8a)[2] This implies the spheres are correlated and resembles the liquid-like ordering. This fluctuation in local concentration directly affect the depletion forces and as $F_{depletion} \sim c(h) - c_{bulk}$, depletion forces follows the concentration fluctuation. When two interfaces approach, at separation distances close to the size of the spheres, the concentration of the sphere in the interspace increases and decreases compared to the bulk concentration. This leads to repulsive and attractive depletion forces which appear in the form of decaying oscillatory forces.[2] (Figure 8b) These types of forces can be mathematically modeled at large distances with an exponentially damped cosine function as follows:

$$F(h) \propto e^{-\frac{h}{\xi}} \cos(\frac{2\pi h}{\lambda} + \theta) \tag{1.61}$$

Where ξ represents the correlation length, λ the wavelength of oscillation and θ the phase of oscillation. This type of force has been theoretically predicted and experimentally observed for many different liquids as separation distance close to the molecular sizes. As the origin of this force is related to correlation and ordering of the spheres, it is known as '*structural forces*'.

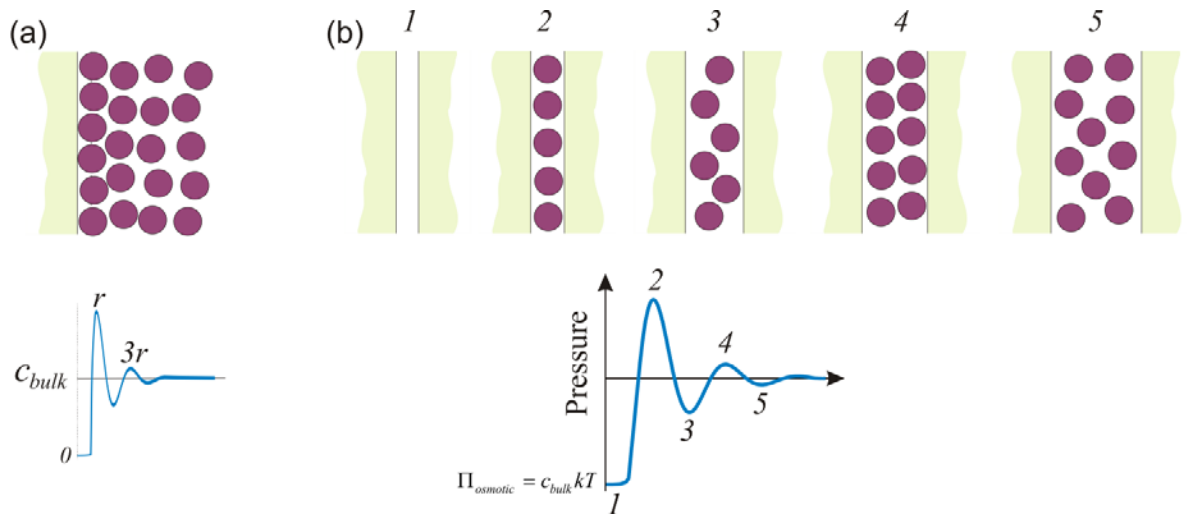

Figure 8. *(a) Structuring of the hard spheres next to a wall and corresponding concentration profile (bottom). (b) Schematic representing depletants structuring and corresponding surface pressure (bottom). The pressure at zero distance recovers the osmotic pressure of the bulk.*

In the cases where the depletants are charged, the probability of finding a depletant adjacent to another one is suppressed significantly due to electrostatic repulsion. This repulsion among the charged depletants leads to strong correlation, as well. Therefore, structural forces are often observed between charged interfaces interacting through medium containing like-charged depletants. Due to the long ranged electrostatic interaction, these structural forces can be detected at low concentration of depletant compared to the one for hard spheres.[78,79] This can be intuitively understood by considering an electrical double layer around depletant which increase their effective volume.

1.6- Colloidal probe AFM

Direct measurement of surface forces allows us to seek for factors affect these forces and also new types of interactions between the interfaces.[24] That is why many efforts were performed to measure the predicted DLVO and non-DLVO forces. Preliminary works however were focused

on measuring forces among the macroscopic surfaces such as glass and mica, mainly due to the technological barrier.[16,18-20,72] Even though these studies experimentally proved many fundamentals of surface forces and shed the lights on new intermolecular forces, the direct measurement of forces between macro and nanoscopic colloidal particles remained challenging. Introduction of atomic force microscopy (AFM) at 1986 opened new vista for measuring various types of forces between almost any types of interfaces.[80] The force measurement in AFM relies on monitoring the elastic deformation of a cantilever. This enables measuring forces lower than pico-newton.[80] The breakthrough in measurement of colloidal forces arrived five years later when two independent research teams extended the AFM technique to force measurement between a micron-sized particle, attached to end of the AFM cantilever, and a substrate in aqueous media.[21,22] This technique allows studying forces among various types of particulate synthesis and natural materials such as polymeric particles, minerals, micro and nano fibers, cells, *etc*.[24] These studies can be done in different media such as water, organic solvents, polymer solutions and melts, and molten salts.

The AFM is composed of piezo-driven cantilever, which its deflection is monitored by reflection of a laser beam from the back of cantilever to a photodiode. (Figure 9a) The position of the probe can be controlled using a scanner which enables to scan all three special directions with precision better than Angstrom.[24] For direct force measurement purpose, the probe explores the vertical direction at fixed point at a certain velocity (normally fraction of micron per second). By the aid of the piezo actuator, the probe approaches to the target surface and deflection of the cantilever is recorded at the same time. Once the probe gets close to the surface, the surface forces deflect the cantilever and eventually touch the surface. At a certain deflection, the probe is withdrawn from

the surface. The approach and retract process is repeated several times to acquire the force curves.[81]

The output of the above procedure is piezo displacement, Z_p, *versus* the signal from the photodiode, *S*. (Figure 9b) This raw data should be converted to surface forces *versus* separation distance. As mentioned earlier, a laser beam is emitted to the back of the cantilever which is then reflected to the middle of a split diode. Emission of the laser beam to the diode generates a photocurrent and the signal from the photodiode is related to the potential difference of the top and the bottom of the slit diode.[24] Therefore, the unit of the signal is in volt. If the cantilever deflects, the position of reflected beam changes and the amount of the photons received by the top and the bottom part of the diodes changes as well, which in turn alters the signal value. For the deflection much smaller than the length of the cantilever, the changes in signal are proportional to the cantilever deflection, Z_c.

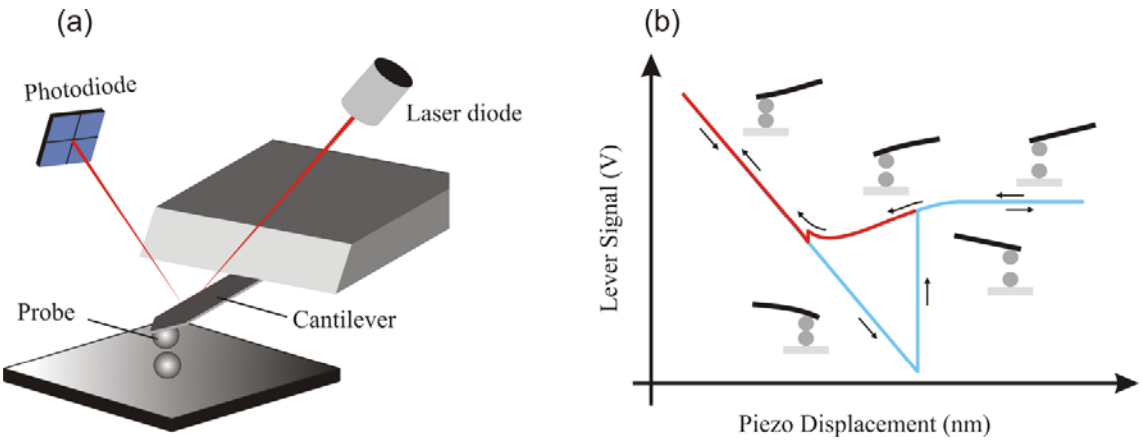

Figure 9. *Scheme of (a) an AFM instrument and (b) a typical output of the force measurement experiment.*

Now, let's consider that the probe is approaching to a hard surface without any specific interaction. Before contact, the signal stays constant, $S=S_0$. However, once the probe touches the surface, the cantilever starts to deflect and the deflection is the same as the piezo displacement.

This part of the force curve is also known as *constant compliance region*.[24] Therefore, Z_p and S are linearly related:

$$S = a \cdot Z_p + b \tag{1.62}$$

By fitting the line to constant compliance region, one can obtain the parameters a and b. The inverse of the slope, a^{-1}, is known as the optical lever sensitivity. Form above relation, one can find the position at which probe touches the surface, *i.e.* contact point:

$$Z_{p0} = \frac{S_0 - b}{a} \tag{1.63}$$

This method determines the contact point with precision of few Angstroms. Once the contact point position is known, the separation distance can be obtained from:

$$h = Z_p - Z_{p0} \tag{1.64}$$

This relation is valid before the contact point and $h=0$ for displacements larger than Z_{p0}. To construct the force curve, one needs to find the cantilever deflection. The Z_c in constant compliance region, $Z_p < Z_{p0}$, is equal to changes of the piezo displacement due to the hard contact, thus:

$$Z_c = Z_p - Z_{p0} = \frac{S - S_0}{a} \tag{1.65}$$

Now, the force can be calculated using Hook's law:

$$F = k \cdot Z_c \tag{1.66}$$

Where k is spring constant of the cantilever. The spring constant of cantilever depends on the size of the lever and also mechanical properties of the materials that the lever is made of.[82] The typical spring constants of AFM cantilevers are in the range of 0.1-10 N/m. Given the deflection of the cantilever can be measured with precision better than one Angstrom, the force resolution of 1-10 pN can be obtained.

In the cases where the surface forces are present, the equation (1.65) is still applicable to derive the cantilever deflection. However, the separation distance should be modified by the deflection of the cantilever:

$$h = Z_c + h_0 = Z_c + Z_p - Z_{p0} \tag{1.67}$$

The results of above mathematical procedure can be seen in Figure 10. In should be noted that the constant compliance region is sometimes hard to determine, especially in the cases of the repulsive forces.[83] (Figure 10b) In the case of the attractive forces, it is possible that the cantilever experience a mechanical instability. In fact, at any equilibrium distance of h, the cantilever bends in a way to satisfies Hook's law. However, if the second gradient of total energy applied on the cantilever becomes negative, then the instability occurs.[24] Form this criterion one fins that the cantilever becomes unstable if:

$$\frac{dF}{dh} > k \tag{1.68}$$

As the probe approaches to the surface by Δh, then applied force on the probe become ΔF larger. Therefore, the probe should bend $\frac{\Delta F}{k}$ more, which if equation (1.68) holds, is larger than Δh. Extra bending in an attractive force field means more forces on the probe and thus the probe

continues to bend till reach to the contact (jump-into-contact) or reach to a point in energy potential where equation (1.68) does not hold any more. This phenomenon is schematically shown in Figure 10d. Existence of the jump into contact in force curves indicates the presence of the strong attractive forces. This problem can be avoided using stiffer cantilever, however, at the expense of losing the force resolution.

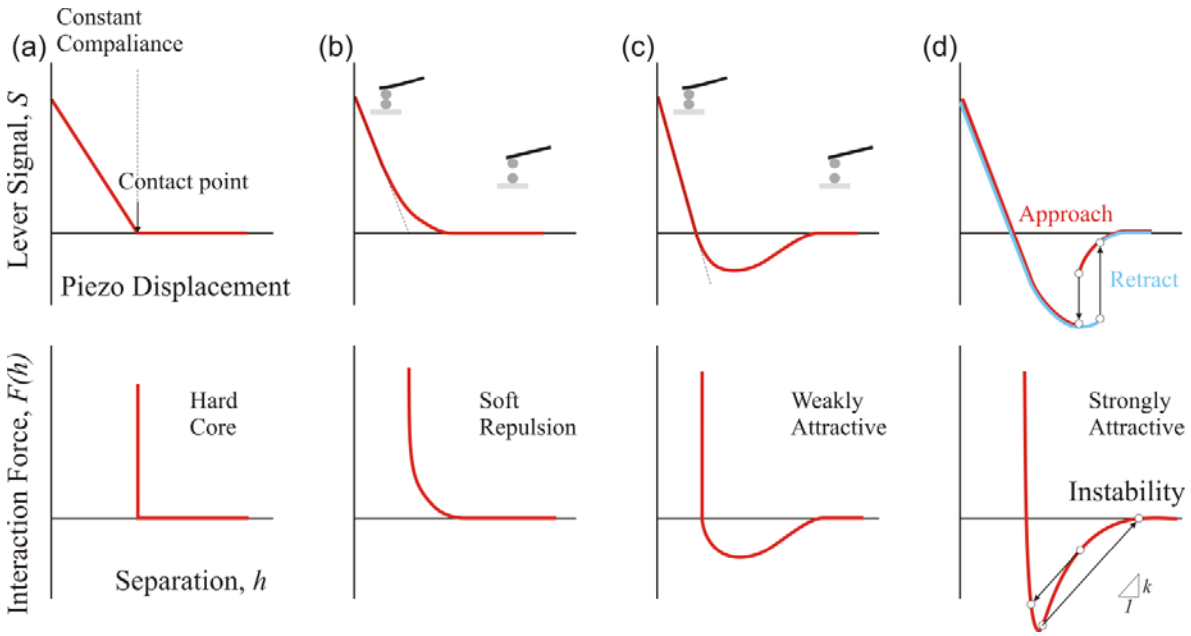

Figure 10. *Response of the probe to the different forces (top row) and their conversion to force-distance curves (bottom row). Different types of interaction are presented: (a) Hard core, (b) soft repulsion, (c) weak attraction and (d) strong attraction.*[83]

The force measurement using AFM is limited by force resolution. As stated before, the force resolution of standard AFM is limited to 1-10 pN. Whether this resolution is enough to resolve the common surface forces depends on the strength of these interactions at relevant distances. The Derjagiun approximation states the surface forces depend on the size of probe and surface energy of the interaction, $F(h) = 2\pi R_{eff} W(h)$. Thus, for the weak interactions such as vdW or depletion interactions the size of probe should be large enough to enable AFM detecting the

interaction. For instance, if the Hamaker constant between a spherical probe and the substrate is 6×10^{-21} J, then in order to detect the vdW forces at separation distances of 10 nm or smaller, the radius of the probe should be larger than 0.1-1 μm (For force resolution of 1-10 pN). The same analysis for depletion forces demonstrates that the size of the probe should be larger than 2 μm in order to detect depletion attraction between the probe and the substrate interacting through a solution containing 1 vol% of 20 nm large non-adsorbing spherical depletant (equation (1.61)). This simple analysis suggests that using micron size probe is ideal to study even very weak surface forces. Therefore, it becomes a common practice to attach large colloidal particles to tip of AFM cantilevers and uses it for force measurements. Employing large particles as probe also has an advantage that the particles can be easily detected using optical microscope which in turn makes it possible to track the position of the probe under the microscope. In addition, wide range of colloidal particles with different sizes and chemistries can be used as a probe. (Figure 11)

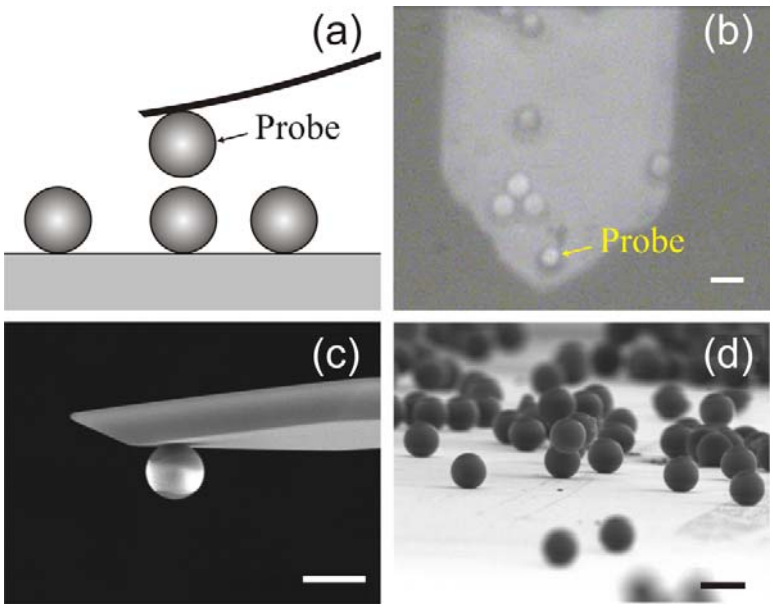

Figure 11. *Colloidal probe AFM: (a) Scheme of direct force measurement between two colloidal particles. (b) Optical micrograph of the polystyrene latex particles, 3.1 μm in diameter, coated on a glass slide. A tip-less AFM*

cantilever is pressed against an individual particle to pick it up as the probe. (c, d) Scanning electron micrographs of silica particles (c) attached to the end of a tip-less cantilever, (d) coated on a quartz slide. Scale bars in (b-d) are 5 μm. [c,d are reproduce with permission from ref. 83-Published by The Royal Society of Chemistry][84]

1.7- Outline of thesis

In this part, I briefly present the subjects of studies in my PhD thesis, the motivation behind the studies and the main finding of this research. The research deals with direct force measurement between different interfaces in the presence of organic multivalent ions and polyelectrolytes.

In the second chapter,[85] surface forces between negatively charged sulfate latex (SL) particles studies in the presence of aliphatic oligoamines as well as a simple monovalent salt, *i.e.* KCl. The central finding of this part is that the DLVO theory is able to interpret the force curves at large distance, > 7 nm, provided that an effective surface potential is assigned to the interface. However, there are ever-present short-ranged attractive force(s) in the presence all investigated electrolytes. Studies of surface potential of the interface show that the counter-ions tend to adsorb to the surface and this tendency strongly depends on the valences of the counter-ions. In the case of tri- and tetra-valent ions, this adsorbtion eventually leads to the charge inversion. On the other hand, the so-called short-ranged attractive forces can be fitted with a single exponential function but with different range and magnitude which also depend on the valency of the counter-ions. This observation leads us to believe the nature and origin of these forces are also different for monovalent and multivalent ions. In the case of monovalent ions, the range of the non-DLVO forces is about 0.3 nm and the magnitude of the forces monotonically decreases by addition of salt. But, in the case of multivalent oligoamines the additional attractive forces are more long ranged with decay length of about 1.0 nm. In addition, the magnitude of the forces peaks at

intermediate concentration of multivalent ions and eventually vanishes at very high ionic strengths. It is also found the higher the valance is, the stronger these forces are.

In third chapter,[86] the study of the surface forces between dissimilar interfaces in the presence of an organic multivalent ion is presented. Oppositely charged SL and amidine latex (AL) particles were used to evaluate the impact of an aliphatic hexamine (N6) (the largest member of amines studies in the previous chapter) on the surface forces. N6 is expected to strongly adsorb to the SL particles but not to the AL particles. Therefore, a rich gallery of forces is anticipated as the AL particles always stay positively charged but the SL particles are negatively charged or neutral or positively charged depending on the dose of N6 in solution. Forces in three different fashions namely AL-AL, SL-SL (symmetric) and AL-SL (asymmetric) were measured. At large distances the forces curve can be interpreted using the DLVO, provided the double layer forces are derived at full Poisson-Boltzmann (PB) level. In the case of asymmetric measurements, the charge regulation of the SL particles plays a key role, especially close to charge reversal point. An interesting outcome of studies of forces at shorter distances is that non-DLVO forces are present in all three sets of measurements. The range and the magnitude of the non-DLVO forces for asymmetric cases are found to be close to the harmonic means of those for symmetric cases.

The origin of these non-DLVO interactions remains elusive to us, especially in the cases of multivalent counter-ions. Theoretical studies since 80's have proposed the presence additional attractive forces between interfaces interacting in solutions of the multivalent ions due to strong ion-ion correlations between multivalent ions themselves and with interface.[87] Our finding that these interactions become stronger as the valence of ions increases is consistent with explanations based on ion-ion correlation.[88,89] However, a direct correlation between the multivalent ions concentration and magnitude of the ion-ion correlation interaction is usually predicted which is

not consistent with experimental observation is this work. In addition, predicting the net charge of interface in the presence of multivalent counter-ions is theoretically challenging as chemical interactions of ions with interface play a key role as well as electrostatic interactions.[39] Similar argument can be valid for other types of interactions such as attraction induced by surface charge heterogeneities,[90] hydrophobic forces,[48] charge fluctuation[91] or electrolyte depletion.[50] For instance, attraction induced by electrolyte depletion again predicts a monotonic increase in magnitude of attractive forces by increasing the electrolyte concentration.[50] Combination of two or more of these forces and possibly others may control the non-DLVO forces at different ranges of ion concentration.

Above studies showed the double layer forces in the presence of the multivalent ions do not follow the DH approximation and PB theory needs to be considered. This becomes crucial in the cases where multivalent ions act as co-ion, whether due to overcharging or intrinsic charge of the interface. These observations were generic for other multivalent ions as well. That is why the chapter four[92] is devoted to this issue. In agreement with PB theory, it is found that the double layer forces in the presence of multivalent co-ions are not exponential. This deviation is assigned to exclusion of the multivalent co-ions from the interspace of interacting surfaces at a critical distance. After depletion of the co-ions, the behavior of double layer forces becomes identical to counter-ion only double layer. This is a general feature for highly charged co-ions and is found to be independent of the chemistry of the surface and ions.

The depletion of highly charged ions from the gallery of like-charged interfaces resembles to depletion of particles and polymers from the interface of similarly charged surfaces. Does this picture hold in the case of highly asymmetric ions such as polyelectrolytes? This question is answered in the chapter five[93] of this thesis. The surface forces between negatively charged silica

particles in solution of a like-charge polyelectrolyte are studied using colloidal probe AFM. Indeed, this study confirms the double layer forces in the presence of like-charge polyelectrolytes can be described using PB theory provided that polyelectrolytes are treated as highly asymmetric ions. This leads to highly non-exponential double layer forces. The assigned valence to polyelectrolyte molecules is always smaller than nominal charge of polymer which can be adequately explained using ion condensation theory. At large distances, structuring of the polyelectrolytes molecules in bulk generates oscillatory depletion forces. It is shown that the onset of these oscillatory forces is in fact the distance that the polyelectrolyte molecules deplete due to the electrostatic repulsion. The PB theory predicts the depletion thickness satisfactory well which in turn leads to acceptable prediction of phase of the oscillation.

In chapter six,[94] the interplay of double layer and depletion forces in the presence of like-charge polyelectrolytes and its mixtures with monovalent salt is studied in more details. The factors controlling the oscillatory forces are clarified. The validity of PB theory for prediction of double layer forces in mixtures highly asymmetric and monovalent electrolytes is checked with extensive direct force measurements. The findings on the dependence of the effective charge of polyelectrolyte molecules on the salt level and the molecular mass agree well with theoretical predictions and other experimentations in literature. An interesting observation in this study is adsorbtion of polyelectrolytes to the like-charged interfaces at intermediate salt and polymer concentrations. It is found that at the certain concentration of ions, polymer segments can overcome the electrostatic barrier to adsorb on the similarly charged interfaces.

1.8- References

1. Parry, R. Empedocles. https://plato.stanford.edu/archives/fall2016/entries/empedocles/
2. Israelachvili, J., *Intermolecular and Surface Forces*. 3 ed.; Academic Press: London, 2011.
3. Vincent, B., *Early (pre-DLVO) studies of particle aggregation*. *Adv. Colloid Interface Sci.* **2012**, 170, 56-67.
4. Hauser, E. A., *The history of colloid science: In memory of Wolfgang Ostwald. J. Chem. Educ.* **1955**, 32, 2.
5. van der Waals, J. D. Nobel Lecture: The equation of state for gases and liquids. http://www.nobelprize.org/nobel_prizes/physics/laureates/1910/waals-lecture.html
6. London, F., *The general theory of molecular forces*. *Trans. Fadad. Soc.* **1937**, 33, 8b-26.
7. Kallmann, H.; Willstaetter, M., *Zur theorie des aufbaues kolloidaler systeme*. *Naturwissenschaften* **1932**, 20, 952-953.
8. Hamaker, H. C., *The London—van der Waals attraction between spherical particles*. *Physica* **1937**, 4, 1058-1072.
9. Langmuir, I., *The role of attractive and repulsive forces in the formation of tactoids, thixotropic gels, protein crystals and coacervates*. *The Journal of Chemical Physics* **1938**, 6, 873-896.
10. Freundlich, H., *The colloidal state: Thixotropy*. Hermann et Cie: Paris, 1935.
11. Verwey, E. J. W.; Overbeek, J. T. G., *Theory of Stability of Lyophobic Colloids*. Elsevier: Amsterdam, 1948.
12. Derjaguin, B., *A theory of interaction of particles in presence of electric double-layers and the stability of lyophobe colloids and disperse systems*. *Acta Phys. Chim.* **1939**, 10, 333-346.
13. Derjaguin, B.; Landau, L. D., *Theory of the stability of strongly charged lyophobic sols and of the adhesion of strongly charged particles in solutions of electrolytes*. *Acta Phys. Chim.* **1941**, 14, 633-662.
14. Lifshitz, E., *The theory of molecular attractive forces between solids*. **1956**.
15. Dzyaloshinskii, I. E. e.; Lifshitz, E.; Pitaevskii, L. P., *General theory of van der Waals' forces*. *Physics-Uspekhi* **1961**, 4, 153-176.
16. Overbeek, J. T. G.; Sparnaay, M. J., *Experiments on long-range attractive forces between macroscopic objects*. *J. Colloid Sci.* **1952**, 7, 343-345.
17. Overbeek, J. T. G.; Sparnaay, M. J., *Classical coagulation. London-van der Waals attraction between macroscopic objects*. *Discuss. Faraday Soc.* **1954**, 18, 12-24.
18. Derjaguin, B. V.; Titijevskaia, A. S.; Abricossova, I. I.; Malkina, A. D., *Investigations of the forces of interaction of surfaces in different media and their application to the problem of colloid stability*. *Discuss. Faraday Soc.* **1954**, 18, 24-41.
19. Tabor, D.; Winterton, R. H. S., *Surface forces: Direct measurement of normal and retarded van der Waals forces*. *Nature* **1968**, 219, 1120-1121.
20. Israelachvili, J. N.; Tabor, D., *The measurement of van der Waals dispersion forces in the range 1.5 to 130 nm*. *Proceedings of the Royal Society of London. A. Mathematical and Physical Sciences* **1972**, 331, 19-38.

21. Ducker, W. A.; Senden, T. J.; Pashley, R. M., *Direct measurement of colloidal forces using an atomic force microscope*. *Nature* **1991**, 353, 239-241.

22. Butt, H. J., *Measuring electrostatic, van der Waals, and hydration forces in electrolyte solutions with an atomic force microscope*. *Biophys. J.* **1991**, 60, 1438-1444.

23. Prieve, D. C.; Alexander, B. M., *Hydrodynamic measurement of double-Layer repulsion between colloidal particle and flat plate*. *Science* **1986**, 231, 1269-1270.

24. Butt, H. J.; Cappella, B.; Kappl, M., *Force measurements with the atomic force microscope: Technique, interpretation and applications*. *Surf. Sci. Rep.* **2005**, 59, 1-152.

25. Trefalt, G.; Palberg, T.; Borkovec, M., *Forces between colloidal particles in aqueous solutions containing monovalent and multivalent ions*. *Current Opinion In Colloid & Interface Science* **2017**, 27, 9-17.

26. Carnie, S. L.; Chan, D. Y. C., *Interaction free energy between plates with charge regulation: A linearized model*. *J. Colloid Interface Sci.* **1993**, 161, 260-264.

27. Pericet-Camara, R.; Papastavrou, G.; Behrens, S. H.; Borkovec, M., *Interaction between charged surfaces on the Poisson-Boltzmann level: The constant regulation approximation*. *J. Phys. Chem. B* **2004**, 108, 19467-19475.

28. Borkovec, M.; Behrens, S. H., *Electrostatic double layer forces in the case of extreme charge regulation*. *J. Phys. Chem. B* **2008**, 112, 10795-10799.

29. Trefalt, G.; Behrens, S. H.; Borkovec, M., *Charge regulation in the electrical double layer: Ion adsorption and surface interactions*. *Langmuir* **2016**, 32, 380-400.

30. Chan, D.; Healy, T. W.; White, L. R., *Electrical double layer interactions under regulation by surface ionization equilibria-dissimilar amphoteric surfaces*. *Journal of the Chemical Society, Faraday Transactions 1: Physical Chemistry in Condensed Phases* **1976**, 72, 2844-2865.

31. Valmacco, V.; Elzbieciak-Wodka, M.; Herman, D.; Trefalt, G.; Maroni, P.; Borkovec, M., *Forces between silica particles in the presence of multivalent cations*. *J. Colloid Interface Sci.* **2016**, 472, 108-115.

32. Zhao, C.; Ebeling, D.; Siretanu, I.; van den Ende, D.; Mugele, F., *Extracting local surface charges and charge regulation behavior from atomic force microscopy measurements at heterogeneous solid-electrolyte interfaces*. *Nanoscale* **2015**, 7, 16298-16311.

33. Brown, M. A.; Abbas, Z.; Kleibert, A.; Green, R. G.; Goel, A.; May, S.; Squires, T. M., *Determination of surface potential and electrical double-layer structure at the aqueous electrolyte-nanoparticle interface*. *Physical Review X* **2016**, 6, 011007.

34. Popa, I.; Sinha, P.; Finessi, M.; Maroni, P.; Papastavrou, G.; Borkovec, M., *Importance of charge regulation in attractive double-layer forces between dissimilar surfaces*. *Phys. Rev. Lett.* **2010**, 104, 228301.

35. Boroudjerdi, H.; Kim, Y. W.; Naji, A.; Netz, R. R.; Schlagberger, X.; Serr, A., *Statics and dynamics of strongly charged soft matter*. *Physics Reports* **2005**, 416, 129-199.

36. Dan, B.-Y.; David, A.; Daniel, H.; Rudi, P., *Beyond standard Poisson–Boltzmann theory: ion-specific interactions in aqueous solutions*. *J. Phys. Condens. Matter* **2009**, 21, 424106.

37. Schulze, H., *Schwefelarsen in wässriger Lösung*. *J. Prakt. Chem.* **1882**, 25, 431-452.

38. Hardy, W. B., *A preliminary investigation of the conditions which determine the stability of irreversible hydrosols*. *Proc. Roy. Soc. London* **1900**, 66, 110-125.

39. Grosberg, A. Y.; Nguyen, T. T.; Shklovskii, B. I., *Colloquium: The physics of charge inversion in chemical and biological systems*. *Rev. Mod. Phys.* **2002**, 74, 329-345.

40. Matijevic, E.; Broadhurst, D.; Kerker, M., *On coagulation effects of highly charged counterions*. *J. Phys. Chem.* **1959**, 63, 1552-1557.

41. Spalla, O.; Belloni, L., *Long range electrostatic attraction between neutral surfaces*. *Phys. Rev. Lett.* **1995**, 74, 2515-2518.

42. Podgornik, R., *Electrostatic correlation forces between surfaces with surface specific ionic interactions*. *The Journal of Chemical Physics* **1989**, 91, 5840-5849.

43. Yan, L., *Electrostatic correlations: from plasma to biology*. *Rep. Prog. Phys.* **2002**, 65, 1577.

44. Besteman, K.; Zevenbergen, M. A. G.; Lemay, S. G., *Charge inversion by multivalent ions: Dependence on dielectric constant and surface-charge density*. *Phys. Rev. E* **2005**, 72, 061501.

45. Zohar, O.; Leizerson, I.; Sivan, U., *Short range attraction between two similarly charged silica surfaces*. *Phys. Rev. Lett.* **2006**, 96, 177802.

46. Sinha, P.; Szilagyi, I.; Montes Ruiz-Cabello, F. J.; Maroni, P.; Borkovec, M., *Attractive forces between charged colloidal particles induced by multivalent ions revealed by confronting aggregation and direct force measurements*. *The Journal of Physical Chemistry Letters* **2013**, 4, 648-652.

47. Adar, R. M.; Andelman, D.; Diamant, H., *Electrostatics of patchy surfaces*. *Adv. Colloid Interface Sci.* **2017**.

48. Donaldson, S. H.; Royne, A.; Kristiansen, K.; Rapp, M. V.; Das, S.; Gebbie, M. A.; Lee, D. W.; Stock, P.; Valtiner, M.; Israelachvili, J., *Developing a general interaction potential for hydrophobic and hydrophilic interactions*. *Langmuir* **2015**, 31, 2051-2064.

49. Adžić, N.; Podgornik, R., *Field-theoretic description of charge regulation interaction*. *The European Physical Journal E* **2014**, 37, 49.

50. Curtis, R. A.; Lue, L., *Depletion forces due to image charges near dielectric discontinuities*. *Current Opinion In Colloid & Interface Science* **2015**, 20, 19-23.

51. Kunz, W.; Lo Nostro, P.; Ninham, B. W., *The present state of affairs with Hofmeister effects*. *Current Opinion In Colloid & Interface Science* **2004**, 9, 1-18.

52. Szilágyi, I.; Trefalt, G.; Tiraferri, A.; Maroni, P.; Borkovec, M., *Polyelectrolyte adsorption, interparticle forces, and colloidal aggregation*. *Soft Matter* **2014**, 10, 2479-2502.

53. Dobrynin, A. V.; Rubinstein, M., *Theory of polyelectrolytes in solutions and at surfaces*. *Prog. Polym. Sci.* **2005**, 30, 1049-1118.

54. Decher, G., *Fuzzy Nanoassemblies: Toward Layered Polymeric Multicomposites*. *Science* **1997**, 277, 1232-1237.

55. Richardson, J. J.; Björnmalm, M.; Caruso, F., *Technology-driven layer-by-layer assembly of nanofilms*. *Science* **2015**, 348.

56. Elimelech, M.; Gregory, J.; Jia, X.; Williams, R. A., *Particle Deposition and Aggregation: Measurement, Modeling, and Simulation*. Butterworth-Heinemann Ltd.: Oxford, 1995.

57. Popa, I. Surface interactions induced by polyelectrolytes, dendrimers, and dendronized polymers. University of Geneva, 2010.

58. Tadmor, R.; Hernandez-Zapata, E.; Chen, N.; Pincus, P.; Israelachvili, J. N., *Debye length and double-layer forces in polyelectrolyte solutions*. *Macromolecules* **2002**, 35, 2380-2388.

59. Pashley, R. M.; Ninham, B. W., *Double-layer forces in ionic micellar solutions*. *J. Phys. Chem.* **1987**, 91, 2902-2904.

60. Tang, K.-T.; Toennies, J. P., *Johannes Diderik van der Waals: A pioneer in the molecular sciences and Nobel Prize winner in 1910*. *Angewandte Chemie International Edition* **2010**, 49, 9574-9579.

61. Rodriguez, A. W.; Capasso, F.; Johnson, S. G., *The Casimir effect in microstructured geometries*. *Nat Photon* **2011**, 5, 211-221.

62. Parsegian, V. A., *Van der Waals forces*. Cambridge University Press: New York, 2006.

63. De Rocco, A. G.; Hoover, W. G., *On the interaction of colloidal particles*. *Proceedings of the National Academy of Sciences* **1960**, 46, 1057-1065.

64. Casimir, H. B. G.; Polder, D., *The influence of retardation on the London-van der Waals forces*. *Phys. Rev.* **1948**, 73, 360-372.

65. Russel, W. B.; Saville, D. A.; Schowalter, W. R., *Colloidal Dispersions*. Cambridge University Press: Cambridge, 1989.

66. Petrache, H. I.; Zemb, T.; Belloni, L.; Parsegian, V. A., *Salt screening and specific ion adsorption determine neutral-lipid membrane interactions*. *Proc. Natl. Acad. Sci. U. S. A.* **2006**, 103, 7982-7987.

67. Hamaker, H. C., *A general theory of lyophobic colloïds. I. Recueil des Travaux Chimiques des Pays-Bas* **1936**, 55, 1015-1026.

68. Von Smoluchowski, M., *Drei vortrage uber diffusion. Brownsche bewegung und koagulation von kolloidteilchen*. *Z. Phys.* **1916**, 17, 557-585.

69. Meyer, E. E.; Lin, Q.; Hassenkam, T.; Oroudjev, E.; Israelachvili, J. N., *Origin of the long-range attraction between surfactant-coated surfaces*. *Proc. Natl. Acad. Sci. U. S. A.* **2005**, 102, 6839-6842.

70. Chandler, D., *Interfaces and the driving force of hydrophobic assembly*. *Nature* **2005**, 437, 640-647.

71. Huang, X.; Margulis, C. J.; Berne, B. J., *Dewetting-induced collapse of hydrophobic particles*. *Proc. Natl. Acad. Sci. U. S. A.* **2003**, 100, 11953-11958.

72. Israelachvili, J.; Pashley, R., *The hydrophobic interaction is long-range decaying exponentially with distance*. *Nature* **1982**, 300, 341-342.

73. Tyrrell, J. W.; Attard, P., *Images of nanobubbles on hydrophobic surfaces and their interactions*. *Phys. Rev. Lett.* **2001**, 87, 176104.

74. Meyer, E. E.; Rosenberg, K. J.; Israelachvili, J., *Recent progress in understanding hydrophobic interactions*. *Proc. Natl. Acad. Sci. U. S. A.* **2006**, 103, 15739-15746.

75. Remsing, R. C.; Xi, E.; Vembanur, S.; Sharma, S.; Debenedetti, P. G.; Garde, S.; Patel, A. J., *Pathways to dewetting in hydrophobic confinement*. *Proceedings of the National Academy of Sciences* **2015**, 112, 8181-8186.

76. Kanduč, M.; Schlaich, A.; Schneck, E.; Netz, R. R., *Water-mediated interactions between hydrophilic and hydrophobic surfaces*. *Langmuir* **2016**, 32, 8767-8782.

77. Asakura, S.; Oosawa, F., *On interaction between two bodies immersed in a solution of macromolecules*. *J. Chem. Phys.* **1954**, 22, 1255-1256.

78. Ji, S.; Walz, J. Y., *Depletion forces and flocculation with surfactants, polymers and particles — Synergistic effects*. *Current Opinion In Colloid & Interface Science* **2015**, 20, 39-45.

79. Kralchevsky, P. A.; Danov, K. D.; Anachkov, S. E., *Depletion forces in thin liquid films due to nonionic and ionic surfactant micelles*. *Current Opinion In Colloid & Interface Science* **2015**, 20, 11-18.

80. Binnig, G.; Quate, C. F.; Gerber, C., *Atomic force microscope*. *Phys. Rev. Lett.* **1986**, 56, 930.

81. Borkovec, M.; Szilagyi, I.; Popa, I.; Finessi, M.; Sinha, P.; Maroni, P.; Papastavrou, G., *Investigating forces between charged particles in the presence of oppositely charged polyelectrolytes with the multi-particle colloidal probe technique*. *Adv. Colloid Interface Sci.* **2012**, 179-182, 85-98.

82. Sader, J. E.; Chon, J. W. M.; Mulvaney, P., *Calibration of rectangular atomic force microscope cantilevers*. *Rev. Sci. Instrum.* **1999**, 70, 3967-3969.

83. Borkovec, M., Advanced analytical and instrumental chemistry I: Colloidal probe technique and surface forces. In University of Geneva: Geneva, 2016.

84. Valmacco, V.; Elzbieciak-Wodka, M.; Besnard, C.; Maroni, P.; Trefalt, G.; Borkovec, M., *Dispersion forces acting between silica particles across water: influence of nanoscale roughness*. *Nanoscale Horizons* **2016**, 1, 325-330.

85. Moazzami-Gudarzi, M.; Trefalt, G.; Szilagyi, I.; Maroni, P.; Borkovec, M., *Forces between negatively charged interfaces in the presence of cationic multivalent oligoamines measured with the atomic force microscope*. *J. Phys. Chem. C* **2015**, 119, 15482-15490.

86. Moazzami-Gudarzi, M.; Trefalt, G.; Szilagyi, I.; Maroni, P.; Borkovec, M., *Nanometer-ranged attraction induced by multivalent ions between similar and dissimilar surfaces probed using an atomic force microscope (AFM)*. *Physical Chemistry Chemical Physics* **2016**, 18, 8739-8751.

87. Pegado, L.; Jönsson, B.; Wennerström, H., *Attractive ion–ion correlation forces and the dielectric approximation*. *Adv. Colloid Interface Sci.* **2016**, 232, 1-8.

88. Boroudjerdi, H.; Kim, Y.-W.; Naji, A.; Netz, R. R.; Schlagberger, X.; Serr, A., *Statics and dynamics of strongly charged soft matter*. *Physics reports* **2005**, 416, 129-199.

89. Kanduc, M.; Moazzami-Gudarzi, M.; Valmacco, V.; Podgornik, R.; Trefalt, G., *Interactions between charged particles with bathing multivalent counterions: experiments vs. dressed ion theory*. *Phys. Chem. Chem. Phys.* **2017**, 19, 10069-10080.

90. Miklavic, S. J., *Double-layer farces between heterogeneous charged surfaces: The effect of net surface-charge*. *J. Chem. Phys.* **1995**, 103, 4794-4806.

91. Adžić, N.; Podgornik, R., *Charge regulation in ionic solutions: Thermal fluctuations and Kirkwood-Schumaker interactions*. *Phys. Rev. E* **2015**, 91, 022715.

92. Ruiz-Cabello, F. J. M.; Moazzami-Gudarzi, M.; Elzbieciak-Wodka, M.; Maroni, P.; Labbez, C.; Borkovec, M.; Trefalt, G., *Long-ranged and soft interactions between charged colloidal particles induced by multivalent coions*. *Soft Matter* **2015**, 11, 1562-1571.

93. Moazzami-Gudarzi, M.; Kremer, T.; Valmacco, V.; Maroni, P.; Borkovec, M.; Trefalt, G., *Interplay between Depletion and Double-Layer Forces Acting between Charged Particles in Solutions of Like-Charged Polyelectrolytes*. *Physical review letters* **2016**, 117, 088001.

94. Moazzami-Gudarzi, M.; Maroni, P.; Borkovec, M.; Trefalt, G., *Depletion and double layer forces acting between charged particles in solutions of like-charged polyelectrolytes and monovalent salt*. *Soft Matter* **2017**.

CHAPTER 2

Forces between negatively charged interfaces in the presence of cationic multivalent oligoamines measured with the atomic force microscope

Moazzami Gudarzi, M.; Trefalt, G.; Szilagyi, I.; Maroni, P.; Borkovec, M., *The Journal of Physical Chemistry C* 2015, 119, 15482-15490.

THE JOURNAL OF PHYSICAL CHEMISTRY C

Article

pubs.acs.org/JPCC

Forces between Negatively Charged Interfaces in the Presence of Cationic Multivalent Oligoamines Measured with the Atomic Force Microscope

Mohsen Moazzami Gudarzi, Gregor Trefalt, Istvan Szilagyi, Plinio Maroni, and Michal Borkovec*

Department of Inorganic and Analytical Chemistry, University of Geneva, Sciences II, 30 Quai Ernest-Ansermet, 1205 Geneva, Switzerland

ABSTRACT: The colloidal probe technique was used to accurately measure forces between water−solid interfaces of negatively charged latex particles in aqueous solutions of linear, cationic oligoamines of different valence up to roughly +4. These measurements were realized between pairs of particles with the atomic force microscope. Monovalent and divalent amines behave as simple electrolytes, and the forces are dominated by double layer repulsion at low concentrations and van der Waals attraction at high concentrations, as suggested by the classical theory by Derjaguin, Landau, Verwey, and Overbeek (DLVO). Additional attractive non-DLVO force of a short range can be evidenced, and its origin is attributed to hydrophobic interaction between the surfaces. Trivalent and tetravalent oligoamines induce a charge reversal and equally an additional attractive non-DLVO force. The charge reversal originates from the adsorption of these oligoamines to the particle surface. The additional non-DLVO force is more long-ranged than the ones observed in the presence of amines of low valence. This additional attraction is probably related to ion−ion correlations, existing surface heterogeneities, and the chainlike nature of the amines investigated.

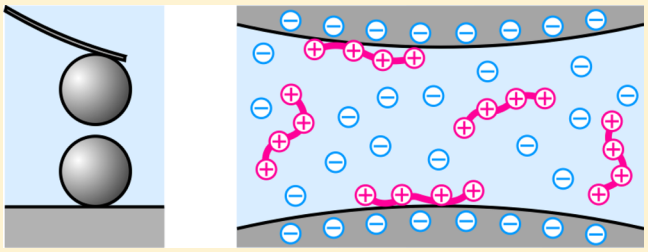

INTRODUCTION

Forces acting between charged interfaces in aqueous suspensions represent a central question in material sciences and environmental engineering. Such forces control the formation of green bodies in ceramic processing, flow of particle suspensions, formation of particle aggregates in wastewater treatment, or particle deposition to surfaces.[1−5] These forces can be modified through various additives, including salts, polymers, or polyelectrolytes.[6−17] Among those, salts containing multivalent ions are of particular interest, as they may induce particle aggregation at substantially lower salt concentrations than monovalent ones. Such multivalent ions may include various metal ions, metal ion complexes, but equally short oligomers of polyelectrolytes.[6−12]

The accurate measurements of forces between water−solid interfaces remained elusive for a long time. The breakthrough came with the invention of the surface forces apparatus, which still offers unsurpassed distance resolution.[18−20] More recently, additional techniques to directly measure surface forces became available, such as total internal reflection microscopy (TIRM),[21,22] optical tweezers combined with videomicroscopy,[10,23,24] and atomic force microscopy (AFM).[14,25,26] TIRM and optical tweezers offer an excellent force resolution, but their distance resolution remains limited to a few nanometers. The AFM can be used to measure forces involving colloidal particles by means of the colloidal probe technique, either in the sphere−plate or in the sphere−sphere geometry. The latter technique offers a subnanometer distance resolution, and with modern AFMs, a good force resolution can be obtained as well. Currently, the colloidal probe technique can be routinely used to measure forces involving colloidal particles down to about 1 μm in diameter.[11,12,14,27]

On the other hand, the theory of forces between charged water−solid interfaces has a long history. The cornerstone represents the theory of Derjaguin, Landau, Verwey, and Overbeek (DLVO), which was developed more than half a century ago.[28] This approach suggests that forces between two interfaces have two main contributions, namely, an attractive van der Waals force and a repulsive double layer force. Subsequently, this approach was refined by considering more precise models of the respective interactions. The calculation of van der Waals forces may consider retardation or include effects of surface roughness.[28−30] Double layer forces may be obtained not only on the basis of Debye−Hückel theory but also from Poisson−Boltzmann (PB) theory, and they may include effects of charge regulation.[31−33] More recently, it was suggested that the PB approach may break down due to neglect of ion−ion correlations or finite size of the ions.[34−36] Forces involving colloidal particles can be obtained from the plate−plate geometry by means of the Derjaguin approximation.[28]

In recent years, there was a substantial interest whether other ionic properties, besides their valence, are relevant in

Received: May 8, 2015
Revised: June 4, 2015
Published: June 4, 2015

DOI: 10.1021/acs.jpcc.5b04426
J. Phys. Chem. C 2015, 119, 15482−15490

Table 1. Ionization Properties for the Oligoamine Cations Used

name[a]	mole fraction and ionization constant[b]					
	+1	+2	+3	+4	+5	+6
methylamine, N1	>0.99					
CH_3NH_2	10.63					
ethyelenediamine, N2	<0.01	>0.99				
$H_2NCH_2CH_2NH_2$	9.93	6.85				
diethylenetriamine, N3	<0.01	0.33	0.67			
$H_2NCH_2CH_2NHCH_2CH_2NH_2$	9.80	8.75	3.73			
triethylenetetramine, N4	<0.01	<0.01	0.85	0.15		
$H_2N(CH_2CH_2NH)_2CH_2CH_2NH_2$	9.73	8.86	6.12	2.60		
pentaethylenehexamine, N6	<0.01	<0.01	0.01	0.88	0.11	<0.01
$H_2N(CH_2CH_2NH)_4CH_2CH_2NH_2$	9.89	9.06	6.03	5.77	2.96	1.28

[a]Chemical name, abbreviation, and chemical formula. [b]Mole fraction of the species of charge indicated (above) and respective pK value at infinite dilution (below).

determining forces between colloidal particles. Several authors have investigated their size, while others have focused on their shape, or electric multipole moments.[35−37] In this context, rodlike multivalent ions were investigated in detail.[37] The latter study concluded that rodlike ions lead to weaker attractions than their point-like counterparts.

In the present work, we experimentally investigate forces between charged colloidal particles in the presence of linear aliphatic polyamines with the colloidal probe technique. By measuring forces between a pair of similar colloidal particles, one can well realize a symmetric situation. While the ions investigated have an internal flexibility, they do represent an experimental realization of the rodlike multivalent ions discussed above. We explore forces in these systems over a wide range of concentrations and for different valences. These forces can be modeled with DLVO theory, provided one includes an additional attractive force. The present findings are compared to recent studies of similar systems containing multivalent ions of simpler structure.

EXPERIMENTAL SECTION

Materials. Negatively charged sulfate-functionalized polystyrene latex particles were purchased from Invitrogen. The mean diameter of these particles is 3.0 μm and their relative polydispersity is 4.1%, as determined by the manufacturer with electron microscopy. The stock dispersion of particles was dialyzed against pure water with a cellulose membrane having a cutoff in the molecular mass of 50 kg/mol until the conductivity of the surrounding solution reached the one of pure water. Milli-Q water (Millipore) was used throughout. The particle concentration after dialysis was obtained by comparing the light-scattering intensities of the dialyzed and nondialyzed suspensions. The particles have a root-mean-square (RMS) roughness of 0.8 nm, as obtained by AFM imaging. The same particles were used in an earlier study, where more details on their characterization can be found.[38]

Oligoamines of linear polyethyleneimine containing different numbers of amine groups were purchased from Aldrich. Their chemical formula is given in Table 1. They will be abbreviated in the following as N1, N2, N3, N4, and N6. In particular, we used the chloride salts in the case of methylamine hydrochloride, ethylenediamine dihydrochloride, triethylenetetramine tetrahydrochloride, and the basic forms of diethylenetriamine and pentaethylenehexamine. Stock solutions of oligoamines in the concentration range of 4−20 g/L were prepared, and their pH was adjusted to 4.0 with HCl and KOH. The final concentrations of oligomers in these solutions were verified with a total organic carbon and nitrogen analyzer (TOCV, Shimadzu). The solutions were prepared by dilution of stock solutions with a 1.0 mM solution of KCl, which was previously adjusted to pH 4.0. At the experimental conditions used, these molecules are highly charged, but they are not fully ionized. The concentration of the different ionic species in the polyamine solutions was obtained by calculating the fraction of the differently charged oligoamines at pH 4.0 from tabulated ionization constants at infinite dilution.[39] The resulting fractions are summarized in Table 1. At higher ionic strength, the ionic composition was slightly different due screening-induced shifts of the ionization constants. However, these differences had only minor effects on the results obtained, and therefore, the composition at infinite dilution was used throughout. Control experiments were carried out in KCl solutions adjusted to pH 4.0. All experiments were performed at a room temperature of 21 ± 3 °C.

Electrophoresis. Charging properties of latex particles were studied with electrophoresis. The measurements were performed with a ZetaNano ZS (Malvern Instruments, Worcestershire, U.K.). Particle suspensions were prepared with appropriate concentrations of oligoamines at particle concentrations of 80 and 200 mg/L. They were equilibrated overnight, and their electrophoretic mobility was obtained as an average of five individual measurements. The mobility data were converted to surface potential (ζ-potential) with Henry's model.[28] The validity of this model was checked for KCl against the standard electrokinetic model,[40] and the respective differences were maximally 10%, but mostly smaller.

Direct Force Measurements. Forces between two individual latex particles were measured with the multiparticle colloidal probe technique. A closed-loop AFM (MFP-3D, Asylum Research) mounted on an inverted optical microscope (IX70, Olympus) was used. The glass plate fitting the bottom of the AFM fluid cell was first cleaned for 2 h in piranha solution, which was prepared by mixing 98% H_2SO_4 and 30% H_2O_2 in a volumetric ratio of 3:1. The plate was then rinsed with pure water and dried in a stream of nitrogen. The dry plate was cleaned for 20 min in an air plasma (PDC-32G, Harrick, New York) and finally silanized overnight in an evacuated container aside a drop of hexamethyldisilazane (Alfa Aesar). A tip-less cantilever (NSC 12, μMash, Estonia) was cleaned by plasma treatment for 20 min, silanized as described above, but only for 2−3 h, and then washed with water.

DOI: 10.1021/acs.jpcc.5b04426
J. Phys. Chem. C 2015, 119, 15482−15490

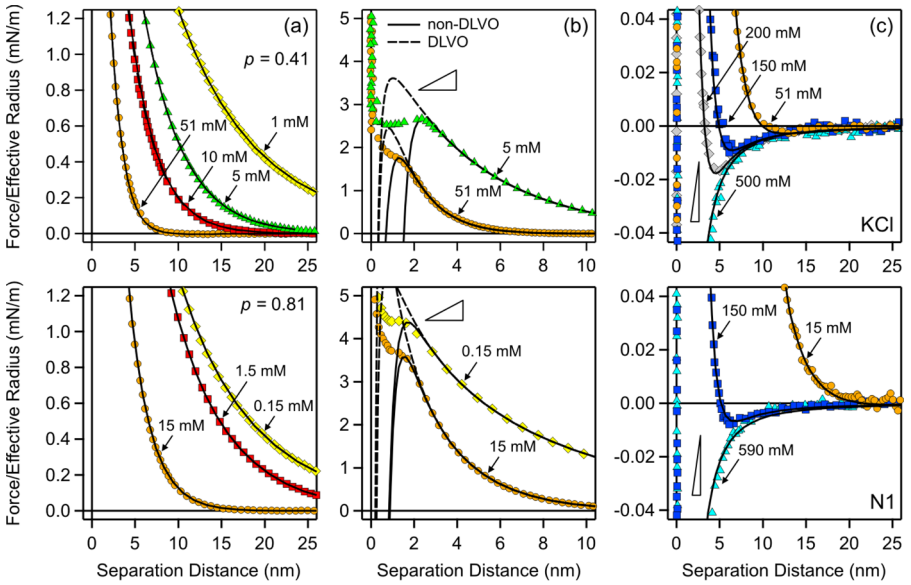

Figure 1. Normalized force profiles in monovalent electrolyte solutions at pH 4.0 for KCl (top) and N1 (bottom). Solid lines are best fits with DLVO theory including an additional non-DLVO short-range exponential attraction with a range of 0.32 nm. Dashed lines are results of DLVO calculations without this additional attraction whenever they are visibly different. The triangles depict the slope of the jump-in instability given by the spring constant of the cantilever. The columns indicate concentration ranges from (a) low with (b) zoom in to (c) high.

The silanized glass plate and cantilever were then mounted in the AFM fluid cell. The cell was flushed with a latex particle suspension of a particle concentration of 100 mg/L adjusted to pH 4.0. The particles were left to deposit on the glass plate for 1 h, and then the cell was amply flushed with the oligoamine solution several times, and left to equilibrate for at least 20 min.

To carry out the force measurement, the functionalized cantilever was approached to a particle deposited on the substrate, which could be picked up by pressing it against the substrate. The particle attached to the cantilever was then centered over another particle that remained deposited on the substrate by observing the interference fringes with the optical microscope with a lateral precision of about 50 nm. Vertical approach−retraction cycles were recorded with a sampling rate of 5 kHz involving the two centered particles with a cycle frequency of 0.5 Hz and velocity of 500 nm/s. The contact point was determined from the constant compliance region with a precision of about 0.5 nm. The forces were calculated with the spring constant of the cantilever. This constant was measured by the method by Sader et al.,[41] which uses the frequency response of the cantilever and its lateral dimensions. The resulting spring constants are in the range of 0.1−0.3 N/m. These values were within 20% with the thermal noise method.[42] Within each electrolyte solution, the measurements were performed at least for 3 different pairs of particles. At least 100 approach−retraction cycles were recorded for each pair. For each cycle, the baseline and the constant compliance region were determined and the resulting force profiles were down-sampled to 3 kHz and averaged over the approach parts of the different cycles. This protocol results in a force resolution of about 0.5 pN. The force profiles were further down-sampled into bins of 0.5 nm. The force profiles normally did not differ more than 10% between different pairs of particles. Further details about the multiparticle colloidal probe technique can be found elsewhere.[14]

Data Analysis. The force profiles were fitted to a modified DLVO theory, whereby the force was decomposed as

$$F = F_{vdW} + F_{dl} + F_{att} \quad (1)$$

whereby F_{vdW} is the van der Waals force, F_{dl} the double layer force, and F_{att} an additional attractive force. These contributions were all evaluated within Derjaguin approximation. The van der Waals force was approximated by the nonretarded expression

$$\frac{F_{vdW}}{R_{eff}} = -\frac{H}{6h^2} \quad (2)$$

where H is the Hamaker constant, h the smallest separation distance between the particle surfaces, and R_{eff} the effective radius, which is given by $R_{eff} = R/2$, where R is the average particle radius. The variations of this quantity due to particle polydispersity are negligible.

The double layer force was calculated numerically by solving the full PB equation between two identical charged plates separated by solution consisting of a mixture of asymmetric electrolytes within the constant regulation approximation. Details of these calculations are given elsewhere.[12,33] The relevant parameters that enter the calculation are the electric diffuse layer potential ψ_D, the regulation parameter p, and the concentrations of the different ionic species in bulk solution. When one sets $p = 1$, one obtains the constant charge boundary condition, whereas, for $p = 0$, one has the constant potential boundary condition. This parameter typically lies in between these two values. The concentrations of the ionic species were estimated from the total oligoamine concentration, and the fractions of the respective species are given in Table 1. The corresponding additional monovalent electrolyte was equally considered. The linearized DH solution is grossly inaccurate, especially when the multivalent ions are the co-ions, and in that case, the force profile cannot be obtained from the ionic strength only.[27]

To rationalize the force curves, it was necessary to introduce an additional attractive force. In monovalent salt solutions, this attraction is probably related to the hydrophobic force.[43] This force was described by an exponential profile

DOI: 10.1021/acs.jpcc.5b04426
J. Phys. Chem. C 2015, 119, 15482−15490

$$\frac{F_{att}}{R_{eff}} = -Ae^{-qh} \quad (3)$$

where q^{-1} is the range of this force and A its amplitude ($A > 0$).

RESULTS AND DISCUSSION

Direct force measurements with the AFM between pairs of negatively charged latex particles were carried out in solutions of multivalent cationic oligoamines over a wide concentration range at pH 4.0. While these molecules behave like simple electrolytes for low valence, they induce charge reversal at higher valences. The force measurements will be discussed qualitatively first, and subsequently, they will be interpreted with DLVO theory quantitatively. However, an additional attractive non-DLVO force is needed to quantify the force profiles accurately.

Generic Features of the Force Profiles. Let us first recall the force profiles in monovalent electrolyte solutions. Figure 1 compares the force profiles in KCl solutions (top) and in N1 solutions (bottom). Since N1 is a simple monovalent electrolyte, the force profiles are very similar in both situations. At low salt concentrations, the forces are soft and long-ranged, as characteristic for double layer repulsion (Figure 1a). With increasing concentration, the range of this repulsion decreases due to progressive screening. With increasing salt concentrations, these forces become more attractive, and jump-in instabilities at distances of 2−4 nm can be observed (Figure 1b). A similar instability is expected on the basis of DLVO theory, since, at short distances, the van der Waals forces dominate over the double layer repulsion. Within this instability, the cantilever should follow a straight line with the slope corresponding to its spring constant, provided that the mechanical equilibrium is established. The data shown indicate that the force acting on the cantilever is more repulsive, probably due to hydrodynamic drag. When the velocity of the cantilever is comparable to the one of the scanner displacement, the influence of hydrodynamic drag of the probe is negligible down to distances of about 2 nm. Within this instability, however, the cantilever will accelerate to higher velocities, which would lead to higher drag and larger repulsive forces. At higher salt concentrations, the forces become attractive at larger distances (Figure 1c). This attraction principally originates from the van der Waals force, but the double layer repulsion overrides this force at intermediate distances. At very short distances, the jump-in is again present (not shown on the scale of Figure 1c). When the electrolyte concentration is high, the force profile becomes fully attractive.

Let us now discuss the more complex force profiles in N6 solutions shown in Figure 2. This oligoamine has a charge of about +4 in the present solution of pH 4.0 (Table 1). The subfigures summarize different concentration regimes. The concentrations indicated always refer to the molar concentration of the amino groups. At very low concentrations, the force profiles are repulsive, soft, and long-ranged (Figure 2a). These forces are reminiscent of the ones observed in monovalent salt solutions, and they again originate from double layer repulsion. With increasing concentration, the forces weaken rapidly, and become fully attractive (Figure 2b). When the concentration is increased further, however, the forces become repulsive. These repulsive forces are again soft and long-ranged, indicating that they originate from repulsion between charged double layers. The natural interpretation of this reentrant transition is a charge neutralization and

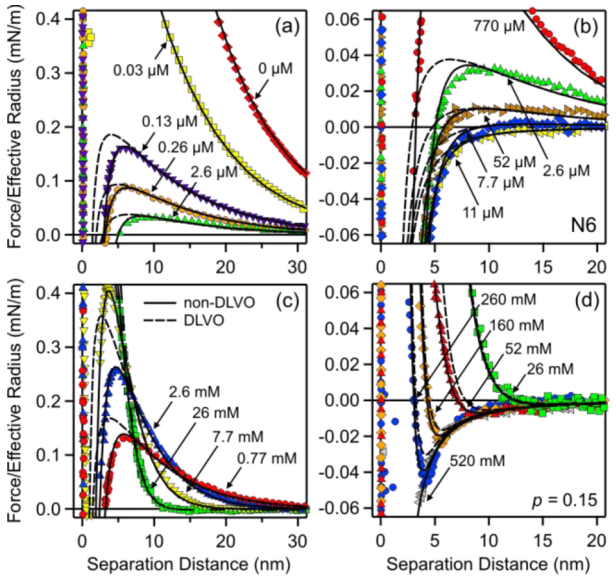

Figure 2. Normalized force profiles in solutions of N6 at pH 4.0. Solid lines are best fits with DLVO theory including an additional non-DLVO short-range exponential attraction with a range of 1.0 nm. Dashed lines are results of DLVO calculations without this additional attraction whenever they are visibly different. The concentration of the amine groups increases from (a) through (d).

subsequent charge reversal due to adsorption of the positively charged polyamines. The charge neutralization point occurs at a concentration of around 11 μM, and at higher concentrations, the particles become positively charged. A similar charge reversal was reported for smaller negatively charged particles with the same oligoamines based on electrophoresis and aggregation rate measurements.[13] When the concentration is increased further, the range of the double layer repulsion decreases due to screening (Figure 2c). At concentrations above 100 mM, van der Waals attraction starts to dominate the interaction at larger distances, but double layer repulsion still remains important at smaller distances (Figure 2d). When the N6 concentration is increased further, the double layer repulsion gets screened completely, and the force profile remains fully attractive.

Figure 3 shows the force profiles for N2, N3, and N4. The profile for N2 resembles the behavior of simple electrolytes with the difference that the transition from repulsive double layer forces to attractive van der Waals forces occurs at lower concentrations. This shift can be rationalized by adsorption of N2 to the particle surface, which leads to a reduction of the surface charge. On the other hand, the behavior of N4 is reminiscent of N6. One also observes a charge reversal, but the charge neutralization point occurs at a substantially higher N4 concentration, namely, around 2.1 mM. This shift can be rationalized by the fact that N4 adsorbs more weakly than N6. The behavior of N3 lies in between. The forces are more attractive at larger distances than for N1 and N2, which can be explained by the fact that the surface charge is neutralized at high N3 concentration. However, the adsorption of N3 is not sufficiently strong such that a charge reversal would occur.

A relevant question is whether additional attractive interactions are present. Figure 4 addresses this question by comparing attractive force profiles at high concentrations with the ones at the charge reversal point. DLVO theory suggests that no double layer forces should be present, due to either

DOI: 10.1021/acs.jpcc.5b04426
J. Phys. Chem. C 2015, 119, 15482−15490

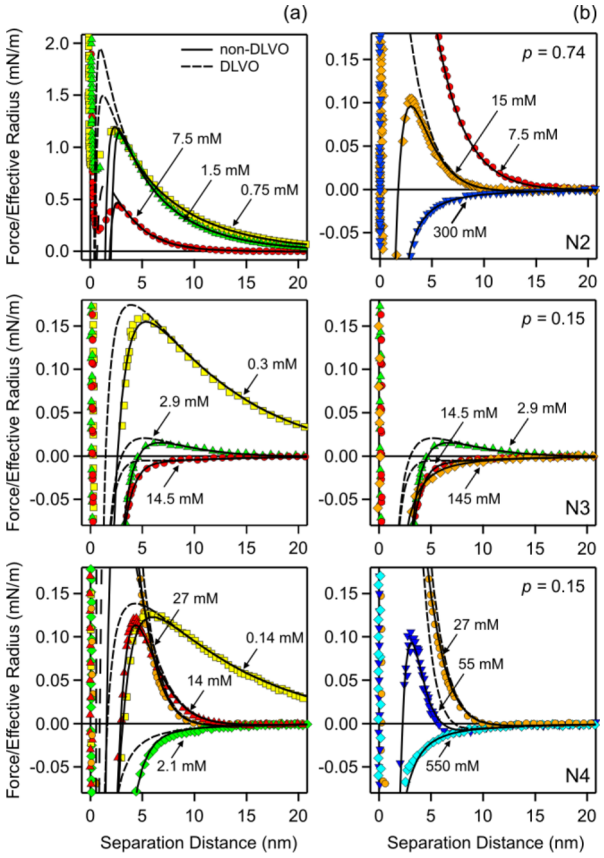

Figure 3. Normalized force profiles in solutions of N2, N3, and N4 at pH 4.0 (top to bottom). Solid lines are best fits with DLVO theory including an additional non-DLVO short-range exponential attraction with a range of 0.32 nm for N2 and 1.0 nm for N3 and N4. Dashed lines are results of DLVO calculations without this additional attraction whenever they are visibly different. The columns indicate concentrations of the amino groups ranging from (a) low to (b) high.

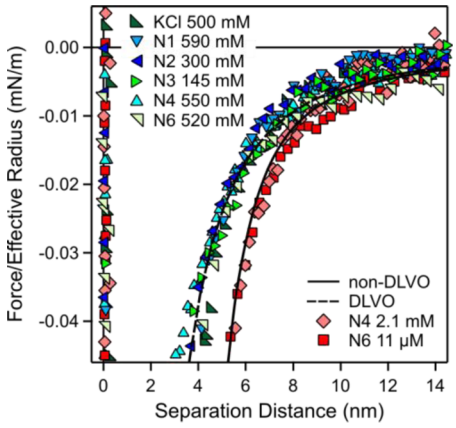

Figure 4. Normalized attractive force profiles in the presence of various oligoamines or KCl. The concentrations refer to molar concentrations of the amino groups, except for KCl, where the molar concentration is used. At high concentrations, the force profiles follow the van der Waals force inherent to DLVO theory with a Hamaker constant of 3.5×10^{-21} J (dashed line). At the charge neutralization point that occurs at lower concentrations for N4 and N6, the forces are more attractive. They can be described with the van der Waals forces and an additional non-DLVO exponential attraction with a range of 1.0 nm and amplitude of 4.0 mN/m.

screening at high salt concentrations or charge neutralization at lower concentrations, and thus solely attractive van der Waals forces should exist. At high concentrations, one observes a common attractive force, which corresponds to the van der Waals attraction. However, the force curves recorded close to the charge neutralization point for N4 and N6 are more strongly attractive. This additional attraction is a non-DLVO force. Such an additional attractive force probably occurs quite universally in the presence of multivalent counterions, since similar additional forces were reported for latex particles in the presence of simple trivalent and tetravalent ions,[12,44] and for silica surfaces in the presence of trivalent cations.[7]

Modeling with DLVO Theory. The measured force profiles were modeled with DLVO theory quantitatively. Our approach relies on the Derjaguin approximation, nonretarded van der Waals forces, and the full solution of the PB equation for a mixture of asymmetric electrolytes within the constant regulation approximation. These approximations are appropriate for the present system. The parameters entering the DLVO theory are the Hamaker constant H, diffuse layer potential ψ_D, and the regulation parameter p of the isolated surface. The solution of the PB equation also requires the ionic concentrations in the bulk solution, but these concentrations are known from the concentration of the oligoamines used and the respective solution speciation due to ionization equilibria (Table 1). Therefore, all ionic concentrations were fixed to the known values in all calculations. In some cases, we have also adjusted the total oligomer concentrations, and the fitted concentrations were always within 10% of the actual concentrations.

However, some features of the force profiles cannot be quantified with DLVO theory. In the monovalent electrolytes, the deficiencies mainly concern the position of the jump-in. In the presence of multivalent ions, the measured attractive forces are stronger than the van der Waals force near the charge neutralization point, and even more so above this point. This additional non-DLVO force was modeled with a simple exponential given in eq 3.

For the monovalent salts, the best fits with the DLVO model including the additional exponential attraction are shown in Figure 1. At low salt concentrations, typically below 30 mM, the force profile is mainly determined by forces acting between double layers, and the profile mainly depends on the diffuse layer potential ψ_D and the regulation parameter p. These two parameters were extracted from these force profiles under these conditions. The regulation parameter was found to be approximately independent of concentration over the concentration range of 1−50 mM. The mean values were 0.41 ± 0.03 for KCl and 0.81 ± 0.05 for N1. For this reason, these parameters were fixed to their mean values.

The Hamaker constant was extracted by fitting the force profiles at high salt concentration (Figures 1c). The extracted value is close to the value of 3.5×10^{-21} J given for the same particles previously.[38] This value should be contrasted to the much larger values of near 1.0×10^{-20} J that result from the full Lifshitz calculation.[29,45] The discrepancy probably originates from the presence of surface roughness, which was measured to have an RMS value of about 0.8 nm. This reduction of the van der Waals attraction results from a combination of retardation and roughness effects. Retardation reduces the apparent Hamaker constant at larger distances, whereas roughness effects are important at small distances. The combination of both effects results in an apparent Hamaker constant that

DOI: 10.1021/acs.jpcc.5b04426
J. Phys. Chem. C 2015, 119, 15482−15490

shows a broad maximum at distances of several nanometers. In this region, the van der Waals interactions can be well approximated with the nonretarded expressions, but with a smaller Hamaker constant. In this fashion, a Hamaker constant of 2.0×10^{-21} J could be rationalized with the measured RMS roughness of 1.1 nm for another type of latex particles.[29] This picture is consistent with the fact that the Hamaker constant measured here is somewhat larger, but accordingly the surface roughness is smaller.

When one combines double layer forces and van der Waals forces with the Hamaker constant reported above, the transition between the repulsive and attractive regime cannot be described very well, especially at short distances. In particular, the position of the jump-in is predicted at substantially smaller distances than observed (Figure 1b). This deficiency can be remedied by introducing an additional attractive exponential force given in eq 3. By fixing the regulation parameter and the Hamaker constant, we have fitted the entire data set including the additional attractive force, and we obtained the two additional parameters, namely, the range q^{-1} and the amplitude A. The range varies relatively weakly, and we found a mean value for q^{-1} of 0.32 ± 0.03 nm. By fixing this value to its mean and refitting the entire data set, we obtain the final set of diffuse layer potentials ψ_D and amplitudes A. These values are shown in Figures 5 and 6a.

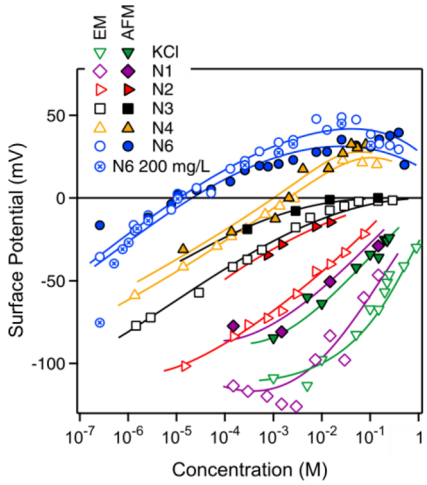

Figure 5. Comparison of surface potentials obtained from AFM and from electrophoretic mobility (EM) versus the concentration for different oligoamines or KCl at pH 4.0. The concentration refers to molar concentration of the amino groups, except for KCl, where the molar concentration is used. Charge neutralization points occur at 2.1 mM and 11 μM for N4 and N6, respectively. The electrophoresis experiments were carried out for N6 at two particle concentrations. They suggest that the adsorbed amount is negligible, and that the concentration shown corresponds to the free equilibrium concentration. The lines help to guide the eye only.

The diffuse layer potentials obtained from the force measurements are compared with surface potentials extracted from electrophoretic mobility (Figure 5). The electrophoresis results further confirm that the particles are negatively charged. The surface potentials increase with the salt concentration, as one would expect from the progressive screening of the surface charge. While the overall trends of the potentials obtained by the two different techniques agree, the magnitude of the electric potentials obtained by electrophoresis is larger. Similar

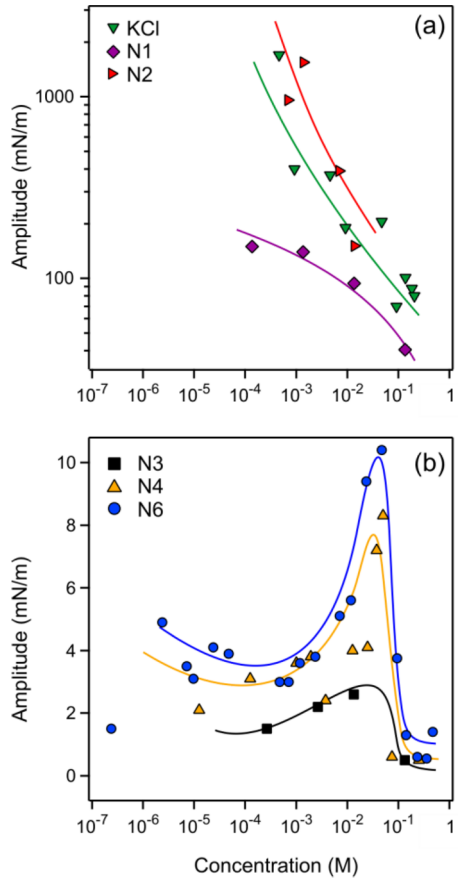

Figure 6. Amplitude of additional non-DLVO exponential attraction versus the concentration for different oligoamines and KCl at pH 4.0. The concentration refers to molar concentration of the amino groups, except for KCl, where the molar concentration is used. (a) For N1, N2, and KCl, the decay lengths are 0.32 nm, and (b) for N3, N4, and N6, 1.0 nm. The lines help to guide the eye only.

discrepancies were reported for other systems.[29,46] This discrepancy could originate from lateral heterogeneities of the surface charge of the latex particles. The presence of such heterogeneities was confirmed on similar particles by rotational electrophoresis of particle doublets.[47] These heterogeneities might also induce rotational motion of the individual particles, which would lead to an enhancement of the electrophoretic mobility.[48]

The amplitude of the additional non-DLVO force decreases with increasing salt concentration (Figure 6a), whereby its magnitude is somewhat weaker for the N1 system than for KCl. Accordingly, the distance of the jump-in in the N1 systems around 1.8 ± 0.1 nm is smaller than 2.5 ± 0.4 nm in KCl. We suspect that this additional attractive force is probably of hydrophobic origin. The fitted mean range of 0.32 nm is fully consistent with the range of the hydrophobic force obtained with the surface forces apparatus[18,43] and theoretical approaches.[49,50] Note that we can only affirm that the present measurements are consistent with an exponential distance dependence of the additional attractive force. Given the experimental noise in the force measurements, one could probably find other functional dependencies that would also be compatible with the data.

A similar fitting strategy was used for the multivalent oligomers. The Hamaker constant was fixed to 3.5×10^{-21} J as before, and this assumption was consistent with the observed

DOI: 10.1021/acs.jpcc.5b04426
J. Phys. Chem. C 2015, 119, 15482−15490

force profiles at high concentrations in all systems studied (Figure 4). The force profiles could also be described with regulation parameters that are independent of the oligomer concentration. No systematic differences between N3, N4, and N6 were found. The mean value of these regulation parameters was 0.15 ± 0.03. For the multivalent oligomers, their values were substantially lower than those for the monovalent ones. This observation is probably related to the fact that the multivalent oligoamines adsorb more strongly, allowing the charge to be regulated more easily. The additional attractive force was equally necessary to describe the force profiles, whereby its range could be assumed to be independent of the oligomer concentration. For N2, the decay length of 0.32 nm obtained for the monovalent ions was consistent with the data, but for N3, N4, and N6, its value was significantly larger. Neither differences between these oligomers nor trends with the concentration could be established, and the overall average yields q^{-1} = 1.00 ± 0.05 nm. This parameter was fixed to the average value in the following. In this fashion, the model again contained only two fitting parameters, namely, the diffuse layer potential ψ_D and the amplitude A.

The values of these parameters are given in Figures 5 and 6b. For the multivalent ions, the diffuse layer potentials are in good agreement with the electrophoresis measurements. In particular, electrophoresis confirms the existence of the charge reversal for N4 and N6. The discrepancies between the surface potentials obtained by AFM and by electrophoresis described above are also apparent for N2. The good agreement between surface potentials obtained from electrophoresis at two different particle concentrations for N6 suggests that the adsorbed amount is negligible with respect to the amount in solution.[51,52] Correspondingly, the total concentration in these experiments corresponds to the free concentration in solution. Deviations occur only at concentrations below 10^{-6} M, where the adsorbed amount is no longer negligible with respect to the total amount of N6. While deviations to the diffuse layer potentials obtained from AFM are equally apparent under these conditions, this concentration range is outside the scope of the present study.

The presence of the additional non-DLVO attraction is obvious for N4 and N6 at the neutralization point. As shown in Figure 4, an additional exponential force profile with a range of 1.0 nm can rationalize the observed dependence reasonably well. In the presence of multivalent ions, the amplitude of the additional attraction is approximately constant at lower concentration, but increases even further after the charge reversal, and finally decreases rapidly at very high concentrations (Figure 6b). A possible interpretation of this additional force is due to ion−ion correlation effects. The PB theory treats the ionic distributions on a mean-field level, and considerations of correlations between the ions introduces new effects, including charge reversal and additional attractive forces.[34−36] The predicted range of these forces is in the subnanometer range,[30,47] but could be compatible with present observations. This elucidation might be not as straightforward as it may seem, since similar attractive non-DLVO forces were observed in solutions containing simple multivalent ions between latex particles and silica surfaces.[7,8,12,44] In these systems, however, the range of these additional forces was 2−3 nm, which is much larger than what one would expect for ion−ion correlation forces. The interpretations put forward for this larger interaction range invoked existing surface heterogeneities or slight asymmetry between the surfaces. Sivan and co-workers have also observed similar additional attraction in the presence of trivalent cobalt complexes.[8] They fitted this attraction to an exponential force profile with a range situated between 0.9 and 2.5 nm. These additional attractive forces are probably related to ion−ion correlations,[34−36] which could lead to the formation of ordered adsorbed layers on the particle surface. However, these forces could be also influenced by surface charge heterogeneities or thermal fluctuations of the surface charge.[11,53,54] While the presence of the oligomers could also induce depletion forces, their range and strength are expected to be too small to be measurable.

The reason for the reduced range of the additional attractive force in the present system with respect to the earlier reports discussed above[7,8,12,44] could be related to the chainlike nature of the ions used, but could also be a consequence of the fact that the adsorbed layers are more homogeneous. In contrast to these experiments, theoretical analysis of forces induced by rodlike multivalent ions actually suggests that the range of attractive forces should be somewhat larger than that for point-like ions.[37] That study, however, assumed perfectly rigid rods, while the present oligomers surely show some flexibility.

CONCLUSION

Forces between negatively charged latex particles were measured in aqueous solutions of linear oligoamines of different valence. Highly charged oligoamines lead to a charge reversal and further induce an additional attractive force. The charge reversal can be explained by adsorption of these cationic chainlike ions to the negatively charged particle surface. The additional non-DLVO force is consistent with an exponential force profile with a range of 1.0 nm. Its magnitude increases with increasing concentration, goes through a maximum, and vanishes at high concentration. This additional attraction is probably related to ion−ion correlations, but it could also be influenced by existing surface heterogeneities and the chainlike nature of the ions investigated. Additional experiments and calculations are needed to elucidate the precise nature of this non-DLVO force.

AUTHOR INFORMATION

Corresponding Author

*Phone: ++41 22 3796405. E-mail: michal.borkovec@unige.ch.

Notes

The authors declare no competing financial interest.

ACKNOWLEDGMENTS

The authors would like to thank Klemen Bohinc, Christophe Labbez, and Rudi Podgornik for illuminating discussions. This research was supported by the Swiss National Science Foundation, University of Geneva, COST Action CM1101, and the Swiss Secretariat of Education and Research.

REFERENCES

(1) Balzer, B.; Hruschka, M. K. M.; Gauckler, L. J. Coagulation Kinetics and Mechanical Behavior of Wet Alumina Green Bodies Produced via DCC. *J. Colloid Interface Sci.* **1999**, *216*, 379−386.

(2) Leong, Y. K.; Scales, P. J.; Healy, T. W.; Boger, D. V. Interparticle Forces Arising from Adsorbed Polyelectrolytes in Colloidal Suspensions. *Colloids Surf., A* **1995**, *95*, 43−52.

(3) Bolto, B.; Gregory, J. Organic Polyelectrolytes in Water Treatment. *Water Res.* **2007**, *41*, 2301−2324.

(4) Adamczyk, Z.; Warszynski, P. Role of Electrostatic Interactions in Particle Adsorption. *Adv. Colloid Interface Sci.* **1996**, *63*, 41−149.

DOI: 10.1021/acs.jpcc.5b04426
J. Phys. Chem. C 2015, 119, 15482−15490

(5) Chen, K. L.; Elimelech, M. Aggregation and Deposition Kinetics of Fullerene (C_{60}) Nanoparticles. *Langmuir* **2006**, *22*, 10994−11001.
(6) Szilagyi, I.; Trefalt, G.; Tiraferri, A.; Borkovec, M. Polyelectrolyte Adsorption, Interparticle Forces, and Colloidal Aggregation. *Soft Matter* **2014**, *10*, 2479−2502.
(7) Dishon, M.; Zohar, O.; Sivan, U. Effect of Cation Size and Charge on the Interaction between Silica Surfaces in 1:1, 2:1, and 3:1 Aqueous Electrolytes. *Langmuir* **2011**, *27*, 12977−12984.
(8) Zohar, O.; Leizerson, I.; Sivan, U. Short Range Attraction between Two Similarly Charged Silica Surfaces. *Phys. Rev. Lett.* **2006**, *96*, 177802.
(9) Rescic, J.; Kovacevic, D.; Tomsic, M.; Jamnik, A.; Ahualli, S.; Bohinc, K. Experimental and Theoretical Study of the Silica Particle Interactions in the Presence of Multivalent Rod-like Ions. *Langmuir* **2014**, *30*, 9717−9725.
(10) Gutsche, C.; Keyser, U. F.; Kegler, K.; Kremer, F. Forces between Single Pairs of Charged Colloids in Aqueous Salt Solutions. *Phys. Rev. E* **2007**, *76*, 031403.
(11) Sinha, P.; Szilagyi, I.; Montes Ruiz-Cabello, F. J.; Maroni, P.; Borkovec, M. Attractive Forces between Charged Colloidal Particles Induced by Multivalent Ions Revealed by Confronting Aggregation and Direct Force Measurements. *J. Phys. Chem. Lett.* **2013**, *4*, 648−652.
(12) Montes Ruiz-Cabello, F. J.; Trefalt, G.; Csendes, Z.; Sinha, P.; Oncsik, T.; Szilagyi, I.; Maroni, P.; Borkovec, M. Predicting Aggregation Rates of Colloidal Particles from Direct Force Measurements. *J. Phys. Chem. B* **2013**, *117*, 11853−11862.
(13) Szilagyi, I.; Sadeghpour, A.; Borkovec, M. Destabilization of Colloidal Suspensions by Multivalent Ions and Polyelectrolytes: From Screening to Overcharging. *Langmuir* **2012**, *28*, 6211−6215.
(14) Borkovec, M.; Szilagyi, I.; Popa, I.; Finessi, M.; Sinha, P.; Maroni, P.; Papastavrou, G. Investigating Forces between Charged Particles in the Presence of Oppositely Charged Polyelectrolytes with the Multi-particle Colloidal Probe Technique. *Adv. Colloid Interface Sci.* **2012**, *179*−*182*, 85−98.
(15) Wei, X. L.; Gong, X. J.; Ngai, T. Interactions between Solid Surfaces Mediated by Polyethylene Oxide Polymers: Effect of Polymer Concentration. *Langmuir* **2013**, *29*, 11038−11045.
(16) Klapp, S. H. L.; Zeng, Y.; Qu, D.; von Klitzing, R. Surviving Structure in Colloidal Suspensions Squeezed from 3D to 2D. *Phys. Rev. Lett.* **2008**, *100*, 118303.
(17) Poptoshev, E.; Rutland, M. W.; Claesson, P. M. Surface Forces in Aqueous Polyvinylamine Solutions. 1. Glass Surfaces. *Langmuir* **1999**, *15*, 7789−7794.
(18) Donaldson, S. H.; Royne, A.; Kristiansen, K.; Rapp, M. V.; Das, S.; Gebbie, M. A.; Lee, D. W.; Stock, P.; Valtiner, M.; Israelachvili, J. Developing a General Interaction Potential for Hydrophobic and Hydrophilic Interactions. *Langmuir* **2015**, *31*, 2051−2064.
(19) Israelachvili, J.; Min, Y.; Akbulut, M.; Alig, A.; Carver, G.; Greene, W.; Kristiansen, K.; Meyer, E.; Pesika, N.; Rosenberg, K.; et al. Recent Advances in the Surface Forces Apparatus (SFA) Technique. *Rep. Prog. Phys.* **2010**, *73*, 036601.
(20) Espinosa-Marzal, R. M.; Drobek, T.; Balmer, T.; Heuberger, M. P. Hydrated-Ion Ordering in Electrical Double Layers. *Phys. Chem. Chem. Phys.* **2012**, *14*, 6085−6093.
(21) Prieve, D. C. Measurement of Colloidal Forces with TIRM. *Adv. Colloid Interface Sci.* **1999**, *82*, 93−125.
(22) Volpe, G.; Brettschneider, T.; Helden, L.; Bechinger, C. Novel Perspectives for the Application of Total Internal Reflection Microscopy. *Opt. Express* **2009**, *17*, 23975−23985.
(23) Crocker, J. C.; Grier, D. G. Microscopic Measurement of the Pair Interaction Potential of Charge-Stabilized Colloid. *Phys. Rev. Lett.* **1994**, *73*, 352−355.
(24) Dobnikar, J.; Brunner, M.; von Grunberg, H. H.; Bechinger, C. Three-Body Interactions in Colloidal Systems. *Phys. Rev. E* **2004**, *69*, 031402.
(25) Ducker, W. A.; Senden, T. J.; Pashley, R. M. Direct Measurement of Colloidal Forces Using an Atomic Force Microscope. *Nature* **1991**, *353*, 239−241.
(26) Butt, H. J.; Cappella, B.; Kappl, M. Force Measurements with the Atomic Force Microscope: Technique, Interpretation and Applications. *Surf. Sci. Rep.* **2005**, *59*, 1−152.
(27) Montes Ruiz-Cabello, F. J.; Moazzami-Gudarzi, M.; Elzbieciak-Wodka, M.; Maroni, P.; Labbez, C.; Borkovec, M.; Trefalt, G. Long-Ranged and Soft Interactions between Charged Colloidal Particles Induced by Multivalent Coions. *Soft Matter* **2015**, *11*, 1562−1571.
(28) Russel, W. B.; Saville, D. A.; Schowalter, W. R. *Colloidal Dispersions*; Cambridge University Press: Cambridge, U.K., 1989.
(29) Elzbieciak-Wodka, M.; Popescu, M.; Montes Ruiz-Cabello, F. J.; Trefalt, G.; Maroni, P.; Borkovec, M. Measurements of Dispersion Forces between Colloidal Latex Particles with the Atomic Force Microscope and Comparison with Lifshitz Theory. *J. Chem. Phys.* **2014**, *140*, 104906.
(30) Kruger, M.; Golyk, V. A.; Bimonte, G.; Kardar, M. Interplay of Roughness/Modulation and Curvature at Proximity. *EPL* **2013**, *104*, 41001.
(31) Carnie, S. L.; Chan, D. Y. C. Interaction Free Energy between Plates with Charge Regulation: A Linearized Model. *J. Colloid Interface Sci.* **1993**, *161*, 260−264.
(32) Behrens, S. H.; Borkovec, M. Electrostatic Interaction of Colloidal Surfaces with Variable Charge. *J. Phys. Chem. B* **1999**, *103*, 2918−2928.
(33) Trefalt, G.; Szilagyi, I.; Borkovec, M. Poisson-Boltzmann Description of Interaction Forces and Aggregation Rates Involving Charged Colloidal Particles in Asymmetric Electrolytes. *J. Colloid Interface Sci.* **2013**, *406*, 111−120.
(34) Guldbrand, L.; Jonsson, B.; Wennerstrom, H.; Linse, P. Electrical Double-Layer Forces: A Monte-Carlo Study. *J. Chem. Phys.* **1984**, *80*, 2221−2228.
(35) Ennis, J.; Marcelja, S.; Kjellander, R. Effective Surface Charge for Symmetric Electrolytes in the Primitive Model Double Layer. *Electrochim. Acta* **1996**, *41*, 2115−2124.
(36) Naji, A.; Kanduc, M.; Forsman, J.; Podgornik, R. Perspective: Coulomb Fluids - Weak Coupling, Strong Coupling, in Between and Beyond. *J. Chem. Phys.* **2013**, *139*, 150901.
(37) Bohinc, K.; Grime, J. M. A.; Lue, L. The Interactions between Charged Colloids with Rod-like Counterions. *Soft Matter* **2012**, *8*, 5679−5686.
(38) Montes Ruiz-Cabello, F. J.; Trefalt, G.; Maroni, P.; Borkovec, M. Accurate Predictions of Forces in the Presence of Multivalent Ions by Poisson-Boltzmann Theory. *Langmuir* **2014**, *30*, 4551−4555.
(39) Martell, A. E.; Smith, R. M. *Critical Stability Constants*; Plenum Press: New York, 1982.
(40) O'Brien, R. W.; White, L. R. Electrophoretic Mobility of a Spherical Colloidal Particle. *J. Chem. Soc., Faraday Trans. 2* **1978**, *74*, 1607−1626.
(41) Sader, J. E.; Chon, J. W. M.; Mulvaney, P. Calibration of Rectangular Atomic Force Microscope Cantilevers. *Rev. Sci. Instrum.* **1999**, *70*, 3967−3969.
(42) Hutter, J. L.; Bechhoefer, J. Calibration of Atomic Force Microscope Tips. *Rev. Sci. Instrum.* **1993**, *64*, 1868−1873.
(43) Meyer, E. E.; Rosenberg, K. J.; Israelachvili, J. Recent Progress in Understanding Hydrophobic Interactions. *Proc. Natl. Acad. Sci. U.S.A.* **2006**, *103*, 15739−15746.
(44) Sinha, P.; Popa, I.; Finessi, M.; Montes Ruiz-Cabello, F. J.; Szilagyi, I.; Maroni, P.; Borkovec, M. Exploring Forces between Individual Colloidal Particles with the Atomic Force Microscope. *Chimia* **2012**, *66*, 214−217.
(45) Bevan, M. A.; Prieve, D. C. Direct Measurement of Retarded van der Waals Attraction. *Langmuir* **1999**, *15*, 7925−7936.
(46) Montes Ruiz-Cabello, F. J.; Maroni, P.; Borkovec, M. Direct Measurements of Forces between Different Charged Colloidal Particles and Their Prediction by the Theory of Derjaguin, Landau, Verwey, and Overbeek (DLVO). *J. Chem. Phys.* **2013**, *138*, 234705.
(47) Feick, J. D.; Velegol, D. Measurements of Charge Non-uniformity on Polystyrene Latex Particles. *Langmuir* **2002**, *18*, 3454−3458.

DOI: 10.1021/acs.jpcc.5b04426
J. Phys. Chem. C 2015, 119, 15482−15490

(48) Anderson, J. L. Effect of Nonuniform Zeta Potential on Particle Movement in Electric Fields. *J. Colloid Interface Sci.* **1985**, *105*, 45−54.
(49) Zangi, R.; Hagen, M.; Berne, B. J. Effect of Ions on the Hydrophobic Interaction between Two Plates. *J. Am. Chem. Soc.* **2007**, *129*, 4678−4686.
(50) Chandler, D. Interfaces and the Driving Force of Hydrophobic Assembly. *Nature* **2005**, *437*, 640−647.
(51) Mezei, A.; Meszaros, R. Novel Method for the Estimation of the Binding Isotherms of Ionic Surfactants on Oppositely Charged Polyelectrolytes. *Langmuir* **2006**, *22*, 7148−7151.
(52) Szilagyi, I.; Polomska, A.; Citherlet, D.; Sadeghpour, A.; Borkovec, M. Charging and Aggregation of Negatively Charged Colloidal Latex Particles in Presence of Multivalent Polyamine Cations. *J. Colloid Interface Sci.* **2013**, *392*, 34−41.
(53) Kirkwood, J. G.; Shumaker, J. B. Forces between Protein Molecules in Solution Arising from Fluctuations in Proton Charge and Configuration. *Proc. Natl. Acad. Sci. U.S.A.* **1952**, *38*, 863−871.
(54) Adzic, N.; Podgornik, R. Field-Theoretic Description of Charge Regulation Interaction. *Eur. Phys. J. E* **2014**, *37*, 49.

DOI: 10.1021/acs.jpcc.5b04426
J. Phys. Chem. C 2015, 119, 15482−15490

CHAPTER 3

Nanometer-ranged attraction induced by multivalent ions between similar and dissimilar surfaces probed by the atomic force microscope (AFM)

Moazzami Gudarzi, M.; Trefalt, G.; Szilagyi, I.; Maroni, P.; Borkovec, M., *Phys. Chem. Chem. Phys.* **2016**, 18, 8739-8751.

Reproduced with permission

PCCP

PAPER

View Article Online
View Journal | View Issue

Cite this: *Phys. Chem. Chem. Phys.*, 2016, **18**, 8739

Nanometer-ranged attraction induced by multivalent ions between similar and dissimilar surfaces probed using an atomic force microscope (AFM)

Mohsen Moazzami-Gudarzi, Gregor Trefalt, Istvan Szilagyi, Plinio Maroni and Michal Borkovec*

Received 18th December 2015,
Accepted 23rd February 2016

DOI: 10.1039/c5cp07830j

www.rsc.org/pccp

Direct force measurements between positively charged amidine latex (AL) and negatively charged sulfate latex (SL) particles are carried out using an atomic force microscope (AFM). Forces between three different pairs, namely AL–AL, AL–SL, and SL–SL, are measured in solutions containing multivalent cationic aliphatic hexamines (N6) and in simple monovalent KCl solutions. The classical theory of Derjaguin, Landau, Verwey, and Overbeek (DLVO) can rationalize the observed force profiles very well, provided the PB equation is solved for the appropriate asymmetric electrolyte and charge regulation effects are included in the analysis. However, the DLVO description is typically valid only at distances beyond several nanometers. At shorter distances, a short-ranged non-DLVO attraction is present, which can be modeled with an exponential force profile. In KCl solutions, the range of this attraction is around 0.3 nm. In N6 solutions, the range of this attraction is about 1.0 nm in the SL–SL system, 0.6 nm in the AL–SL system, and 0.3 nm in the AL–AL system.

Introduction

Multivalent ions strongly affect interactions between charged colloidal particles in electrolyte solutions, and this aspect is essential for numerous applications, such as water purification, concrete hardening, or rheology of drilling fluids.[1,2] Interactions in biological systems are equally strongly influenced by multivalent ions (*e.g.*, phosphate, spermine, spermidine).[3–5] For this reason, substantial effort is devoted to the investigation of the forces acting in such systems, both experimentally and theoretically. On the experimental side, one could recently witness the development of reliable tools capable of measuring forces between individual colloidal particles down to sub-nanometer distances. These methods include the colloidal probe technique based on the atomic force microscope (AFM)[6–8] and video microscopy combined with optical or magnetic tweezers.[9–12] These techniques were used to investigate the influence of multivalent ions on the forces acting between colloidal particles or inducing polyelectrolyte collapse.[5,9,13] On the theoretical side, computer simulations and various approximation schemes (*e.g.*, integral equations, density functionals) were employed to better understand the influence of electrostatic interactions on the forces acting between charged interfaces and those determining polyelectrolyte conformations in the presence of multivalent ions.[3,4,14–16]

The classical view relies on the theory of Derjaguin, Landau, Verwey, and Overbeek (DLVO).[17] This theory suggests that forces acting between colloidal particles are principally governed by van der Waals and double layer interactions, whereby the latter ones are being estimated by the Poisson–Boltzmann (PB) mean-field model. At the same time, however, one must postulate that multivalent ions specifically adsorb to the particle surface, thereby modifying the diffuse layer potential and, as a consequence, the double layer forces. The knowledge of the adsorption characteristics of these ions thus becomes essential within this approach.[18]

Modern theories treat electrostatic interactions between the ions beyond the mean-field PB approximation and include ion–ion correlation effects.[14,15] An interesting consequence of this approach is that electrostatic interactions alone may lead to the adsorption of multivalent ions, and induce a charge reversal.[16,19] However, researchers disagree whether additional specific interactions are relevant or not. Another significant prediction of such theories is that electrostatic interactions may induce additional attractive forces, which cannot be simply explained within the traditional DLVO theory.[14,20] However, interaction forces between particles may further be influenced by additional effects, including finite ionic size, image charge contributions, or the shape of ions.[15,21,22]

Department of Inorganic and Analytical Chemistry, University of Geneva, Sciences II, 30 Quai Ernest-Ansermet, 1205 Geneva, Switzerland. E-mail: michal.borkovec@unige.ch; Tel: +41 22 3796405

The theoretical effort has been accompanied by numerous experimental studies, even though the latter activity was possibly less intense. Nevertheless, the surface force apparatus was used early on to study the influence of multivalent ions on the forces acting between mica surfaces.[23] Reliable measurements involving colloidal particles and multivalent ions are relatively recent, and they mostly rely on the colloidal probe technique. Such force measurements involving a silica particle and an amino-functionalized substrate did provide evidence that multivalent counterions induce a charge reversal of the silica particle.[24] These measurements further confirmed the close relation between double layer forces and ζ-potentials obtained from electrokinetic studies.[16,25] Force measurements between two similar colloidal latex particles lead to similar conclusions.[9,13,26] However, these experiments have further suggested that multivalent ions may induce additional attractive non-DLVO forces.[13,27] While their origin could not yet be clearly established, they have an exponential distance dependence. However, so far such non-DLVO forces have not been reported in systems involving two oppositely charged surfaces in the presence of multivalent ions.

We have recently studied negatively charged colloidal particles in the presence of oligomeric aliphatic amines by electrokinetic techniques and direct force measurements.[28,29] Under mildly acidic conditions, these oligoamines form multivalent ions due to partial ionization of the amino groups. In particular, pentaethylenehexamine (N6) leads to a substantial charge reversal and also induces the typical attractive non-DLVO force.[28] For this reason, we decided to investigate the forces between oppositely charged particles in the presence of this oligoamine. In particular, we focus on positively charged amidine latex (AL) and negatively charged sulfate latex (SL). By quantitatively interpreting the forces acting between three different AL–AL, AL–SL, and SL–SL particle pairs, the present investigation goes substantially beyond the previous study, where only results for the SL–SL system were reported.[28] By scanning a wide concentration range of N6, we are able to identify the attractive non-DLVO force in the asymmetric system for the first time.

Experimental

Materials

Positively charged amidine-terminated polystyrene latex (AL) and negatively charged sulfate-terminated polystyrene latex (SL) particles were purchased from Invitrogen. The mean diameters of AL and SL particles were 0.95 μm and 3.0 μm with relative polydispersities of 3.6% and 4.1%, respectively, as determined by the manufacturer by transmission electron microscopy. The aqueous stock particle suspensions were dialyzed until the conductivity of the surrounding solution reached that of pure water, which typically lasts about one week. A cellulose membrane having a cut-off of 50 kg mol^{-1} was used for both particles. In order to determine the particle concentration in the final dispersions, the light scattering intensities of dialyzed suspensions were calibrated through the ones without dialysis of known concentrations. AFM imaging was used to establish that the root-mean square roughness of both types of particles is <0.8 nm. The same particles were used in previous studies, where more details on the characterization can be found.[28,30]

All measurements were performed in aqueous solutions prepared using Milli-Q water (Millipore) at room temperature of 21 ± 3 °C. Pentaethylenehexamine (N6) with the structural formula $H_2N(CH_2CH_2NH)_4CH_2CH_2NH_2$ was purchased in basic form from Sigma-Aldrich. Stock solutions of N6 were prepared in the concentration range of 4–20 g L^{-1}, and adjusted to pH 4.0 with HCl. The final concentration in stock solutions was measured using a total organic carbon and nitrogen analyzer (TOCV, Shimadzu). The solutions to be used in the experiments were prepared by dilution of stock solutions with a 1.0 mM KCl solution, which was also previously adjusted to pH 4.0 with HCl. N6 is not fully charged under these conditions and the precise ionic composition in solution was calculated based on the tabulated ionization constants at infinite dilution. This solution contains 1% of the species with a +3 charge, 88% with +4 charge, and 11% with +5 charge.[28] The contour length of this molecule is 2.0 nm. This molecule assumes a coiled conformation in solution with a radius of gyration of <1 nm. Further experiments were performed in KCl solutions at pH 4.0.

Electrophoresis

The particle charge was studied by electrophoresis using Zeta-Nano ZS (Malvern Instruments, Worcestershire, UK). Particle suspensions were prepared at particle concentrations of about 80 mg L^{-1} in the appropriate solutions of N6 and/or KCl. The samples were equilibrated overnight and the average of at least 5 mobility measurements was taken. The electrophoretic mobility was converted to the electrokinetic potential (ζ-potential) using Henry's model. This model was found to be accurate within 10% for KCl when compared with the results of the standard electrokinetic model.[17,31]

Electrophoresis experiments were used to demonstrate that N6 is almost entirely dissolved in solution and that the quantity adsorbed is negligible with respect to the one in the solution phase. Electrophoresis measurements were carried out at different particle concentrations for the SL system, which clearly indicate that N6 adsorbs and induces a charge reversal.[28] One finds that the electrophoretic mobilities are independent of the particle concentration for the same N6 concentration, and therefore one can conclude that only a negligible fraction of N6 is adsorbed in the relevant range of particle concentrations.[32] For the AL system, the electrophoretic mobility of the particles was compared for KCl and N6 solutions. The mobility values were converted to surface charge density using the standard electrokinetic model combined with the PB model and plotted *versus* the ionic strength. For the N6 solutions, the ionic strength was calculated by including the appropriate distribution of charged species discussed above. The data for both systems collapse, which suggests that the adsorption of N6 to AL particles is negligible.

Direct force measurements

Forces between a pair of latex particles were measured with the multiparticle colloidal probe technique. A closed-loop AFM

(MFP-3D, Asylum Research) mounted on an inverted optical microscope (IX70, Olympus) was used. The glass plate fitting the bottom of the AFM fluid cell was cleaned in piranha solution consisting of a mixture of 98% H_2SO_4 and 30% H_2O_2 in a volumetric ratio of 3 : 1 for 2 h. Subsequently, the plate was washed with pure water, dried in a stream of nitrogen, and treated for 20 min in an air-plasma (PDC-32G, Harrick, New York). The plate was finally silanized overnight in an evacuated container with hexamethyldisilazane (Alfa Aesar), and rinsed with pure water afterwards. A tipless cantilever was cleaned using the plasma cleaner and silanized in the same fashion, except that the silanization time was reduced to 2–3 h.

The silanized glass plate and the cantilever were then mounted in the AFM fluid cell, and a Teflon spacer was introduced to avoid mixing of the two types of latex particle suspensions during deposition. Colloidal suspensions of AL and SL at a particle concentration of about 100 mg L^{-1} were prepared and adjusted to pH 4.0. Initially, the AL suspension was injected into the cell on the left hand side of the spacer and left to deposit for about 1 h. The cell was then thoroughly flushed with 1.0 mM KCl solution of pH 4.0. Subsequently, the SL suspension was injected into the cell on the right hand side of the spacer and left to deposit for another hour, and the cell was flushed with the 1.0 mM KCl solution again. Finally, the spacer was removed and the cell was amply flushed with KCl or N6 solutions of the appropriate concentration, and left to equilibrate for at least 20 min.

To perform the force measurements, the functionalized cantilever was approached to the substrate, and one particle was picked up by pressing the cantilever against the substrate. The AL and SL particles could be easily distinguished due to the different size. Once one of the particles was picked up, it was centered above another particle by observing the interference fringes using an optical microscope. Centering could be achieved with a lateral precision of about 50 nm. After aligning the particles, vertical approach–retraction cycles were recorded with a sampling rate of 5 kHz. The approach velocity was 500 nm s^{-1} and a cycle frequency of 0.5 Hz was used. For each particle pair, at least 100 cycles were recorded. The contact point was determined from the onset of the constant compliance region with a precision of about 0.5 nm. This region was perfectly linear, which confirms that the deformation of the latex particles is negligible in the contact region. The cantilever deflection was converted to forces by Hook's law with the spring constant of the cantilever. This constant was obtained from the frequency response of the cantilever and its lateral dimensions as proposed by Sader *et al.*[33] The resulting values were about 0.1–0.4 N m^{-1} and were within 20% of the values obtained by the thermal noise method.[7] The force profiles were obtained by down-sampling of the traces to 3 kHz and averaging the approach parts of the different cycles, resulting in a force resolution of about 0.5 pN. For better graphical display, the final force curves were further averaged in distance bins of 0.5 nm. At least 3 particle pairs were examined, and for these pairs the force curves were typically reproducible within 10%, see Fig. 1a. Within the same solution, the three different types of particle pairs could be realized in sequence, namely AL–AL or SL–SL in the two symmetric geometries (similar surfaces) and AL–SL in the asymmetric geometry (dissimilar surfaces). We have also compared results measured in two different geometries. First, an AL particle was attached to the cantilever and measured against a SL particle attached to the substrate. Second, a SL particle was attached to the cantilever and measured against an AL particle attached to the substrate. Both geometries gave very similar results as illustrated in Fig. 1b and they were both used to measure the force profiles in the asymmetric AL–SL systems.

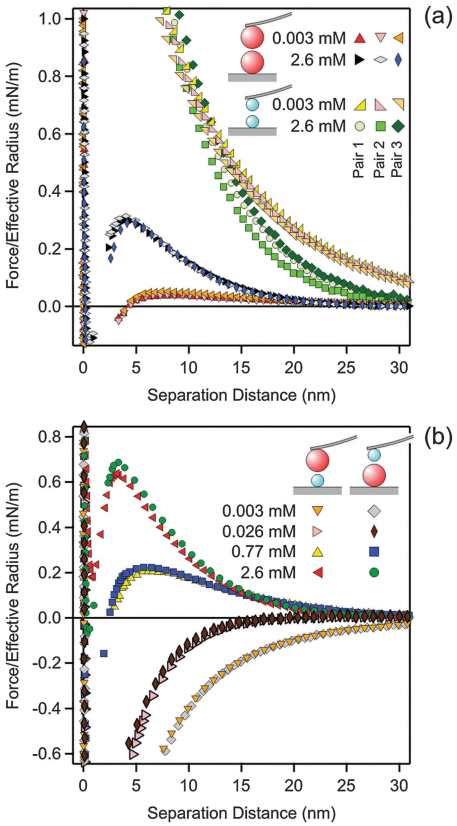

Fig. 1 Reproducibility of the measured force profiles in solutions of N6 in 1.0 mM KCl and pH 4.0 at the concentrations indicated. (a) Comparison of different pairs of particles in the symmetric AL–AL and SL–SL geometries. (b) Comparison of the two realizations of the asymmetric AL–SL system, either with the SL on the cantilever and the AL particle on the substrate, or *vice versa*.

Data analysis

The force profiles were interpreted in terms of a modified DLVO theory. The measured force profile was fitted to the following form:

$$F = F_{vdW} + F_{dl} + F_{att} \quad (1)$$

where F_{vdW} represents the van der Waals force and F_{dl} the double layer force. These two terms correspond to the DLVO contribution, while F_{att} is a short-ranged attractive non-DLVO term. The van der Waals force is modeled with the non-retarded form, namely[17]

$$\frac{F_{vdW}}{R_{eff}} = -\frac{H}{6h^2} \quad (2)$$

where H is the Hamaker constant, h is the separation distance between the surfaces of the particles, and R_{eff} is the effective radius. The latter quantity is given by the relation

$$R_{\mathrm{eff}}^{-1} = R_{\alpha}^{-1} + R_{\beta}^{-1} \quad (3)$$

where R_α and R_β are the radii of the particles α and β. Due to the low polydispersity of the samples, we use the average particle radii. This expression makes use of the Derjaguin approximation, which assumes that the effective radius is much larger than the range of interaction forces.[17] This condition is well satisfied for the particles used here.

The double layer force was evaluated from the PB theory in the plate–plate geometry numerically. This theory describes the electrostatic potential profile $\psi(x)$ as a function of the position x, whereby the two surfaces are located at $x = \pm h/2$. The potential profile satisfied the PB equation

$$\frac{\mathrm{d}^2\psi}{\mathrm{d}x^2} = -\frac{q}{\varepsilon_0\varepsilon}\sum_i z_i c_i \mathrm{e}^{-z_i q\psi/(kT)} \quad (4)$$

where q is the elementary charge, ε_0 the permittivity of vacuum, ε the dielectric constant, k the Boltzmann constant, and T the absolute temperature. The electrolyte solution contains ions of number concentration c_i and valence z_i, and the index i runs over the different ions. This equation is solved for a given separation h subject to the constant regulation (CR) boundary conditions

$$\pm\varepsilon_0\varepsilon\left.\frac{\mathrm{d}\psi}{\mathrm{d}x}\right|_{x=\pm h/2} = \sigma_\pm - C_{\mathrm{I}}^{(\pm)}[\psi(\pm h/2) - \psi_\pm] \quad (5)$$

where $\sigma_\pm$, $\psi_\pm$, and $C_{\mathrm{I}}^{(\pm)}$ are the surface charge density, the diffuse layer potential, and the inner layer capacitance of the respective isolated surfaces. The surface charge density is given by the charge–potential relationship

$$\sigma_\pm = \left\{2kT\varepsilon_0\varepsilon\sum_i c_i\left[\mathrm{e}^{-z_i q\psi_\pm/(kT)} - 1\right]\right\}^{1/2} \quad (6)$$

This relation is valid for $\psi_\pm \geq 0$, while $\sigma_\pm$ must be set to be negative when $\psi_\pm < 0$. Instead of referring to the inner layer capacitance, we introduce the regulation parameter

$$p_\pm = \frac{C_{\mathrm{D}}^{(\pm)}}{C_{\mathrm{D}}^{(\pm)} + C_{\mathrm{I}}^{(\pm)}} \quad (7)$$

where $C_{\mathrm{D}}^{(\pm)}$ is the diffuse layer capacitance of the isolated layer and is given by $C_{\mathrm{D}}^{(\pm)} = \mathrm{d}\sigma_\pm/\mathrm{d}\psi_\pm$. The advantage of introducing the regulation parameter is that it assumes simple values for the classical boundary conditions. For constant charge (CC) conditions one has $p_\pm = 1$, while constant potential (CP) conditions correspond to $p_\pm = 0$. Once the potential profile is known, one can calculate the swelling pressure from the relation

$$\Pi = kT\sum_i c_i\left[\mathrm{e}^{-z_i q\psi/(kT)} - 1\right] - \frac{\varepsilon_0\varepsilon}{2}\left(\frac{\mathrm{d}\psi}{\mathrm{d}x}\right)^2 \quad (8)$$

This pressure is then integrated to obtain the interaction surface energy, which is then converted to the interaction force by means of the Derjaguin approximation, resulting in the relation

$$\frac{F_{\mathrm{dl}}}{R_{\mathrm{eff}}} = 2\pi\int_h^\infty \Pi(h')\mathrm{d}h' \quad (9)$$

here, the PB equation is solved in the KCl system for a 1 : 1 electrolyte, while in the N6 system for a respective mixture of 1 : 1, 3 : 1, 4 : 1, and 5 : 1 electrolytes. Displacement of the plane of origin of the double-layer with respect to the contact point by distances below 1 nm has small effects on the calculated force profiles in the concentration range considered. More details on the numerical procedure can be found elsewhere.[34]

The short-ranged attractive non-DLVO force is modeled with a simple exponential profile

$$\frac{F_{\mathrm{att}}}{R_{\mathrm{eff}}} = -A_{\alpha\beta}\mathrm{e}^{-q_{\alpha\beta}h} \quad (10)$$

where $A_{\alpha\beta}$ is the amplitude and $q_{\alpha\beta}^{-1}$ is the range of the interaction occurring between particles α and β. The observed additional short ranged forces could be successfully described with this functional form in systems containing monovalent and multivalent ions. This observation is in line with previous studies.[27,28,35] The respective parameters will be discussed for the three SL–SL, AL–AL, and AL–SL pairs of particles in the following sections.

Results and discussion

We present direct force measurements between similar and dissimilar particle surfaces in the same electrolyte solutions carried out using the atomic force microscope (AFM). In particular, we study interactions between micrometer-sized positively charged amidine latex (AL) particles and negatively charged sulfate latex (SL) particles in the symmetric AL–AL and SL–SL as well as asymmetric AL–SL geometries. For brevity, we will sometimes denote the AL particles by a + sign and the SL particles by a − sign. This sign refers to the charge of the bare particle. These particles are mainly studied in solutions containing the aliphatic hexamine, denoted as N6, which adsorbs to the SL particles in a flat conformation and induces charge reversal.[28] The three combinations ++, +−, and −− are realized in various electrolyte solutions in the same fluid cell. All experiments are carried out at pH 4.0, whereby N6 predominantly forms tetravalent cations. These experiments are further compared with those in monovalent KCl solutions.

Monovalent salt solutions

The measured force profiles in KCl solutions are shown in Fig. 2. The left column shows the measurements at low salt concentrations, while the right column shows the measurements at higher concentrations. The top row (Fig. 2a) shows the results for the symmetric AL–AL system, the middle row (Fig. 2b) for the asymmetric AL–SL system, and the bottom row (Fig. 2c) for the second symmetric SL–SL system. At high salt concentrations, the forces are attractive and very similar for all the different pairs studied. These attractive forces originate from van der Waals interactions. At lower salt concentrations,

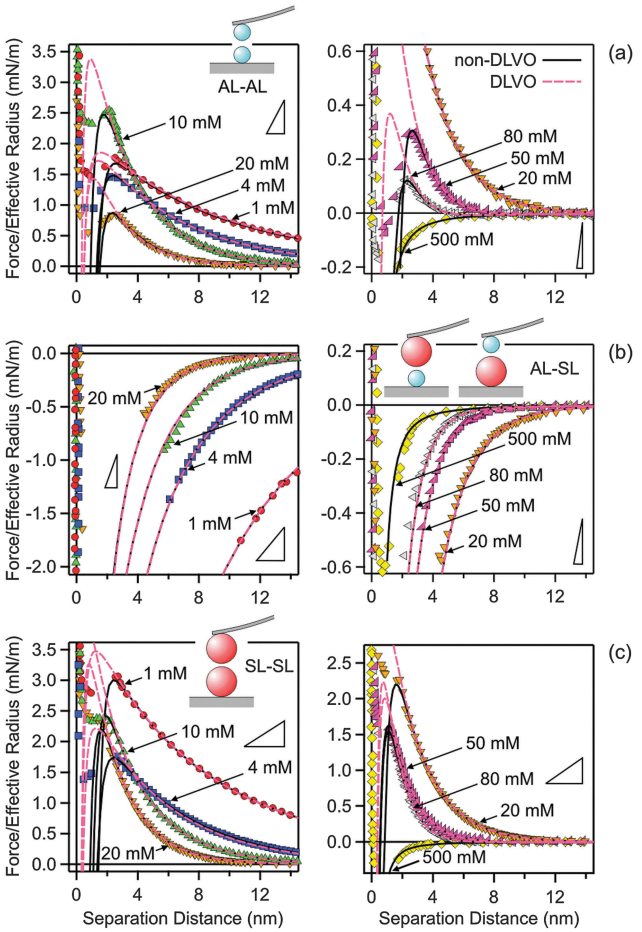

Fig. 2 Comparison of experimental force profiles involving amidine latex (AL) and sulfate latex particles (SL) in KCl solutions at pH 4.0 with calculations based on DLVO theory and those with an additional non-DLVO attraction. Low concentrations are shown in the left column and high concentrations in the right one. The triangles indicate the slope of the expected jump-in instability based on the cantilever spring constant. (a) AL–AL, (b) AL–SL, and (c) SL–SL.

the forces are repulsive for the symmetric AL–AL and SL–SL systems, while they are attractive for the asymmetric AL–SL system. This behavior is typical for double-layer forces. The interacting particles bear the same charge for the symmetric systems, leading to electrostatic repulsion. For the asymmetric systems, the particles are oppositely charged, leading to electrostatic attraction. With increasing salt concentration, the electrostatic interactions are progressively screened, and their contribution disappears at higher concentrations, typically above 100 mM. This behavior is in agreement with DLVO theory. When the forces become strongly attractive, the force profile may not be accessible due to the mechanical jump-in instability of the cantilever. The triangles in Fig. 2 indicate the critical slopes that are given by the spring constant of the cantilever.

The agreement with DLVO theory is only qualitative, however. Quantitative data analysis reveals that additional non-DLVO contributions are important at small separations, and they can be described with an attractive exponential force law given by eqn (10). Best fits of the experimental force profiles with DLVO theory including this non-DLVO contribution are shown as solid lines in Fig. 2. For comparison, results of the DLVO theory without additional attractive contributions are also shown as dashed lines. One observes that DLVO theory is insufficient to model the profiles at intermediate salt concentrations or at smaller distances, especially close to the jump-in occurring around 2 nm.

The quantitative data analysis was carried out according to the following strategy. Initially, van der Waals forces were studied at high salt concentrations, namely in 500 mM KCl solutions. These forces can be only reliably measured under these conditions, since otherwise they are masked by the repulsive double-layer forces. Under these conditions, the double layer interactions are fully screened. The results for the symmetric AL–AL and SL–SL, and the asymmetric AL–SL geometries are shown in Fig. 3. One observes that the data for the three systems coincide within experimental error. The distance dependence can be rather well described using eqn (2) with the common Hamaker constant of $H = (3.5 \pm 0.1) \times 10^{-21}$ J. At larger distances, the experimentally observed force is somewhat weaker than the calculated one, probably due to retardation effects. The reported Hamaker constant is in line with previous studies of the same particles.[28,30] The value is substantially smaller than the non-retarded value of 14.0×10^{-21} J calculated from the dielectric spectra of polystyrene and water from the Lifshitz theory.[17,36] This discrepancy is caused by the combined effect of roughness and retardation, which has been discussed in detail for a similar type of latex particles elsewhere.[37] These effects basically eliminate the salt dependence of the Hamaker constant. They further result in very similar Hamaker constants for the SL and AL particles, probably by coincidence.

Once the Hamaker constant was determined, the force profiles shown in Fig. 2 were quantified in three subsequent steps. In the first step, the force profiles involving the

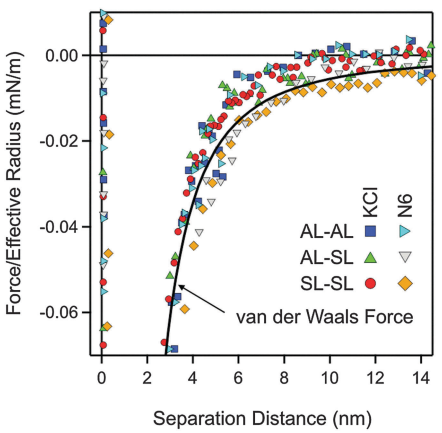

Fig. 3 Experimental force profiles involving different combinations of amidine latex (AL) and sulfate latex particles (SL) at pH 4.0 in 500 mM KCl and in the multivalent N6 systems at a concentration of 520 mM of the amino groups. The solid line is the non-retarded van der Waals force with a Hamaker constant of $H = 3.5 \times 10^{-21}$ J. This value is used in all calculations.

symmetric AL–AL pairs were analyzed (Fig. 2a). Initially, the DLVO theory was used, whereby the double layer forces are calculated using the non-linear PB equation for a simple electrolyte. This description is capable of quantifying the force profiles at larger distances, and yields good estimates of the surface properties, namely the diffuse layer potential and the regulation parameter. At shorter distances, however, the calculated force profiles are more repulsive than the experimental ones. This deficiency can be remedied by adding the exponential attractive non-DLVO contribution given by eqn (10) to the profile. With this modification, the resulting profiles describe the position of the jump-in reasonably well. At smaller distances than the position of the jump-in, the experimental force profiles become unreliable due to the existing mechanical instability and contributions from hydrodynamic interactions. By performing a least-squares fit with the model given by eqn (1), one obtains four different parameters, namely the diffuse layer potential ψ_+, the regulation parameter p_+, as well as the range and the amplitude of the non-DLVO force, namely ${q_{++}}^{-1}$ and A_{++}. Among the fitted parameters, the regulation parameter and the range of the non-DLVO force remained relatively independent of the concentration, leading to the values $p_+ = 0.41 \pm 0.03$ and ${q_{++}}^{-1} = 0.35 \pm 0.02$ nm. Therefore, the AL–AL force profiles were refitted by keeping these quantities fixed to their average values, whereby the diffuse layer potential ψ_+ and the amplitude of the non-DLVO force A_{++} were adjusted. During these and all subsequent fitting procedures, the Hamaker constant was fixed to $H = 3.5 \times 10^{-21}$ J and the salt concentration to the respective nominal value. The diffuse layer potential ψ_+ was assumed to be positive, since ionized amidine groups bear a positive charge.

In the next step, the asymmetric AL–SL force profiles were analyzed (Fig. 2b). In this case, DLVO theory is sufficient to quantify the data. Thereby, the diffuse layer potential ψ_+ and the regulation parameter p_+ of the AL particle were fixed to the previously determined values for the AL–AL pairs, while the corresponding quantities were adjusted for the SL particles, namely ψ_- and p_-. Again, the regulation parameter shows no clear trends with the concentration, and is $p_- = 0.36 \pm 0.07$. This quantity was therefore fixed to the average value, and the entire series of force profiles was refitted, which yields the diffuse layer potential ψ_- of the SL particles. The negative sign of the diffuse layer potential of the SL particles follows from the force profiles in the asymmetric setting unambiguously, since the AL particles are positively charged. These experimental data provide no evidence of an additional non-DLVO attraction, but we will come back to this point later. An earlier study reported a regulation parameter of 0.41 ± 0.03 for the same SL particles in the same electrolyte.[28] This value is in good agreement with the presently reported one.

In the last step, the symmetric SL–SL force profiles were quantified (Fig. 2c). At this point, the surface properties of the SL particles, namely the diffuse layer potential ψ_- and the regulation parameter p_-, are known from the fit of the asymmetric situation, and it was comforting to see that DLVO theory predicts the force profiles at larger distances very well. At shorter distances, however, the forces are again more attractive than what is suggested by the DLVO theory, and this shortcoming can be again remedied by adding an attractive exponential non-DLVO contribution given by eqn (10). Therefore, the fitting of the SL–SL force profiles only involves the determination of the range and amplitude of this interaction, namely ${q_{--}}^{-1}$ and A_{--}. The range was again relatively independent of the concentration, and yields an average value of ${q_{--}}^{-1} = 0.32 \pm 0.05$ nm. The force profiles could be described well by fixing this parameter to the latter value and by fitting the amplitude A_{--} only.

The resulting parameters obtained from these fits are summarized in Table 1 and Fig. 4. Table 1 includes the parameters which can be assumed to be independent of the concentration, while Fig. 4 reports the concentration dependent ones.

First focus on the fitted diffuse layer potentials shown in Fig. 4a. The magnitude of the diffuse layer potential decreases with increasing salt concentration. This trend is expected on the basis of PB theory.[17] The reported potentials for the SL particles compare well with a previous study, where these values were determined from the symmetric SL–SL particle pairs.[28] The electrokinetic potential (ζ-potential) for the two types of particles is equally shown for comparison. These measurements confirm the signs of the potentials, as well as the overall trends. However, the magnitude of the electrokinetic potentials is substantially larger than the ones determined from the AFM experiment. These discrepancies are likely related to surface charge heterogeneities of the latex particles.[38] These heterogeneities could induce an additional rotational motion of the particles, which would lead to an enhancement of the electrophoretic mobility.[39] Similar discrepancies between diffuse layer potentials measured by AFM and electrophoresis were reported earlier in other latex particle systems.[37,40] We suspect that AFM measurements provide a more reliable estimate of the diffuse layer potential, since the interaction force represents an equilibrium quantity, the entire profile is fitted to the model, and the consistency of the measured potentials can be tested independently. On the other hand, electrokinetic techniques require the interpretation of a dynamic quantity and provide only a one point measurement.[31]

Table 1 Summary of parameters obtained from fitting the experimental force profiles

	Regulation parameter		Range of non-DLVO exponential interaction		
Solution	p_+ AL	p_- SL	${q_{++}}^{-1}$ (nm) AL–AL	${q_{+-}}^{-1}$ (nm) AL–SL	${q_{--}}^{-1}$ (nm) SL–SL
KCl	0.41 ± 0.03	0.36 ± 0.07	0.35 ± 0.02	—	0.32 ± 0.05
N6	0.38 ± 0.02	Fig. 7b	0.34 ± 0.02	0.56 ± 0.03	1.0 ± 0.1

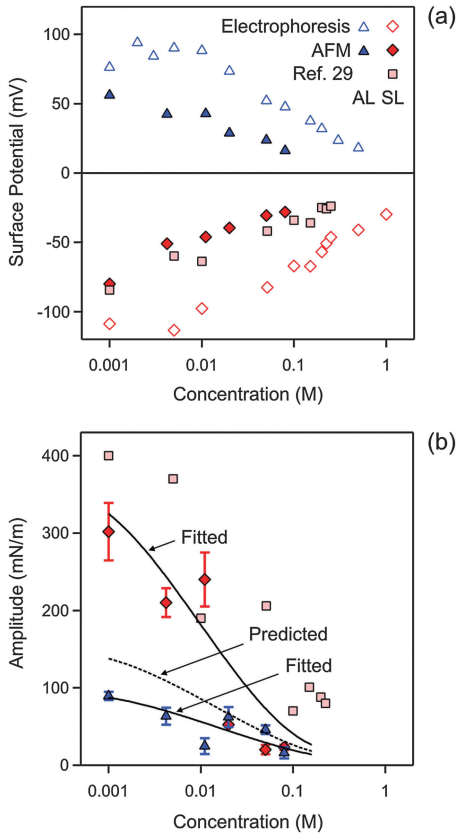

Fig. 4 Concentration dependence of parameters obtained by fitting the experimental force profile with DLVO theory including the non-DLVO attraction in KCl solutions at pH 4.0. (a) Diffuse layer potential obtained from the present AFM measurements compared with the electrokinetic potential (ζ-potential) from electrophoresis. (b) Amplitude of the non-DLVO attraction. The two solid lines are empirical fitting functions of the amplitudes A_{++} and A_{--}, and the dotted line in between is the prediction for A_{+-} using eqn (12). The corresponding data obtained from the symmetric SL–SL system in an earlier study[28] are also shown. Table 1 shows the fitted parameters that are concentration independent. The error bars are indicated in (b), but they are comparable to the size of the data points in (a).

The diffuse layer potentials of the SL particles were obtained from the force profiles in two different ways, namely from the analysis of the AL–AL and AL–SL systems as shown here, and from the symmetric SL–SL system discussed elsewhere[28] (Fig. 4a). These two estimates agree very well, and this agreement confirms the self-consistency of the analysis of the force profiles in terms of DLVO theory. Good agreement between diffuse layer potentials obtained from a similar analysis of force profiles in symmetric and asymmetric systems was also reported in other systems.[34] For this reason, we suspect that the AFM potentials represent more reliable estimates of the diffuse layer potential than the ones obtained from electrokinetics.

The nature of the attractive non-DLVO force, which can be described with an exponential law, resembles results from previous reports.[13,27,35,40] In particular, an earlier study also analyzed short ranged forces between the same SL particles in the KCl electrolyte with an exponential force profile.[28] That study reports the same range as reported here, and the measured amplitudes are very similar to the ones given here. The presently observed range is fully consistent with measurements using the surface force apparatus and theoretical calculations.[35]

Fig. 5 illustrates how the boundary conditions used in the PB calculations affect the force profiles. The respective parameters are summarized in Table 2. Focus on the leftmost column, where the force profiles in 4.0 mM KCl solution are shown. The other columns will be discussed later. The solid lines correspond to the results of DLVO theory including the non-DLVO attraction, while the dashed ones to DLVO theory alone. The underlying PB calculations rely on the CR approximation. The grey regions are delimited with the respective results for CC and CP boundary conditions that also include the non-DLVO attraction. The CC conditions lead to the most repulsive profile, while charge regulation makes the profile less repulsive. One observes that the nature of the boundary conditions is moderately important in all three different geometries.

Multivalent salt solutions

Forces between these particles in the presence of multivalent N6 cations are more complex due to the charge reversal of the SL particles.[28,29] The force profiles measured at pH 4.0 and in the presence of 1.0 mM KCl for different N6 concentrations are summarized in Fig. 6. Again, the profiles for the different pairs of particles are given in different rows, namely AL–AL in the top row (Fig. 6a), AL–SL in the middle row (Fig. 6b), and SL–SL in the bottom row (Fig. 6c). The columns summarize increasing concentrations of N6 (from left to right). The concentrations in the N6 system always refer to the molar concentration of the amino groups. At very high concentrations, the forces are attractive for all different pairs, since they are dominated by van der Waals forces. As illustrated in Fig. 3, these attractive forces are identical to the ones observed in the KCl system within experimental error.

For the symmetric AL–AL system (top row), the repulsive forces at lower N6 concentrations are dominated by double layer interactions between the positively charged particles. The situation resembles the one in monovalent KCl solution. This behavior can be understood due to the multivalent nature of the N6 cations. Highly charged co-ions are expelled from the proximity of the positively charged surface, and therefore they play only a minor role.

On the other hand, the forces acting between the AL–SL and SL–SL pairs in the presence of N6 oligomers are very different from the ones in monovalent salt solutions. This difference is due to the charge reversal induced by the adsorption of the N6 cations to the negatively charged SL particles. This charge reversal can be most clearly seen in the asymmetric AL–SL system. At low N6 concentrations, double layer interactions between the oppositely charged surfaces of the AL and SL particles induce attractive forces. As the N6 concentration is increased, the forces become repulsive. These repulsive forces are again caused by double layer interactions, but now the SL particles become positively charged. This charge reversal is caused by the strong adsorption of the multivalent N6 cations

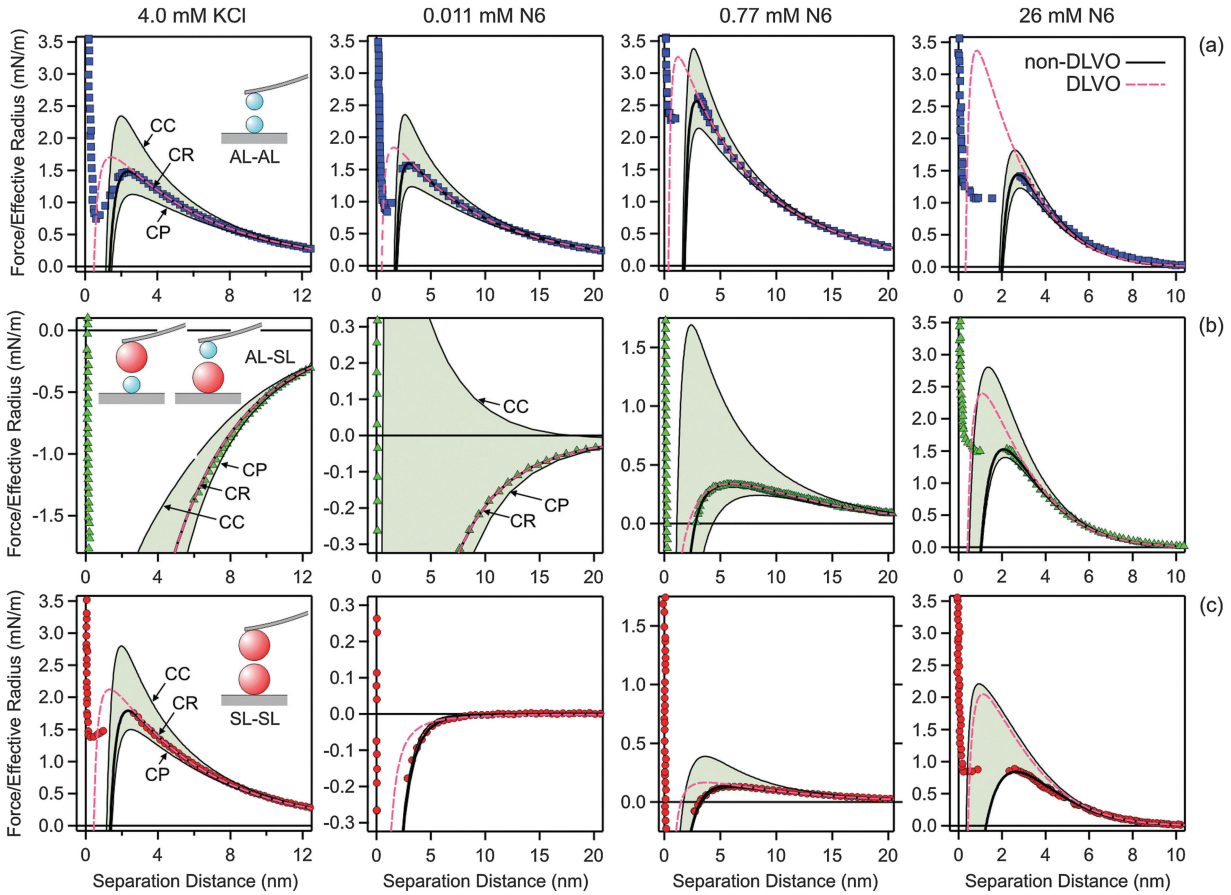

Fig. 5 Comparison of selected experimental force profiles involving amidine latex (AL) and sulfate latex particles (SL) with DLVO theory with CR approximation and the one where the non-DLVO attraction is included. The grey regions are delimited by the corresponding profiles including the non-DLVO attraction with CC and CP conditions. The columns refer to different systems and concentration. The leftmost column 1 is for 4.0 mM KCl solution, while the remaining columns refer to N6 solutions with concentrations of the amino groups of 0.011 mM in column 2, 0.77 mM in column 3, and 26 mM in the rightmost column 4. The parameters used for calculations are given in Table 2. (a) AL–AL, (b) AL–SL, and (c) SL–SL.

Table 2 Parameters used for the calculations shown in Fig. 5

Quantity	Symbol	KCl 4.0 mM	N6 0.011 mM[a]	N6 0.77 mM[a]	N6 26 mM[a]
Diffuse layer potential	ψ_+ (mV)	+44	+56	+68	+41
	ψ_- (mV)	−50	−3.5	+19	+38
Regulation parameter	p_+	0.41	0.38	0.38	0.38
	p_-	0.36	0.13	0.08	0
Amplitude of non-DLVO interaction[b]	A_{++} (mN m^{-1})	65	380	480	800
	A_{+-} (mN m^{-1})	103	5.4	7.0	15
	A_{--} (mN m^{-1})	240	2.7	3.5	7.2

[a] Concentration of amino groups. [b] The range of the interaction $q_{\alpha\beta}^{-1}$ is given in Table 1.

to the SL particle surface. With increasing N6 concentration, this repulsion becomes stronger due to progressive adsorption, but at even higher concentrations, it weakens again due to screening. At very high concentrations, the double layer interactions are completely screened, and the forces become attractive due to van der Waals interactions (Fig. 3). At the charge reversal point, which occurs at around 0.011 mM, the forces are more attractive, but mainly due to charge regulation effects.

The forces between SL–SL pairs are also strongly influenced by charge reversal. At low concentrations, the interactions are dominated by repulsive double layer forces, since the SL particles are negatively charged. When the concentration is increased, the surface undergoes a charge reversal at 0.011 mM. At the charge reversal point, the forces are attractive, as they are dominated by van der Waals interactions. At higher concentration, the surfaces become positively charged, and they repel

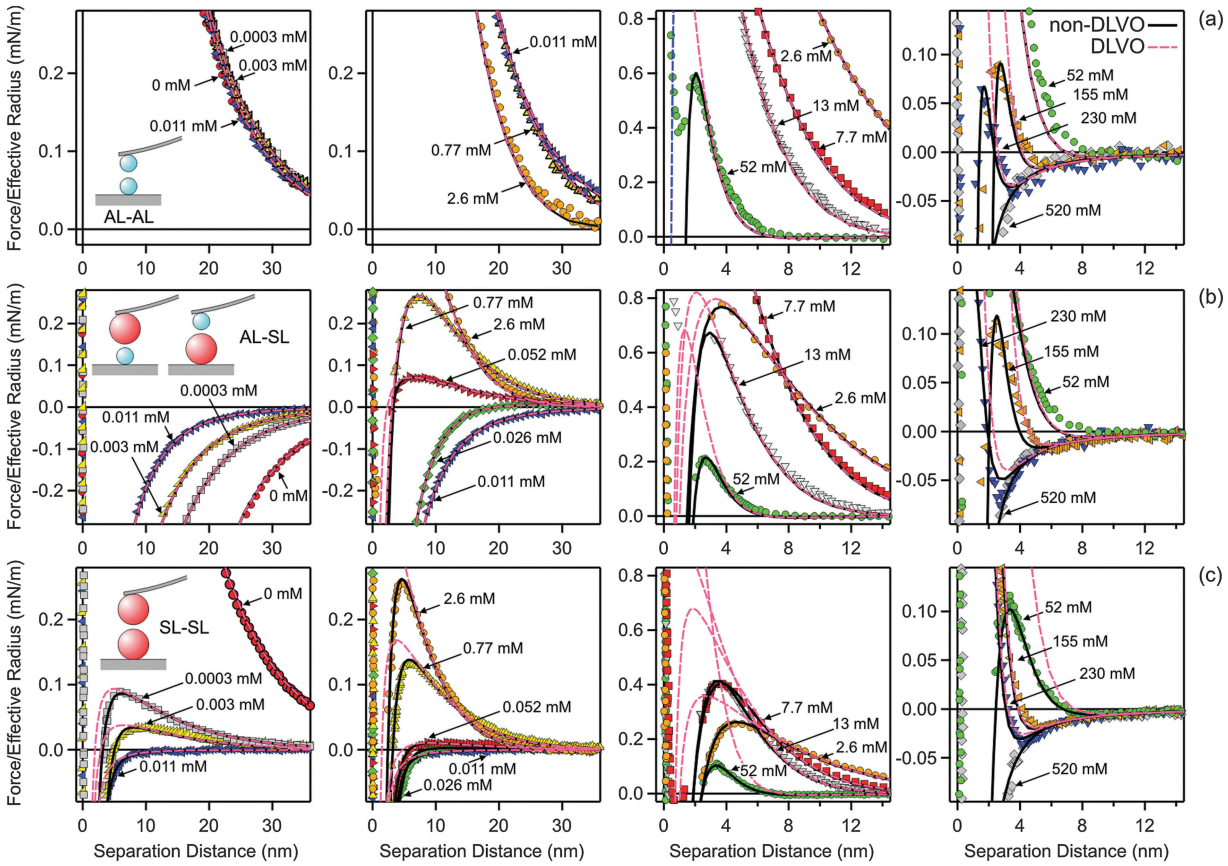

Fig. 6 Comparison of experimental force profiles involving amidine latex (AL) and sulfate latex particles (SL) in N6 solutions at pH 4.0 with calculations based on DLVO theory and those with an additional non-DLVO attraction. The concentration refers to the molar concentration of the amino groups, and they increase from the leftmost column to the rightmost one. (a) AL–AL, (b) AL–SL, and (c) SL–SL.

again through double layer forces. When the concentration is increased further, the double layer forces are weakened by ionic screening, until they disappear completely and the forces become attractive again due to the dominance of van der Waals interactions.

While this mechanism is in line with DLVO theory, a quantitative comparison demonstrates that this theory cannot fully rationalize the data, see Fig. 6. This comparison again reveals the presence of an additional non-DLVO attraction, which can be modeled with an exponential force profile given by eqn (10). A similar fitting strategy as for the monovalent electrolyte was used. However, the double layer forces must be calculated using the non-linear PB equation for the appropriate electrolyte mixture, which includes multivalent cations as well as monovalent cations and anions. The ionic composition was kept fixed during the calculations. The same Hamaker constant as previously determined in the monovalent system was used. The model parameters were determined as follows. In a first step, the forces between AL–AL particles were quantified. Thereby, the surface properties, namely the diffuse layer potential ψ_+ and the regulation parameter p_+, as well as the parameters of the non-DLVO force, namely the range ${q_{++}}^{-1}$ and the amplitude A_{++}, were fitted. The regulation parameter and the range showed no clear trends, with average values $p_+ = 0.38 \pm 0.02$ and ${q_{++}}^{-1} = 0.34 \pm 0.02$ nm. The profiles could be successfully fitted by fixing these parameters to their average values, and only adjusting ψ_+ and A_{++}. In a second step, the forces between AL–SL particles were investigated. Thereby, the surface parameters of the AL particles were fixed to the previously determined values. Therefore, the fitting process involved the surface properties ψ_- and p_-, and the parameters of the non-DLVO force ${q_{+-}}^{-1}$ and A_{+-}. Within this series, the range ${q_{+-}}^{-1}$ remained approximately constant, and could be fixed to its average value of ${q_{+-}}^{-1} = 0.56 \pm 0.03$ nm. The remaining parameters, namely ψ_-, p_-, and A_{+-}, had to be adjusted for each profile. In contrast to the monovalent situation, the regulation parameter p_- could not be kept fixed within the concentration series, but could be constrained to $p_- > 0$. In a third step, the forces between SL–SL were analyzed. The surface properties of the SL particles, namely ψ_- and p_-, were taken from the asymmetric system, and the fitting involved only the parameters of the short-ranged exponential non-DLVO force, namely its range ${q_{--}}^{-1}$ and the amplitude A_{--}. The range could be again fixed to its average value of ${q_{--}}^{-1} = 1.0 \pm 0.1$ nm, and the entire series could be rationalized with a single adjustable parameter, namely the amplitude A_{--}.

The resulting parameters are summarized in Table 1 and Fig. 7 and 8. Table 1 displays the parameters that remained

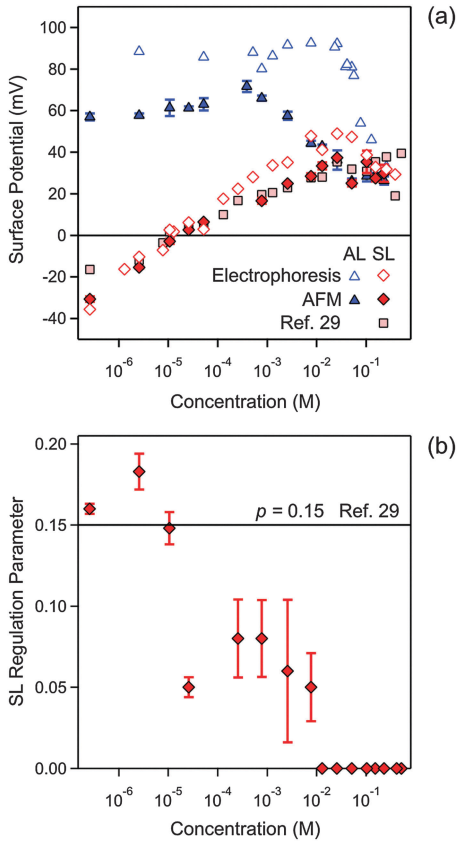

Fig. 7 Concentration dependence of parameters obtained by fitting the experimental force profile with DLVO theory including the non-DLVO attraction in N6 solutions at pH 4.0. The concentration refers to molar concentration of the amino groups. (a) Diffuse layer potential obtained from the present AFM measurements compared with the electrokinetic potential (ζ-potential) from electrophoresis (b) and regulation parameter. The corresponding data obtained from the symmetric SL–SL system in an earlier study[28] are also shown. Table 1 shows the fitted parameters that are concentration independent. The error bars are indicated in (b), but they are comparable to the size of the data points in (a).

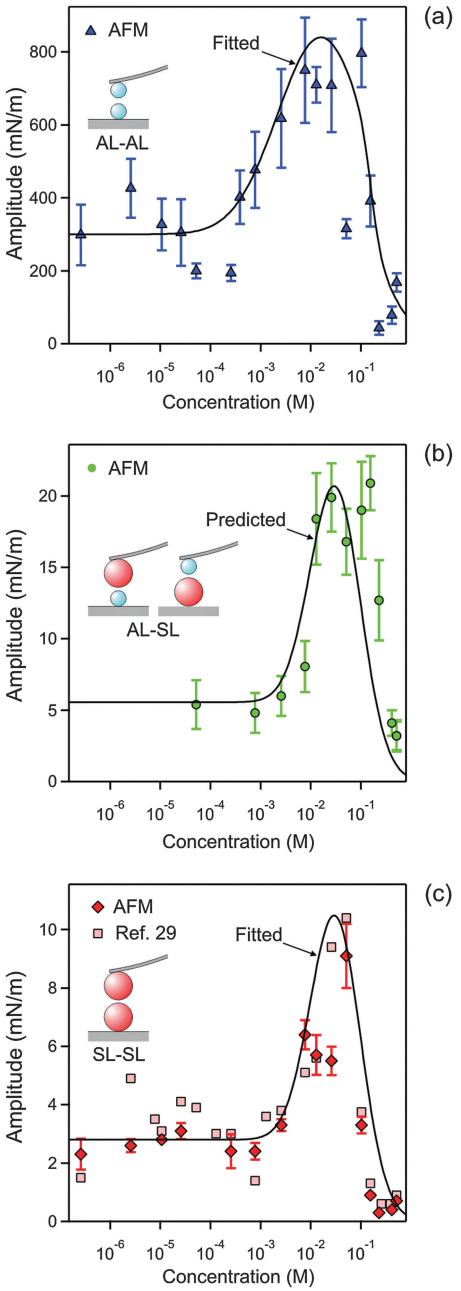

Fig. 8 Concentration dependence of the amplitude of the non-DLVO attraction in N6 solutions at pH 4.0 obtained by fitting the force profiles measured with the AFM. The concentration refers to molar concentration of the amino groups. (a) AL–AL, (b) AL–SL, and (c) SL–SL. The lines in (a and c) are empirical fitting functions of the amplitudes A_{++} and A_{--}, and the one in (b) is the prediction of A_{+-} with eqn (12). The corresponding data obtained from the symmetric SL–SL system in an earlier study[28] are also shown in (c). Table 1 shows the fitted parameters that are concentration independent.

fixed within the series, while the figures illustrate parameters that vary with the N6 concentration.

Fig. 7 summarizes the concentration dependence of the surface properties. The diffuse layer potentials of the AL and SL particles are shown in Fig. 7a. The diffuse layer potentials obtained from the force measurements are compared with the electrokinetic potentials (ζ-potential) measured by electrophoresis. These values agree very well for the SL particles, but the electrokinetic potentials are larger for the AL particles. A similar disagreement was observed for the monovalent electrolyte (Fig. 4a) and for other latex particles.[37,40] The diffuse layer potential of AL particles is positive, and goes through a weak maximum as a function of concentration. At high concentrations, this behavior resembles the monovalent case, and is characteristic of a surface, which interacts weakly with the ions present. For the SL particles, however, the potential strongly increases due to adsorption of the multivalent cationic N6 species. The diffuse layer potential vanishes at 0.011 mM, increases further, and after passing through a weak maximum it decreases again. The electrokinetic potentials now agree rather well with the diffuse layer potentials obtained by AFM. Such a charge reversal is characteristic of multivalent ions adsorbing to oppositely charged surfaces, and it was reported in similar systems earlier.[24,28–30]

The diffuse layer potentials of the SL particles obtained from the present analysis of the AL–AL and AL–SL systems compare favorably with the ones obtained from the symmetric SL–SL

system as discussed elsewhere (Fig. 7a).[28] This agreement again provides solid evidence of the self-consistency of the present DLVO analysis of the force profiles. In this situation, the diffuse layer potentials obtained from the AFM experiments also agree well with the electrokinetic ζ-potentials. The latter agreement probably results from the smoothing out of the surface charge heterogeneities through the adsorption of N6 oligomers.

In the presence of N6, the regulation parameter decreases with concentration for the SL particles, see Fig. 7b. Such a decrease is unusual, since in various other situations, the force profiles were compatible with a regulation parameter that was independent of concentration.[30,41] A constant regulation parameter is also consistent with the force profiles in the present system, in particular, for monovalent salt solutions, and for the AL particles in the presence of N6 (Table 1). A previous study reported a concentration independent regulation parameter $p_- = 0.15$ in the same SL–SL system containing N6 cations.[28] While a constant regulation parameter is consistent with the data for the symmetric SL–SL system, but when this parameter is calculated from the asymmetric AL–SL system, one observes the decrease shown in Fig. 7b. This discrepancy illustrates the difficulties in estimating regulation parameters reliably, especially from data obtained in symmetric systems near a charge reversal.

The resulting parameters for the exponential non-DLVO attractive force are given in Table 1 and Fig. 8. For the AL–SL pairs, this additional force can only be reliably quantified for sufficiently high concentrations, roughly above 0.05 mM. The observed range for the AL–AL system of ${q_{++}}^{-1} = 0.34 \pm 0.02$ nm is well comparable with the values measured in the KCl electrolyte. For the SL–SL system, however, the range is substantially larger, namely ${q_{--}}^{-1} = 1.0 \pm 0.1$ nm. For the AL–SL system, the range lies in between. Previous force measurements across electrolyte solutions containing multivalent counterions in symmetric systems indicate the presence of an additional non-DLVO attraction with a range of a few nm.[13,27,28]

The amplitudes determined for the AL–AL, AL–SL, and SL–SL pairs follow similar trends (Fig. 8). This amplitude remains relatively constant at low N6 concentrations, but then goes through a maximum located around 30 mM, and finally decreases sharply to vanishingly small values. The magnitude of the amplitude decreases with increasing range of attraction, namely in the sequence AL–AL, AL–SL, and SL–SL. The amplitudes for the short-ranged exponential attraction were equally extracted from the SL–SL data in a previous study, albeit assuming a constant regulation parameter.[28] These values are also presented in Fig. 8c, and they agree with the present results very well. Previous measurements with latex particles in the presence of multivalent ions also report comparable strength of the short-ranged attraction and amplitudes passing through a maximum with increasing salt concentrations.[13]

Fig. 5 illustrates the major influence of boundary conditions in the PB calculations on the force profiles for the system containing N6. The parameters used in the calculations are given in Table 2. The column depicts force profiles for three different concentrations, namely 0.011 mM (column 2), 0.77 mM (column 3), and 26 mM (rightmost column 4). The shaded regions are again delimited with the results for CC and CP boundary conditions. The concentration of 0.011 mM reflects the charge neutralization point of the SL particles (Fig. 5, column 2). The forces in the AL–AL system are controlled by repulsive double layer forces, since these particles are highly charged. In this situation, the boundary conditions do play some role. For the SL–SL system, the forces are attractive, since the particles are neutral and their interaction is dominated by van der Waals forces and additional attractive non-DLVO forces. Since the double layer forces are negligible, the boundary conditions have no influence. The forces in the AL–SL system are attractive, but they are again dominated by double layer forces. In this case, however, boundary conditions are extremely important, since CC conditions lead to repulsion, while CP conditions to attraction. Therefore, the force profiles are highly sensitive to the regulation parameter of the SL particles, and this sensitivity permits that its value can be accurately extracted from such force profiles. The importance of the boundary conditions in similar asymmetric systems was also pointed out recently.[26,30,41] The presence of an additional non-DLVO attraction is clearly evident in the SL–SL systems, since the observed attractive force is substantially stronger than the van der Waals force. Similar enhancement of the attraction by multivalent counterions at the charge neutralization point was also reported in other systems.[27,28,30] This attractive force cannot be fitted with eqn (2) alone, but rather a superposition of eqn (2) and (10) is needed. For the concentration of 0.77 mM (Fig. 5, column 3), both particles are positively charged, but the surface charge density of the SL particle is small, while that of the AL particle is substantial. The force profiles for the AL–SL systems are again dominated by double layer forces, but they are repulsive at larger distances, while they become attractive upon approach. This characteristic shape can be well described by PB theory, provided one uses the correct values of the regulation parameters. In these situations, the boundary conditions are extremely important. For the concentration of 26 mM (Fig. 5, rightmost column 4), the effect of boundary conditions is relatively small for the AL–AL system, moderate for AL–SL, and largest for SL–SL. Under these conditions, however, the contribution of the non-DLVO attraction is substantial.

Mixing rule for the non-DLVO attraction

Given the ranges and amplitudes of the exponential non-DLVO attraction, one would like to have a simple mixing rule, which could predict the parameters of this force for the asymmetric system from the two symmetric ones. An arithmetic mean of the decay constants yields a relatively good estimate of the decay constant in the mixed system, namely

$$q_{+-} = \frac{1}{2}(q_{++} + q_{--}) \tag{11}$$

With ${q_{++}}^{-1} = 0.34$ nm and ${q_{--}}^{-1} = 1.0$ nm eqn (11) leads to the estimate ${q_{+-}}^{-1} = 0.51$ nm. This value is in good agreement with the experimentally observed value of ${q_{+-}}^{-1} = 0.56$ nm (Table 1).

The amplitudes can be calculated from the harmonic mean of the values for the symmetric system reasonably well, namely

$$A_{+-}{}^{-1} = \frac{1}{2}\left(A_{++}{}^{-1} + A_{--}{}^{-1}\right) \quad (12)$$

This result is illustrated with solid lines in Fig. 8. The data for the symmetric AL–AL and SL–SL were fitted with an empirical function, and these two functions were used to calculate the resulting harmonic mean, which is then shown as the dotted line together with the AL–SL data. One observes that the simple harmonic mean is capable of predicting the amplitudes in the AL–SL system quite well.

One can also investigate whether this simple mixing rule is consistent with the findings in the monovalent KCl system. Recall that an additional attractive component could not be identified between the AL–SL pairs, since the relevant part of the force curves was inaccessible due to the jump-in instability of the cantilever. Nevertheless, the data obtained in the symmetric systems can be used to calculate the effect of the non-DLVO attraction on the forces in the asymmetric system with the proposed mixing rules given in eqn (11) and (12). The predicted range of the exponential force for the AL–SL system is 0.33 nm, and the corresponding amplitudes are indicated in Fig. 4b. These parameters can be used to calculate the expected contribution of the non-DLVO forces in the AL–SL system, and the results are shown in Fig. 2. The contribution of the additional attraction is small, and cannot be seen on the scale of the graph. Still, the calculated force profiles that include the predicted non-DLVO force do not contradict the experimental data, and we conclude that the proposed mixing rule is also consistent with the data obtained in the monovalent KCl system.

One must stress, however, that this mixing rule is purely empirical, and this rule might not be applicable to other types of electrolytes or in other systems.

Conclusion

This study presents a comprehensive set of direct force measurements involving positively charged AL and negatively charged SL particles, particularly investigating forces between three different pairs, namely AL–AL, AL–SL, and SL–SL. Measurements in solutions containing multivalent cationic aliphatic amines N6 are compared with those in simple monovalent KCl solutions. In all situations, the DLVO theory is capable of describing the force profiles very well. To obtain good agreement with experiment, however, the PB equation must be solved for the appropriate asymmetric electrolyte and charge regulation effects must be included in the analysis. The observed force profiles cannot be rationalized without detailed consideration of charge regulation effects.

However, the description by DLVO theory is only valid at distances beyond 5 nm. At shorter distances, one observes a short-ranged non-DLVO attraction, which can be modeled with an exponential force profile. In the monovalent system, the range of this attraction is around 0.3 nm. In the multivalent symmetric systems, the range of this attraction is about 1.0 nm in the SL–SL system, where the multivalent ions represent the counterions, but is again 0.3 nm in the AL–AL system, where the multivalent ions are the co-ions. For the first time, we were able to identify the non-DLVO attraction in the asymmetric AL–SL system. Here, we find an intermediate range of about 0.6 nm. The amplitude of this attraction decreases with increasing concentration for the monovalent system, while it passes through a maximum for the multivalent system. These findings are in line with previous reports.[13,40] The origin of this attraction is currently not clear to us, but it could be related to ion–ion correlations, surface charge heterogeneities, hydrophobic forces, charge fluctuations, or electrolyte depletion.[15,35,42,43] While ion–ion correlations represent an interesting possibility, theoretical studies suggest that the strength of these forces should increase with increasing salt concentrations,[15,20] and the present experiments suggest a weakening of the additional attraction under these conditions. This observation points towards the importance of other forces as well.

Acknowledgements

This work was supported by the Swiss National Science Foundation and the University of Geneva.

References

1 B. Bolto and J. Gregory, *Water Res.*, 2007, **41**, 2301–2324.
2 B. Jonsson, A. Nonat, C. Labbez, B. Cabane and H. Wennerstrom, *Langmuir*, 2005, **21**, 9211–9221.
3 Y. Burak, G. Ariel and D. Andelman, *Curr. Opin. Colloid Interface Sci.*, 2004, **9**, 53–58.
4 M. O. Khan and B. Jonsson, *Biopolymers*, 1999, **49**, 121–125.
5 K. Besteman, K. Van Eijk and S. G. Lemay, *Nat. Phys.*, 2007, **3**, 641–644.
6 W. A. Ducker, T. J. Senden and R. M. Pashley, *Nature*, 1991, **353**, 239–241.
7 H. J. Butt, B. Cappella and M. Kappl, *Surf. Sci. Rep.*, 2005, **59**, 1–152.
8 G. Toikka, R. A. Hayes and J. Ralston, *Langmuir*, 1996, **12**, 3783–3788.
9 C. Gutsche, U. F. Keyser, K. Kegler and F. Kremer, *Phys. Rev. E: Stat., Nonlinear, Soft Matter Phys.*, 2007, **76**, 031403.
10 J. Baumgartl, J. L. Arauz-Lara and C. Bechinger, *Soft Matter*, 2006, **2**, 631–635.
11 K. C. Neuman and A. Nagy, *Nat. Methods*, 2008, **5**, 491–505.
12 D. R. Baselt, G. U. Lee, M. Natesan, S. W. Metzger, P. E. Sheehan and R. J. Colton, *Biosens. Bioelectron.*, 1998, **13**, 731–739.
13 F. J. Montes Ruiz-Cabello, G. Trefalt, Z. Csendes, P. Sinha, T. Oncsik, I. Szilagyi, P. Maroni and M. Borkovec, *J. Phys. Chem. B*, 2013, **117**, 11853–11862.
14 R. Kjellander and S. Marcelja, *Chem. Phys. Lett.*, 1984, **112**, 49–53.

15 A. Naji, M. Kanduc, J. Forsman and R. Podgornik, *J. Chem. Phys.*, 2013, **139**, 150901.
16 A. Martin-Molina, C. Rodriguez-Beas, R. Hidalgo-Alvarez and M. Quesada-Perez, *J. Phys. Chem. B*, 2009, **113**, 6834–6839.
17 W. B. Russel, D. A. Saville and W. R. Schowalter, *Colloidal Dispersions*, Cambridge University Press, Cambridge, 1989.
18 D. A. Sverjensky, *Geochim. Cosmochim. Acta*, 2006, **70**, 2427–2453.
19 S. Raafatnia, O. A. Hickey, M. Sega and C. Holm, *Langmuir*, 2014, **30**, 1758–1767.
20 J. Forsman, *J. Phys. Chem. B*, 2004, **108**, 9236–9245.
21 K. Bohinc, J. M. A. Grime and L. Lue, *Soft Matter*, 2012, **8**, 5679–5686.
22 M. M. Hatlo and L. Lue, *Soft Matter*, 2008, **4**, 1582–1596.
23 R. M. Pashley, *J. Colloid Interface Sci.*, 1984, **102**, 23–35.
24 K. Besteman, M. A. G. Zevenbergen, H. A. Heering and S. G. Lemay, *Phys. Rev. Lett.*, 2004, **93**, 170802.
25 R. O. James and T. W. Healy, *J. Colloid Interface Sci.*, 1972, **40**, 53–64.
26 C. Zhao, D. Ebeling, I. Siretanu, D. van den Ende and F. Mugele, *Nanoscale*, 2015, **7**, 16298–16311.
27 O. Zohar, I. Leizerson and U. Sivan, *Phys. Rev. Lett.*, 2006, **96**, 177802.
28 M. Moazzami-Gudarzi, G. Trefalt, I. Szilagyi, P. Maroni and M. Borkovec, *J. Phys. Chem. C*, 2015, **119**, 15482–15490.
29 I. Szilagyi, A. Polomska, D. Citherlet, A. Sadeghpour and M. Borkovec, *J. Colloid Interface Sci.*, 2013, **392**, 34–41.
30 F. J. Montes Ruiz-Cabello, G. Trefalt, P. Maroni and M. Borkovec, *Langmuir*, 2014, **30**, 4551–4555.
31 A. V. Delgado, F. Gonzalez-Caballero, R. J. Hunter, L. K. Koopal and J. Lyklema, *J. Colloid Interface Sci.*, 2007, **309**, 194–224.
32 A. Mezei and R. Meszaros, *Langmuir*, 2006, **22**, 7148–7151.
33 J. E. Sader, J. W. M. Chon and P. Mulvaney, *Rev. Sci. Instrum.*, 1999, **70**, 3967–3969.
34 F. J. Montes Ruiz-Cabello, G. Trefalt, P. Maroni and M. Borkovec, *Phys. Rev. E: Stat., Nonlinear, Soft Matter Phys.*, 2014, **90**, 012301.
35 S. H. Donaldson, A. Royne, K. Kristiansen, M. V. Rapp, S. Das, M. A. Gebbie, D. W. Lee, P. Stock, M. Valtiner and J. Israelachvili, *Langmuir*, 2015, **31**, 2051–2064.
36 M. A. Bevan and D. C. Prieve, *Langmuir*, 1999, **15**, 7925–7936.
37 M. Elzbieciak-Wodka, M. Popescu, F. J. Montes Ruiz-Cabello, G. Trefalt, P. Maroni and M. Borkovec, *J. Chem. Phys.*, 2014, **140**, 104906.
38 J. D. Feick and D. Velegol, *Langmuir*, 2002, **18**, 3454–3458.
39 J. L. Anderson, *J. Colloid Interface Sci.*, 1985, **105**, 45–54.
40 F. J. Montes Ruiz-Cabello, G. Trefalt, T. Oncsik, I. Szilagyi, P. Maroni and M. Borkovec, *J. Phys. Chem. B*, 2015, **119**, 8184–8193.
41 I. Popa, P. Sinha, M. Finessi, P. Maroni, G. Papastavrou and M. Borkovec, *Phys. Rev. Lett.*, 2010, **104**, 228301.
42 N. Adzic and R. Podgornik, *Eur. Phys. J. E: Soft Matter Biol. Phys.*, 2014, **37**, 49.
43 R. A. Curtis and L. Lue, *Curr. Opin. Colloid Interface Sci.*, 2015, **20**, 19–23.

CHAPTER 4

Long-ranged and soft interactions between charged colloidal particles induced by multivalent coions

Ruiz-Cabello, F. J. M.; Moazzami-Gudarzi, M.; Elzbieciak-Wodka, M.; Maroni, P.; Labbez, C.; Borkovec, M.; Trefalt, G., *Soft Matter* **2015**, 11, 1562-1571.

Reproduced with permission

Soft Matter

PAPER

View Article Online
View Journal | View Issue

Cite this: *Soft Matter*, 2015, **11**, 1562

Long-ranged and soft interactions between charged colloidal particles induced by multivalent coions

F. Javier Montes Ruiz-Cabello,[a] Mohsen Moazzami-Gudarzi,[a] Magdalena Elzbieciak-Wodka,†[a] Plinio Maroni,[a] Christophe Labbez,[b] Michal Borkovec[a] and Gregor Trefalt*[a]

Forces between charged particles in aqueous solutions containing multivalent coions and monovalent counterions are studied by the colloidal probe technique. Here, the multivalent ions have the same charge as the particles, which must be contrasted to the frequently studied case where multivalent ions have the opposite sign as the substrate. In the present case, the forces remain repulsive and are dominated by the interactions of the double layers. The valence of the multivalent coion is found to have a profound influence on the shape of the force curve. While for monovalent coions the force profile is exponential down to separations of a few nanometers, the interaction is much softer and longer-ranged in the presence of multivalent coions. The force profiles in the presence of multivalent coions and in the mixtures of monovalent and multivalent coions can be accurately described by Poisson–Boltzmann theory. These results are accurate for different surfaces and even in the case of highly charged particles. This behavior can be explained by the fact that the force profile follows the near-field limit to much larger distances for multivalent coions than for monovalent ones. This limit corresponds to the conditions with no salt, where the coions are expelled between the two surfaces.

Received 12th November 2014
Accepted 2nd January 2015

DOI: 10.1039/c4sm02510e

www.rsc.org/softmatter

Introduction

Electric double layer forces between solid substrates across aqueous solutions are currently a topic of intense research.[1–8] Such forces are becoming routinely accessible by various methods, including the surface force apparatus, the colloidal probe technique, or total internal reflection microscopy.[1–6,9–16] Double layer forces originate from overlapping diffuse layers forming near charged water–solid interfaces. Their range can be substantial at low salt levels, but decreases with increasing salt level due to progressive screening. The systems investigated mostly included simple monovalent electrolytes and surfaces of mica, latex, or various oxides (*e.g.*, silica, alumina, titania).[5,9–20] These studies reveal that at lower salt concentrations the force profiles in these systems are dominated by double layer forces, and they can be well described by the mean-field Poisson–Boltzmann (PB) theory or at lower charge densities by the linearized Debye–Hückel (DH) theory.[2,21,22] To obtain accurate description of the force profiles at shorter distances, classical boundary conditions of constant charge (CC) and constant potential (CP) might be inaccurate, and a more detailed description of charge regulation effects may be necessary.[13,23–25] The easiest way to incorporate such regulation effects is the constant regulation (CR) approximation. This approximation assumes a constant capacitance of the inner layer, and introduces only one additional parameter.[23,26,27] The PB theory fails at smaller distances or higher salt levels, where one must consider additional interactions, especially van der Waals or hydration forces.[11,14,15]

Forces between charged surfaces in solutions containing multivalent ions came into focus more recently.[1,8,28–36] The existing studies support the picture that the PB theory provides a reasonably accurate description of the forces, at least at distances larger than several nanometers and in sufficiently dilute solutions. They further confirm that multivalent counterions interact strongly with charged surfaces.[29,32,33,37] In this commonly studied case, multivalent ions are oppositely charged than the surface, and therefore they adsorb strongly. Thereby, they reduce the surface charge density, eventually to the point that the surface undergoes a charge reversal. Multivalent ions may also induce additional attractive forces, which can make the total force stronger than the van der Waals force.[30–33] These additional attractions are likely related to ion correlation effects.[35,38–40] These effects are not treated in the classical mean-field PB theory, but they could also be responsible for adsorption of multivalent ions.[29,41,42]

[a]*Department of Inorganic and Analytical Chemistry, University of Geneva, Sciences II, Quai Ernest-Ansermet 30, 1205 Geneva, Switzerland. E-mail: gregor.trefalt@unige.ch*
[b]*Laboratoire Interdisciplinaire Carnot de Bourgogne, UMR 6303 CNRS, Université de Bourgogne, FR-21078, France*
† Present address: Jerzy Haber Institute of Catalysis and Surface Chemistry, Polish Academy of Science, 30-239 Krakow, Poland.

On the other hand, multivalent coions adsorb onto surfaces only weakly or not at all.[37] In this case, the charge of the multivalent ions has the same sign as the charge of the surface. The strong electrostatic repulsion leads to a depletion of these ions from the surface, and to a modification of the structure of the diffuse layer.[43,44] This situation has not been much investigated experimentally so far.[7,8,37]

The question whether the decay length of the double layer forces might deviate from the Debye length was equally raised.[7,8,45,46] While PB theory predicts that double layer forces decay with the Debye length at large distances, theoretical studies of charge renormalization effects suggest that this decay length might be different, especially in asymmetric electrolytes.[45,46] The currently available experimental results indicate that the measured screening lengths agree with the Debye length within experimental error, especially when complexation in solution is being considered.[5,7,8,32,33] One should realize, however, that the theoretically predicted deviations from the Debye length are relatively small, and probably within experimental error.

Force measurements involving multivalent ions almost exclusively involved multivalent counterions, meaning that the ions are oppositely charged as the surface. Multivalent coions that are equally charged as the surface were hardly addressed. We are aware only of a limited number of studies, where these conditions were realized,[7,8,37] but these studies did not analyze the respective force profiles in any detail. This situation prompted us to reinvestigate these conditions more carefully. We show that multivalent coions may induce unusually soft and long-ranged double layer forces, which can be accurately described by PB theory.

Poisson–Boltzmann (PB) theory

Electric double layer forces between colloidal particles can be analyzed by the classical PB theory.[21,23,47,48] This approach treats all ions as point charges in a dielectric continuum. Their interactions are described in a mean-field fashion, whereby ion–ion correlations are being neglected. When the particles are sufficiently large, the situation can be simplified by calculating the net pressure $\Pi(h)$ between two identical planar surfaces *versus* the surface separation h. Free energy per unit area can be then obtained by integrating the pressure profile, and the force between two particles follows from the Derjaguin approximation, which involves the effective radius.[21] In the case of two spherical particles of the same size, the effective radius is half of the particle radius.

The net pressure can be calculated by solving the PB equation, which defines the electric potential $\psi(x)$ as a function of the position x, whose origin is taken at the mid-plane of the two surfaces located at $x = \pm h/2$. When the solution contains different ions of number concentrations c_i and valence z_i, the PB equation reads[23,47]

$$\frac{\mathrm{d}^2\psi}{\mathrm{d}x^2} = -\frac{q}{\varepsilon_0\varepsilon}\sum_i z_i c_i \mathrm{e}^{-z_i\beta q\psi}, \tag{1}$$

where q is the elementary charge, ε_0 the dielectric permittivity of vacuum, ε the dielectric constant, and $\beta = 1/(kT)$ the inverse thermal energy. The latter relationship defines T as the absolute temperature and k as the Boltzmann constant. We use $\varepsilon = 80$ as appropriate for water at room temperature. The solution of the PB equation is found within the constant regulation (CR) approximation.[23,45] In the CR approximation, each surface is characterized by the diffuse layer potential ψ_D and the regulation parameter p. The diffuse layer potential can be equally expressed in terms of the diffuse layer charge density σ. The regulation parameter represents the generalization of the constant charge (CC, $p = 1$) and constant potential (CP, $p = 0$) boundary conditions.[23,47] In general, the regulation parameter can also become negative.[49]

We assume that the solution contains a mixture of strong monovalent (1 : 1) and multivalent (1 : z or z : 1) salts of known concentrations from which the respective ionic concentrations c_i can be evaluated. The net pressure is the difference between the pressure in the slit and the bulk pressure, and in the symmetric situation the former is obtained from the electric potential at the midplane $\psi_\mathrm{M} = \psi(0)$.[21,47] The midplane potential is calculated from the PB equation numerically subject to the boundary condition $\mathrm{d}\psi/\mathrm{d}x = 0$ at $x = 0$. To gain better insight into the different regimes, we further investigate two asymptotic solutions, namely the far-field and the near-field. The far-field regime reflects large separations and is equivalent to DH theory, where the solution composition enters only through the Debye length. The near-field regime describes small separations, where only the counterions neutralizing the surface charge contribute. This regime is equivalent to conditions without added salt.

Far-field regime

At large separations, the electric potentials are small, and thus the PB equation can be linearized, leading to the DH equation

$$\frac{\mathrm{d}^2\psi}{\mathrm{d}x^2} = \kappa^2\psi \tag{2}$$

where κ is the inverse Debye length defined as

$$\kappa^2 = \frac{2q^2 I}{\varepsilon_0\varepsilon kT} \tag{3}$$

and I is the ionic strength

$$I = \frac{1}{2}\sum_i z_i{}^2 c_i \tag{4}$$

which is also expressed as a number concentration. The DH equation can be solved analytically leading to the result

$$\Pi = 2\varepsilon_0\varepsilon\kappa^2\psi_\mathrm{eff}{}^2\mathrm{e}^{-\kappa h} \tag{5}$$

This relationship reflects the PB situation at larger separations, but ψ_eff depends on the surface potential in a non-linear fashion with the limiting behavior

$$\psi_\mathrm{eff} = \begin{cases} \psi_\mathrm{D} & \text{for } \psi_\mathrm{D} \to 0 \\ \alpha kT/q & \text{for } \psi_\mathrm{D} \to \infty \end{cases} \tag{6}$$

The above relationship applies when the potential is positive, otherwise the appropriate negative signs must be introduced. For pure electrolytes, the reduced values for the saturation potential α are known,[43,44] and they are summarized for multivalent coions in Table 1. The characteristic feature is that these values strongly increase with valence. Note that the far-field regime is independent of the boundary conditions.

Near-field regime

When the distance between the surfaces is small, the coions are expelled, and their charge is fully neutralized by the remaining counterions. This situation corresponds to no added salt, and the PB equation simplifies to[42–44]

$$\frac{\mathrm{d}^2\psi}{\mathrm{d}x^2} = \frac{qc}{\varepsilon_0\varepsilon}\mathrm{e}^{\beta q\psi}, \tag{7}$$

where we assume that the surface is positively charged, and that the counterions are monovalent anions of concentration c. The case with the opposite signs of the charge is obtained by replacing q by $-q$. The solution of this equation reads[2,50]

$$\psi = \psi_{\mathrm{M}} - \frac{1}{q\beta}\ln\cos^2\left(\frac{x\gamma}{\lambda}\right), \tag{8}$$

where $\gamma = \mathrm{e}^{\beta q(\psi_{\mathrm{M}}-\psi_{\mathrm{D}})/2}$ and

$$\lambda = \frac{2\varepsilon_0\varepsilon}{\beta q\sigma}, \tag{9}$$

is the Gouy–Chapman length. The net pressure is now given by

$$\Pi = kTc\mathrm{e}^{\beta q\psi_{\mathrm{M}}} \tag{10}$$

and it is equal to the pressure in the slit, since the bulk pressure vanishes without salt. The pressure can be parameterized through the dimensionless quantity γ defined above, namely

$$\Pi = \frac{2\varepsilon_0\varepsilon}{\beta^2q^2\lambda^2}\gamma^2 \tag{11}$$

By invoking the potential profile given by eqn (8) and using the constant regulation boundary conditions one finds that the pressure is determined by

$$p[\gamma\tan(\ell\gamma) - 1] + (1-p)\ln\left[\frac{\gamma}{\cos(\ell\gamma)}\right] = 0 \tag{12}$$

where $\ell = h/(2\lambda)$ and p is the regulation parameter. When one analyses eqn (12) for large separation distances, the pressure profile again becomes independent of the boundary conditions, and reads

Table 1 Far-field limit for the saturation values of effective potentials for $z:1$ electrolytes containing multivalent coions

z	1	2	3	4	5
α	4	6	8.707	12.314	17.337
ψ_{eff} (mV)	102.7	154.0	223.5	316.1	445.0

$$\Pi = \frac{2\pi^2\varepsilon\varepsilon_0}{\beta^2q^2}\frac{1}{h^2} \tag{13}$$

The free energy can be calculated through integration of the pressure, but the appropriate integration constant must be inferred from the solution of the full PB equation.

Experimental

Materials

Two different types of polystyrene latex particles were used, namely sulfate-terminated latex (SL) and amidine-terminated latex (AL), and they were obtained from Invitrogen. Further experiments were carried out with silica particles obtained from Bangs Laboratories Inc., USA. Table 2 summarizes the mean diameters and polydispersities as determined by the manufacturer.

Experiments were carried out at 22 ± 2 °C in solutions of KCl, K_2SO_4, $LaCl_3$, $K_3Fe(CN)_6$, and $K_4Fe(CN)_6$ in Milli-Q water. For the SL particles pH 5.6 was used, while for AL particles the solutions were adjusted to pH 4.0 with HCl, and for the silica particles with KOH to pH 10.0. The specific pH values were chosen in order to increase the magnitude of the surface charge density, while keeping the ionic strength low. Some experiments were also performed in solutions of aliphatic polyamine, namely of 3,6,9,12-tetraazatetradecane-1,14-diamine (N6) with chemical formula H_2N–$(CH_2$–CH_2–$NH)_4$–CH_2–CH_2–NH_2, obtained from Sigma-Aldrich (St. Louis, USA). At pH 4.0, La^{3+} does not hydrolyze, and N6 has the +4 cation as the predominant species.[51] The experiments were carried out at ionic strengths between 1 and 3.1 mM. The ionic strength was chosen as low as possible, such that the low salt regime is well developed, while high enough, such that ions originating from the self-dissociation of water or carbonate dissolution remain negligible.

Direct force measurements

Forces between particles were measured with a closed-loop AFM (MFP-3D, Asylum Research) mounted on an inverted optical microscope (Olympus IX70).[13,52] The particles were attached on tip-less cantilevers (MikroMasch, HQ CSC37, without Al coating) and to the substrate. A pair of particles was centered laterally through optical fringes viewed in the optical microscope with an accuracy of about 100 nm. For one pair of particles, we typically recorded about 100 vertical approach-retraction cycles with an approach-retraction velocity of 300 nm s^{-1}, a sampling rate of 5 kHz, and a cycle frequency of 0.5 Hz. The contact point was obtained from the constant compliance region. The cantilever deflection recorded in the approach part was transformed into force profiles by means of the spring constant of the cantilever. The latter constant was measured by the method developed by Sader *et al.*,[53] which relies on the frequency response of the cantilever and its geometrical dimensions. Typical values of the spring constants were 0.1–0.3 N m^{-1}. These values agreed within about 10% with those determined through the thermal fluctuations of the cantilever.[54] The forces were subsequently down-sampled to 150 Hz and

Table 2 Particle and selected solution characteristics

Particles	Abbreviation	Diameter (μm)	Polydispersity (%)	RMS roughness (nm)	pH	Charge density (mC m^{-2})	Regulation parameter p
Sulfate latex	SL	3.0	4.1	0.8	5.6	−9.3	0.64
Amidine latex	AL	0.95	3.6	0.5	4.0	+7.5	0.31
Silica	SiO_2	5.2	10	1.4	10.0	−4.4	0.66

averaged over the different approach curves, leading to a force resolution of about 1 pN. All measurements were repeated with at least three pairs of different particles, and they were well reproducible. The relative error between the resulting double layer potentials, which was determined by fitting the force curves for every pair of particles under the same conditions, was below 15%.

Latex particles were mounted in solution within the AFM fluid cell. A glass plate fitting the fluid cell was used as the substrate. The glass plate and cantilevers were cleaned overnight in a piranha solution, which consists of H_2SO_4 98% and H_2O_2 30% mixed in ratio 3 : 1. They were further rinsed with water, dried, and cleaned in an air-plasma for 20 min. Silanization of the plate and cantilevers was carried out overnight in an evacuated container aside two drops of 20 μL of 3-ethoxydimethylsilylpropylamine and 100 μL of (3-glycidoxypropyl) dimethylethoxysilane. The silanized plate was then introduced into the AFM fluid cell, and the cantilever into the cantilever holder. Before the experiments, the stock latex particle suspension was purified by dialysis against Milli-Q (Millipore) until the conductivity of the dialysate reached the value of the pure water. The particle suspensions were prepared in the respective electrolyte solutions at a particle concentration of 80 mg L^{-1}, and injected into the fluid cell. The particles were allowed to settle for a few hours, and the cell was then rinsed with the pure electrolyte solution. By pressing the particle against the substrate with the cantilever, one could firmly attach a particle to the cantilever. For the latex particles, the constant compliance region could be identified after the jump-in in the load range of 5–10 nN with an absolute accuracy of about 0.3 nm.

The silica particles were attached by sintering in the dry state. Cantilevers were cleaned in air-plasma for 5 minutes. Few silica particles were placed on a glass slide and tiny drops of about 5 μL of glue (Araldite 2000+) were deposited in their proximity. The cantilever was mounted in the AFM, brought in contact with the glue with the translation stage, and used to pick up the particle. The cantilever was removed from the AFM, and placed into an oven at 1150 °C for 3 h. The same particles were attached to the glass slide sealing the AFM fluid cell as follows. The slide was cleaned with piranha solution for 2 hours, then rinsed with water, and dried under a stream of nitrogen. Subsequently, particles were spread onto a square quartz slide of 19 mm (Edmund Optics), and then sintered at 1150 °C for 3 hours. The reverse side of the slide with the sintered particles was glued (Pattex 100% Repair Gel) onto a glass slide sealing the AFM cell. After sintering, the substrate and the cantilevers were again cleaned in an air-plasma. This procedure leads to a firm attachment of the particles to the substrate and to the cantilever, while completely removing traces of the glue and of any organic impurities. For the silica particles, the contact point was identified at a load of about 5 nN. The precision of the contact position is inferior to the latex particles, but typically below 1 nm.

Particle roughness

The root mean square (RMS) roughness of the particles was measured by AFM imaging. The latex particles were deposited for about 1 hour on a piranha-cleaned and silanized glass slide with dimensions about 1 cm × 1 cm. These slides were silanized overnight in an evacuated glass container aside a 50 μL drop of 3-ethoxydimethylsilylpropylamine (for SL) or (3-glycidoxypropyl)dimethylethoxysilane (for AL). After the deposition of the particles, the substrate was rinsed in 10 mM KCl solution. The images were recorded in liquid with a Cypher AFM instrument (Asylum Research, Santa Barbara, USA) with BioLever Mini cantilevers (BL-AC40TS, Olympus, Japan). They had a nominal tip radius of <9 nm and a resonance frequency of around 30 kHz in water. The scan rate was 2.0 Hz, the scan size 0.5 μm × 0.5 μm, and the free oscillation amplitude (FOA) 20 nm. The set-point was fixed at around 70% of the FOA.

The roughness of the silica particles was determined as follows. The particles sintered onto a quartz slide, which was previously cleaned with piranha solution, rinsed with water, and finally treated in air plasma for 20 min. The particles were imaged in air with the MFP-3D in amplitude modulation mode. Silicon cantilevers (OMCL-AC240TS, Olympus) with a nominal tip radius <10 nm and a resonance frequency of about 70 kHz were used. Images were acquired with a scan rate of 2 μm s^{-1}, an FOA of about 40 nm, and a set point around 80% of the FOA. The roughness was determined for an area of 1 μm × 1 μm. The RMS roughness of the particles is summarized in Table 2. These values are <1 nm for the latex particles, and 1.4 nm for the silica particles. All particles used can be thus considered to be smooth for the relevant surface separations considered.

Results and discussion

We present direct force measurements between pairs of similar colloidal particles in aqueous solutions containing multivalent coions. These multivalent ions have the same sign of the charge as the surface, and they do not adsorb on the surface. With respect to the monovalent situation, however, one obtains much softer and long-ranged force profiles. Several types of

particles and different coions are compared with PB theory, which captures the observed profiles very well.

Pressure profiles

Let us first discuss pressure profiles between two charged plates calculated with PB theory. These profiles are shown in Fig. 1, and they reveal the relevant features more clearly than the force profiles discussed below. At larger distances, the profiles decay exponentially as one expects from the far-field linearized DH solution. This decay is evident from the linear dependence in the semi-logarithmic representation. As the separation decreases, the coions are progressively being expelled between the plates. When their concentration becomes negligible, the pressure profile follows the near-field solution of the PB equation. This solution assumes that the charge of the plates is fully neutralized by counterions, which corresponds to the situation of no added salt.

Fig. 1b shows the calculated force profiles for plates of a surface change density of -10 mC m^{-2} in a solution of an ionic strength of 1.05 mM. This surface charge density corresponds to the diffuse layer potentials -87 mV and -114 mV in 1 : 1 and 1 : 5 electrolytes, respectively. The left panel shows the familiar situation of monovalent 1 : 1 salt. The pressure profile is dominated by the exponential far-field DH profile down to separations of a few nanometers. The effective potential is -69 mV, which is about half of the saturation value. The near-field profile sets in at small separation distances only. For a pentavalent 1 : 5 electrolyte, the profile is much softer and longer-ranged, and features a sigmoidal shape. At larger distances the pressure is again exponential, but this dependence only sets in at relatively large distances, around 80 nm here. The effective potential is now -293 mV, which is still substantially below the saturation value. At smaller distances, the pressure follows the near-field regime, but this regime now sets in at much larger distances than for the monovalent ones, about 30 nm in this case. This wider region of validity is related to the larger magnitude of the effective potential. This larger value results from the fact that the multivalent coions get expelled from the slit at larger distances than the monovalent ones. This difference is a consequence of the higher charge of the multivalent ions, which leads to their higher electrostatic energy when they are situated between the plates.

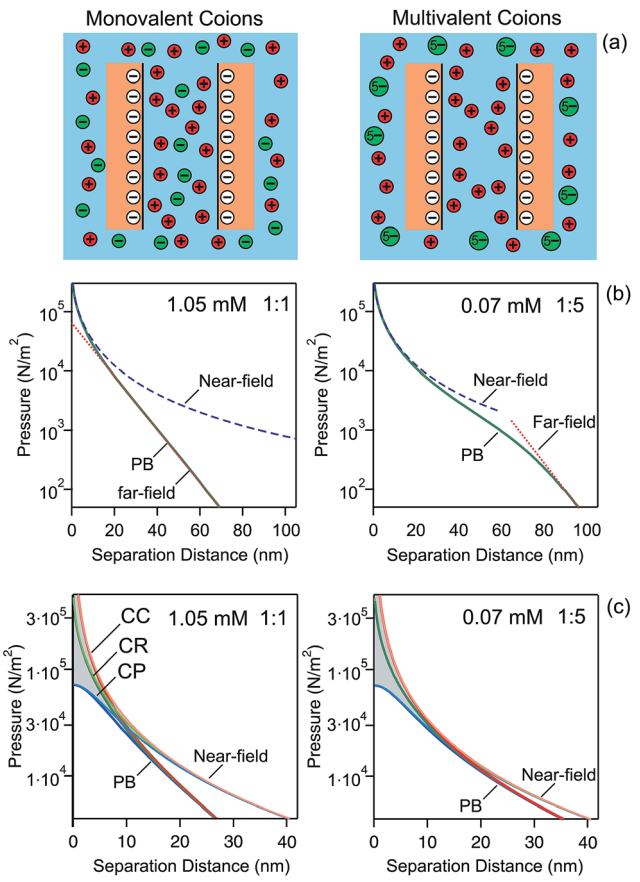

Fig. 1 (a) Schematic presentation of expulsion of the multivalent coions between the charged walls. (b) Net pressure between charged plates in the presence of 1.05 mM 1 : 1 and 0.05 mM 1 : 5 electrolyte calculated with the PB theory. The near and far-field asymptotes are denoted by dashed lines. (c) The effect of the CC, CR, and CP boundary conditions for the same surfaces. Near-field solution is also shown. A surface charge density of -10 mC m^{-2} and regulation parameter $p = 0.5$ are used throughout. Ionic strength is 1.05 mM.

The details of the pressure profiles at smaller distances are shown in Fig. 1c. At small separations, the effect of boundary conditions is substantial. The CC conditions, characterized by the regulation parameter $p = 1$, result in the strongest repulsion by the double layer forces. Regulation effects are reflected by smaller regulation parameters and they lead to the decrease of the strength of the repulsion, as illustrated with $p = 0.5$ and $p = 0$ (CP conditions). At larger distances, the effect of boundary conditions disappears, and the near-field solution converges to eqn (13). The near-field solution reproduces the full PB calculations at small distances. However, its region of validity is much wider for the multivalent coions than for the monovalent ones.

Characteristic length scales in the far-field and near-field regimes are the Debye length κ^{-1} and Gouy–Chapman length λ. In this example, we approximately have $\kappa^{-1} = 9.5$ nm and $\lambda = 3.6$ nm. The Debye length reflects the range of the exponential decay at larger distances, while the Gouy–Chapman length measures the thickness of the layer containing counterions only.

Sulfate latex particles

Let us first discuss the effect of multivalent coions on experimentally measured force profiles between negatively charged SL particles of 3 μm in diameter. Fig. 2 compares forces in 1.0 mM KCl solutions and 0.1 mM $K_4Fe(CN)_6$ solutions. These strong electrolytes fully dissociate into $Fe(CN)_6^{4-}$ or Cl^-, which are the coions, K^+ being the counterion. The ionic strength of both solutions is the same, namely 1.0 mM. The force profile in the monovalent electrolyte shown in Fig. 2a is exponential down to a few nanometers, as was the case for the pressure. The profile in the presence of multivalent coions shown in Fig. 2b is much softer, and features a sigmoidal shape. In this case, the

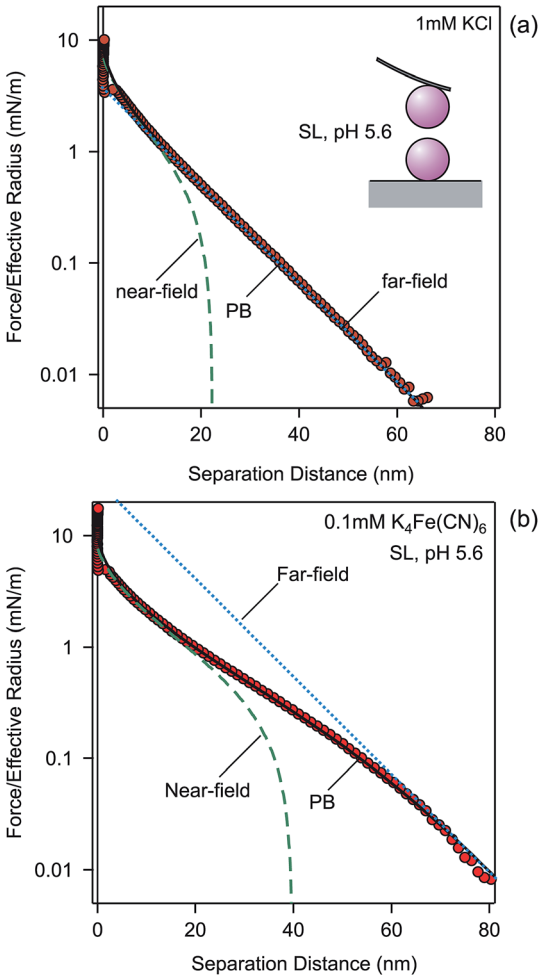

Fig. 2 Forces between SL particles in (a) 1 mM KCl and (b) 0.1 mM $K_4Fe(CN)_6$ at pH 5.6. Points designate the experiments, while solid lines are PB calculations with a surface charge density of -9.3 mC m^{-2} and regulation parameter $p = 0.64$. The far-field and near-field asymptotes are presented with dashed lines.

exponential dependence sets in only around 60 nm. In both cases, one observes a jump-in close to contact, which occurs due to additional van der Waals attraction and hydrophobic forces.

The measured force profiles can be described with PB theory perfectly well. By fitting the force profile measured in the KCl solution, we extract the surface charge density $\sigma = -9.3 \pm 0.1$ mC m^{-2} and a regulation parameter $p = 0.64 \pm 0.02$ (see also Table 2). The calculation uses the fixed analytical KCl concentration of 1.0 mM. When this concentration would be adjusted, the fitted concentration will remain within 5% of this value. We now keep the same surface parameters, and predict the force profile in 0.10 mM $K_4Fe(CN)_6$ solution with the PB theory. Again, the analytical concentration is being fixed. The calculation reproduces the sigmoidal shape of the measured force curve extremely well. The fact that the force profiles are consistent with the same surface charge density for monovalent and multivalent coions suggests that the multivalent ions adsorb onto the surface very weakly, or not at all. The lack of adsorption is obviously related to the strong electrostatic repulsion between multivalent coions and the surface.

The reason for the different appearance of the force curves is related to the fact that multivalent coions are being expelled from the gap between the surfaces at much larger separations than the monovalent ones. Therefore, the near-field solution provides a good description of the force profile to larger distances, albeit not as large as was the case for the pressure profile. The sigmoidal dependence is reinforced by the larger magnitude of the effective potential entering the far-field profile for the multivalent salts. For KCl, the effective potential is $\psi_{eff} = -67$ mV, while for $K_4Fe(CN)_6$ one has $\psi_{eff} = -176$ mV. The magnitude of these values is still substantially below the saturation values given in Table 1. At the same time, the force profile must converge into the near-field profile at small distances. While for KCl, the far-field asymptote lies below the near-field profile, for $K_4Fe(CN)_6$ the far-field asymptote lies above it, and thus the force curve makes the sigmoidal transition converge into the near-field profile.

Further force measurements with other solution compositions confirm that PB theory describes the force profiles quantitatively. Fig. 3 shows measurements in $K_4Fe(CN)_6$ solutions of varying concentrations. Thereby, the charge density and regulation properties of the surface were kept at the previous values (Table 2) and the solution concentrations were fixed to the known analytical concentrations of the solutions. These calculations contain no adjustable parameters, and provide very satisfactory results.

Fig. 4a shows another test of the PB theory, as these experiments were carried out in mixtures of KCl and $K_4Fe(CN)_6$ solutions at a constant ionic strength of 1.0 mM. The calculations rely on the solution of the PB equation for mixed electrolytes, and they predict the observed force profiles very well. Again, no adjustable parameters were used.

Fig. 4b summarizes the effect of the valence of different coions. These experiments were carried out in solutions of KCl, K_2SO_4, $K_3Fe(CN)_6$, and $K_4Fe(CN)_6$, thus covering valences of

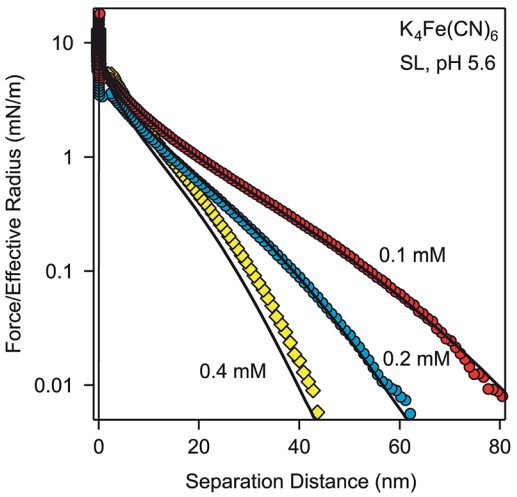

Fig. 3 Forces between SL particles in different concentrations of $K_4Fe(CN)_6$ at pH 5.6. Points designate the experiments, while solid lines are predictions with the PB theory with a surface charge density of -9.3 mC m^{-2} and regulation parameter $p = 0.64$.

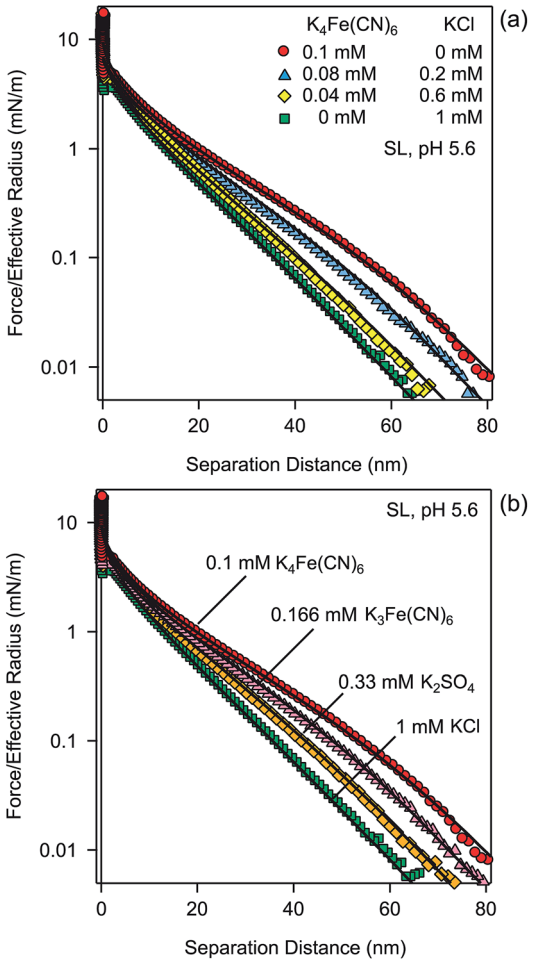

Fig. 4 (a) Forces between SL particles in a mixture of KCl and $K_4Fe(CN)_6$ at pH 5.6 and fixed ionic strength of 1 mM. (b) Forces in KCl, K_2SO_4, $K_3Fe(CN)_6$, and $K_4Fe(CN)_6$ solutions at pH 5.6 and constant ionic strength of 1 mM. Points designate the experiments, while solid lines are predictions of the PB theory with a surface charge density of -9.3 mC m^{-2} and regulation parameter $p = 0.64$.

coions of -1, -2, -3, and -4. The ionic strength was fixed to 1.0 mM. The corresponding predictions of the PB theory, which contain no adjustable parameters, are again in excellent agreement with experiment.

In all cases, a fixed value of surface charge density satisfactorily describes the forces, which implies that the ions involved do not adsorb onto the particles. This behavior is characteristic for multivalent coions, and is in contrast to multivalent counterions, which readily adsorb onto the surfaces and modify the surface charge or even induce charge reversal.[29,32,33] However, the assumption of a fixed surface charge density leads to minor discrepancies, for example, for the highest concentration shown in Fig. 3. These discrepancies are probably related to small variations of the surface charge density and the surface regulation properties. These variations could be caused by weak adsorption of the ions involved onto the surface.

All calculations used the analytical concentrations. While the analytical concentrations are accurate within <1%, some modification might result from chemical decomposition of $Fe(CN)_6^{4-}$ due to oxidation. We find that the analytical concentrations are consistent with the measured force profiles to an accuracy of about <10%. This agreement is comparable to previous studies that attempted to determine the salt concentrations from measured force profiles.[5,7,8,32,33]

Amidine latex particles

A similar set of experiments was carried out with positively charged AL particles of a diameter of 0.95 μm. For these particles, the cations are the coions, and for this reason we investigated solutions containing La^{3+} and K^+. The forces in mixtures of KCl and $LaCl_3$ solutions at a fixed ionic strength of 3.1 mM are shown in Fig. 5a. One observes the same features as in the previously discussed case with the SL particles. In the monovalent salt, the decay is exponential of larger part of the accessible distance range, typically down to a few nanometers. For multivalent coions, the exponential decay sets in at larger

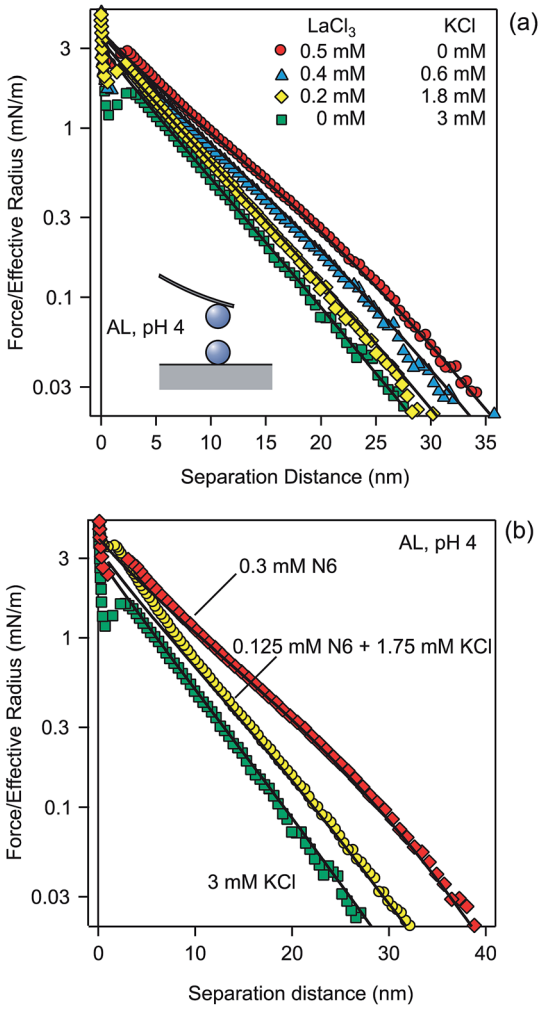

Fig. 5 (a) Forces between AL particles in a mixture of KCl and $LaCl_3$ at pH 4 and a fixed ionic strength of 3.1 mM. (b) Forces in the presence of N6 polyamine and its mixture with KCl. Points designate the experiments, while solid lines are predictions with the PB theory with a surface charge density of +7.5 mC m^{-2} and regulation parameter $p = 0.31$.

distances, at about 30 nm. Again, the characteristic soft and sigmoidal force profile is observed. For the AL particles, one observes a more pronounced jump-in close to contact, which probably occurs since the hydrophobic forces are stronger for AL than for SL .

The surface properties of the particles were again determined by fitting the force profile in KCl solutions, whereby the solution concentrations were fixed to the analytical values. The respective surface charge density was $\sigma = +7.5 \pm 0.1$ mC m^{-2} and the regulation parameter $p = 0.31 \pm 0.02$ (Table 2). With these values, one can correctly predict the force profiles in all mixtures. These calculations contain again no adjustable parameters, since the analytical concentrations and the surface properties are kept fixed (Table 2). We have also fitted the electrolyte concentrations, and we found that they agreed within 10% with the analytical ones. A small discrepancy could also be related to the formation of $LaCl^{2+}$ complexes in solution.[33,55] The reason for the softer repulsion is again related to the more effective exclusion of the multivalent coions from the gap and to the larger effective potentials for the multivalent coions (Table 1). The near-field profile again remains a good approximation at much larger distances for multivalent coions than for monovalent ones.

Fig. 5b shows a similar effect with highly charged organic aliphatic polyamine. N6 is a linear amine, which does not ionize fully, and the prevalent species has a valence of +4. The forces in the presence of N6 and its mixture with KCl are predicted with PB theory only by invoking the respective concentrations. Again the ionic strength is fixed to 3.1 mM. No parameter adjustment was made, as the same surface properties as before were used. Good agreement with the observed force profiles was found. The minor discrepancies could be related to weak adsorption onto the surface or due to the contribution of other valences, which occur in small concentrations due to the multi-step dissociation equilibria.

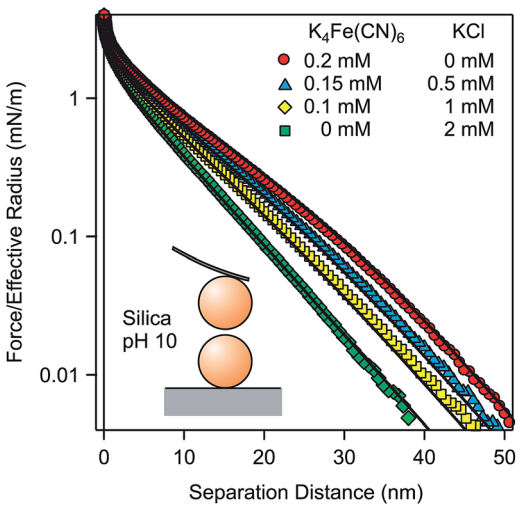

Fig. 6 Forces between silica particles in a mixture of KCl and $K_4Fe(CN)_6$ at pH 10 and a fixed ionic strength of 2.1 mM. Points designate the experiments, while solid lines are predictions of PB theory with a surface charge density of -4.4 mC m^{-2} and regulation parameter $p = 0.66$.

Silica particles

To confirm that the described effects are generic for various types of materials, forces between negatively charged silica particles of 5.2 μm in diameter were measured in solutions of $K_4Fe(CN)_6$, KCl, and their mixtures at an ionic strength of 2.1 mM (Fig. 6). As for the previously discussed systems, one observes softer profiles in the presence of multivalent coions. The main difference to the previous force profiles is that forces remain repulsive down to contact and that one cannot observe a jump-in at short distances. This feature is probably related to repulsive short-ranged hydration forces acting between silica surfaces.[17,19,20]

Surface properties of silica were determined by fitting the force profile in KCl solution with PB theory. Thereby, the analytical salt concentration was used as before. From this fit, we obtain the surface charge density $\sigma = -4.4 \pm 0.1$ mC m^{-2} and a regulation parameter $p = 0.66 \pm 0.02$ (Table 2). These parameters are then used to predict the force profiles in $K_4Fe(CN)_6$ solutions and their mixtures with KCl. Since the appropriate salt concentrations were kept fixed, no adjustable parameters enter the calculation. The PB theory again describes the measured force profiles very well. The characteristic features observed for the force profiles in the presence of multivalent coions do not depend on the nature of the particles. The obtained surface charge density is well comparable to the published values measured for silica surfaces at pH $\sim$ 10 at low salt concentrations.[17–20,56] These values were determined by force measurements and they are in the range from -8 to -4 mC m^{-2}.

Conclusions

Direct force measurements were carried out with different types of negatively and positively charged colloidal particles in aqueous electrolyte solutions containing multivalent coions. In all situations studied, the multivalent ions have the same sign of charge as the particles. While these ions hardly adsorb onto such surfaces, they strongly modify the structure of the diffuse layer. As a consequence, one observes unusually softer and longer-ranged force profiles than for monovalent electrolytes. These profiles have a sigmoidal appearance in the popular semi-logarithmic representation and they can be described with PB theory for asymmetric electrolytes very well. These characteristic features reflect the fact that multivalent coions get expelled from the gap between the surfaces at larger distances than for monovalent ones. At short distances, the force profile converges to the near-field solution of the PB equation, which reflects the situation where the surface charge is neutralized by counterions only, as is the case without added salt. In the presence of multivalent coions, the near-field profile represents a good approximation up to larger separation distances than for monovalent coions. This fact is also reflected by the effective potentials entering the

far-field DH theory, which are higher for the multivalent coions than for the monovalent ones. These findings demonstrate that the PB theory can accurately describe forces in the presence of multivalent coions even when surfaces are highly charged.

The measured force profiles reflect the analytical electrolyte concentrations very well. While the observed discrepancies are typically <10%, these deviations could also be related to complexation in solution or to a chemical decomposition of the ions. The present work confirms the findings of previous studies,[7,8] which concluded that salt concentrations determined from direct force measurements are in agreement with the analytical ones. Systematic deviations between experimentally observed decay lengths in the far-field regime and the Debye lengths cannot be confirmed even in the presence of multivalent ions. While these deviations might exist, they are beyond the resolution of the surface force instruments currently in use.

The present work contributes to the current discussion on the role of multivalent ions in electrostatic interactions between charged surfaces.[8,29–34,36] Thereby, a major difference between multivalent counterions and multivalent coions must be stressed. Multivalent counterions strongly adsorb onto charged surfaces, and they may eventually lead to overcharging. Multivalent coions do not adsorb onto such surfaces, or eventually only weakly. Therefore, they do not affect the surface charge, but they strongly modify the structure of the electric double layer and the resulting interaction forces. Therefore, addition of multivalent coions provides a new means of tuning repulsive double layer forces. This possibility might be of relevance in colloidal self-assembly, where delicate balance between interactions must be achieved in order to obtain the regular particle arrangements.[57,58] In this respect, a more detailed understanding how multivalent ions influence forces between dissimilar surfaces would be desirable as well.

Acknowledgements

This research was supported by the Swiss National Science Foundation, University of Geneva, COST Action CM1101, and the Swiss Secretariat of Education and Research. We acknowledge helpful discussions with Jordi Faraudo and Peter Kralchevsky.

References

1 R. M. Pashley and J. N. Israelachvili, *J. Colloid Interface Sci.*, 1984, **97**, 446–455.
2 J. Israelachvili, *Intermolecular and Surface Forces*, Academic Press, London, 2nd edn, 1992.
3 T. Baimpos, B. R. Shrestha, S. Raman and M. Valtiner, *Langmuir*, 2014, **30**, 4322–4332.
4 H. J. Butt, B. Cappella and M. Kappl, *Surf. Sci. Rep.*, 2005, **59**, 1–152.
5 A. Tulpar, V. Subramanian and W. Ducker, *Langmuir*, 2001, **17**, 8451–8454.
6 M. Borkovec, I. Szilagyi, I. Popa, M. Finessi, P. Sinha, P. Maroni and G. Papastavrou, *Adv. Colloid Interface Sci.*, 2012, **179–182**, 85–98.
7 M. Nayeri, Z. Abbas and J. Bergenholtz, *Colloids Surf., A*, 2013, **429**, 74–81.
8 M. M. Kohonen, M. E. Karaman and R. M. Pashley, *Langmuir*, 2000, **16**, 5749–5753.
9 R. M. Pashley, *J. Colloid Interface Sci.*, 1981, **83**, 531–546.
10 G. Toikka, R. A. Hayes and J. Ralston, *Langmuir*, 1996, **12**, 3783–3788.
11 M. Elzbieciak-Wodka, M. Popescu, F. J. Montes Ruiz-Cabello, G. Trefalt, P. Maroni and M. Borkovec, *J. Chem. Phys.*, 2014, **140**, 104906.
12 F. J. Montes Ruiz-Cabello, P. Maroni and M. Borkovec, *J. Chem. Phys.*, 2013, **138**, 234705.
13 I. Popa, P. Sinha, M. Finessi, P. Maroni, G. Papastavrou and M. Borkovec, *Phys. Rev. Lett.*, 2010, **104**, 228301.
14 R. M. Espinosa-Marzal, T. Drobek, T. Balmer and M. P. Heuberger, *Phys. Chem. Chem. Phys.*, 2012, **14**, 6085–6093.
15 M. A. Bevan and D. C. Prieve, *Langmuir*, 1999, **15**, 7925–7936.
16 M. Dishon, O. Zohar and U. Sivan, *Langmuir*, 2009, **25**, 2831–2836.
17 W. A. Ducker, T. J. Senden and R. M. Pashley, *Langmuir*, 1992, **8**, 1831–1836.
18 K. Hu and A. J. Bard, *Langmuir*, 1997, **13**, 5114–5119.
19 M. Giesbers, J. M. Kleijn and M. A. Cohen Stuart, *J. Colloid Interface Sci.*, 2002, **248**, 88–95.
20 J. Morag, M. Dishon and U. Sivan, *Langmuir*, 2013, **29**, 6317–6322.
21 W. B. Russel, D. A. Saville and W. R. Schowalter, *Colloidal Dispersions*, Cambridge University Press, Cambridge, 1989.
22 M. Elimelech, J. Gregory, X. Jia and R. A. Williams, *Particle Deposition and Aggregation: Measurement, Modeling, and Simulation*, Butterworth-Heinemann Ltd., Oxford, 1995.
23 R. Pericet-Camara, G. Papastavrou, S. H. Behrens and M. Borkovec, *J. Phys. Chem. B*, 2004, **108**, 19467–19475.
24 B. V. Zhmud, A. Meurk and L. Bergstrom, *J. Colloid Interface Sci.*, 1998, **207**, 332–343.
25 S. Rentsch, H. Siegenthaler and G. Papastavrou, *Langmuir*, 2007, **23**, 9083–9091.
26 S. L. Carnie and D. Y. C. Chan, *J. Colloid Interface Sci.*, 1993, **161**, 260–264.
27 S. H. Behrens and M. Borkovec, *J. Phys. Chem. B*, 1999, **103**, 2918–2928.
28 R. M. Pashley, *J. Colloid Interface Sci.*, 1984, **102**, 23–35.
29 K. Besteman, M. A. G. Zevenbergen, H. A. Heering and S. G. Lemay, *Phys. Rev. Lett.*, 2004, **93**, 170802.
30 O. Zohar, I. Leizerson and U. Sivan, *Phys. Rev. Lett.*, 2006, **96**, 177802.
31 M. Dishon, O. Zohar and U. Sivan, *Langmuir*, 2011, **27**, 12977–12984.
32 P. Sinha, I. Szilagyi, F. J. Montes Ruiz-Cabello, P. Maroni and M. Borkovec, *J. Phys. Chem. Lett.*, 2013, **4**, 648–652.
33 F. J. Montes Ruiz-Cabello, G. Trefalt, Z. Csendes, P. Sinha, T. Oncsik, I. Szilagyi, P. Maroni and M. Borkovec, *J. Phys. Chem. B*, 2013, **117**, 11853–11862.

34 D. Ebeling, D. van den Ende and F. Mugele, *Nanotechnology*, 2011, **22**, 305706.
35 R. Kjellander, S. Marcelja, R. M. Pashley and J. P. Quirk, *J. Chem. Phys.*, 1990, **92**, 4399–4407.
36 C. Gutsche, U. F. Keyser, K. Kegler and F. Kremer, *Phys. Rev. E: Stat., Nonlinear, Soft Matter Phys.*, 2007, **76**, 031403.
37 F. J. Montes Ruiz-Cabello, G. Trefalt, P. Maroni and M. Borkovec, *Langmuir*, 2014, **30**, 4551–4555.
38 J. Forsman, *J. Phys. Chem. B*, 2004, **108**, 9236–9245.
39 M. M. Hatlo and L. Lue, *Soft Matter*, 2009, **5**, 125–133.
40 K. Bohinc, J. M. A. Grime and L. Lue, *Soft Matter*, 2012, **8**, 5679–5686.
41 M. Kanduc, A. Naji, J. Forsman and R. Podgornik, *Phys. Rev. E: Stat., Nonlinear, Soft Matter Phys.*, 2011, **84**, 011502.
42 B. I. Shklovskii, *Phys. Rev. E: Stat., Nonlinear, Soft Matter Phys.*, 1999, **60**, 5802–5811.
43 G. Tellez, *Philos. Trans. R. Soc., A*, 2011, **369**, 322–334.
44 M. Han and X. J. Xing, *J. Stat. Phys.*, 2013, **151**, 1121–1139.
45 R. Kjellander and D. J. Mitchell, *J. Chem. Phys.*, 1994, **101**, 603–626.
46 A. McBride, M. Kohonen and P. Attard, *J. Chem. Phys.*, 1998, **109**, 2423–2428.
47 G. Trefalt, I. Szilagyi and M. Borkovec, *J. Colloid Interface Sci.*, 2013, **406**, 111–120.
48 S. H. Behrens and M. Borkovec, *Phys. Rev. E: Stat., Nonlinear, Soft Matter Phys.*, 1999, **60**, 7040–7048.
49 M. Borkovec and S. H. Behrens, *J. Phys. Chem. B*, 2008, **112**, 10795–10799.
50 A. C. Cowley, N. L. Fuller, R. P. Rand and V. A. Parsegian, *Biochemistry*, 1978, **17**, 3163–3168.
51 A. E. Martell, R. M. Smith and R. J. Motekaitis, *Critically Selected Stability Constants of Metal Complexes: Version 8.0.*, National Insitutue of Standards and Technology, Gainesburg, 2004.
52 I. Popa, G. Gillies, G. Papastavrou and M. Borkovec, *J. Phys. Chem. B*, 2009, **113**, 8458–8461.
53 J. E. Sader, J. W. M. Chon and P. Mulvaney, *Rev. Sci. Instrum.*, 1999, **70**, 3967–3969.
54 J. L. Hutter and J. Bechhoefer, *Rev. Sci. Instrum.*, 1993, **64**, 1868–1873.
55 C. F. Baes and R. E. Mesmer, *The Hydrolysis of Cations*, Krieger Publishing, Malabar1976.
56 V. Kuznetsov and G. Papastavrou, *J. Phys. Chem. C*, 2014, **118**, 2673–2685.
57 Q. Chen, S. C. Bae and S. Granick, *Nature*, 2011, **469**, 381–384.
58 F. Li, D. P. Josephson and A. Stein, *Angew. Chem., Int. Ed.*, 2011, **50**, 360–388.

CHAPTER 5

Interplay between depletion and double layer forces acting between charged particles in solutions of like-charged polyelectrolytes

Moazzami-Gudarzi, M.; Kremer, T.; Valmacco, V.; Maroni, P.; Borkovec, M.; Trefalt, G., *Phys. Rev. Lett.* **2016**, 117, 088001.

Reproduced with permission

Interplay between Depletion and Double-Layer Forces Acting between Charged Particles in Solutions of Like-Charged Polyelectrolytes

Mohsen Moazzami-Gudarzi, Tomislav Kremer, Valentina Valmacco, Plinio Maroni, Michal Borkovec, and Gregor Trefalt*
Department of Inorganic and Analytical Chemistry, University of Geneva, Sciences II, 30 Quai Ernest-Ansermet, 1205 Geneva, Switzerland
(Received 3 May 2016; published 15 August 2016)

Direct force measurements between negatively charged silica particles in the presence of a like-charged strong polyelectrolyte were carried out with an atomic force microscope. The force profiles can be quantitatively interpreted as a superposition of depletion and double-layer forces. The depletion forces are modeled with a damped oscillatory profile, while the double-layer forces with the mean-field Poisson-Boltzmann theory for a strongly asymmetric electrolyte, whereby an effective valence must be assigned to the polyelectrolyte. This effective valence is substantially smaller than the bare valence due to ion condensation effects. The unusual aspect of the electrical double layer in these systems is the exclusion of the like-charged polyelectrolyte from the vicinity of the surface, leading to a strongly nonexponential diffuse ionic layer that is dominated by counterions and has a well-defined thickness. As the oscillatory depletion force sets in right after this layer, this condition can be used to predict the phase of the oscillatory depletion force.

DOI: 10.1103/PhysRevLett.117.088001

Since the pioneering work of Asakura and Oosawa [1], depletion forces remained in the focus of the soft condensed matter community [2–4]. Much theoretical progress has been made by studying mixtures of hard spheres, and within the mean spherical approximation analytical expressions for the depletion potential between a pair of particles in a suspension of smaller depletants have been derived [3,5]. On the experimental side, spectacular results were obtained by exploring the possibility of tuning the range and strength of the interaction potential between colloidal particles through depletion forces induced by dissolved neutral polymers [6–8]. The availability of these systems opened the possibility to study their phase behavior and establish conditions concerning the occurrence of the gas-liquid phase transition [7] and its relation to colloidal aggregation [8].

More recently, the focus shifted towards charged depletants, including nanoparticles [9,10], micelles [11,12], or polyelectrolytes [13–15]. For a wide range of systems, these forces could be rationalized with a simple damped oscillatory profile, which follows from the large-distance asymptotics of the hard-sphere depletion potential [3,9]. The dependence of the free energy per unit area W with separation distance h as induced by the depletion interaction can be expressed as

$$W_{\mathrm{de}}(h) = Ae^{-h/\xi}\cos(2\pi h/\lambda + \theta), \qquad (1)$$

where A is the amplitude, ξ the correlation length, λ the wavelength, and θ the phase shift. In contrast to hard-sphere systems, however, the wavelength shows a characteristic dependence on the number concentration c of the depletants, typically with scaling behavior as $\lambda \propto c^{-\alpha}$, where $1/3 \leq \alpha \leq 1/2$. Recently, it was shown that this wavelength closely corresponds to the position of the structural peak observed in small angle scattering experiments [9].

When studying depletion forces, one always attempts to minimize interactions between the depletants and the respective substrate. For neutral polymers, the particles are often protected by alkyl-chain brushes [6]. For charged depletants, the larger particles are chosen to be highly charged and with a charge of the same sign as the one of the depletants [9,11,14]. In this way, the deposition of the depletants to the larger particles can be avoided. In such a system, however, the larger particles will interact by repulsive double-layer forces [2] and shorter-ranged depletion interactions [16]. Counterions may also alter the solvent structure close to the interface and affect the surface charge [17]. Double-layer forces will be intimately linked to depletion forces, since the charged depletants will contribute to screening. However, the combined action of the double-layer and depletion force was hardly studied. The reason could possibly be that the double-layer force does not decay exponentially, as one would naively expect from the simple theory of the electrical double layer.

Here, we investigate the interplay between the depletion and double-layer forces acting between charged colloidal silica particles in solutions of strong like-charged polyelectrolytes. We are able to quantify the forces measured with an atomic force microscope (AFM) by means of a superposition of the damped oscillatory depletion forces and repulsive double-layer forces. The double-layer force can be calculated accurately within the mean-field Poisson-Boltzmann (PB) theory by considering highly asymmetric electrolytes. Such electrolytes induce unusual nonexponential force profiles and a well-defined thickness of the diffuse part of the electrical double layer. This thickness then determines the onset of the depletion force and, in turn, its phase.

The double-layer force between two equally charged plates is obtained by numerically solving the PB equation for constant charge boundary conditions [2]. For a solution containing different ions of number concentrations c_i and valence z_i, the PB equation reads

$$\frac{d^2\psi}{dx^2} = -\frac{q}{\varepsilon_0\varepsilon}\sum_i z_i c_i\, e^{-z_i q\psi/kT}, \tag{2}$$

where q is the elementary charge, ε_0 the dielectric permittivity of vacuum, ε the dielectric constant of water, T the absolute temperature, and k the Boltzmann constant. We use $T = 298$ K and $\varepsilon = 80$ as appropriate for water at room temperature. From the electric potential at the midplane ψ_M, one obtains the double-layer disjoining pressure Π_{dl} given by [2]

$$\Pi_{\mathrm{dl}} = kT\sum_i c_i(e^{-z_i q\psi_M/kT} - 1), \tag{3}$$

which is then integrated to obtain the interaction energy

$$W_{\mathrm{dl}} = \int_h^\infty \Pi_{\mathrm{dl}}(h')\, dh'. \tag{4}$$

In the present situation of a highly asymmetric $1:Z$ electrolyte, where the multivalent coions have the same sign of charge as the surface, the pressure profile is determined by the salt-free situation. In this situation, the surface charge is only neutralized by the monovalent counterions, and the PB equation can be solved analytically. For large distances, the pressure is given by

$$\Pi_{\mathrm{dl}} = \frac{\pi}{2}\frac{kT}{l_B(h + 2l_{\mathrm{GC}})^2} - kT(1+Z)c, \tag{5}$$

where $l_B = q^2/(4\pi\varepsilon_0\varepsilon kT)$ is the Bjerrum length, $l_{\mathrm{GC}} = 2\varepsilon_0\varepsilon kT/(q\sigma)$ is the Gouy-Chapman length, whereby σ is the surface charge density, and c is the number concentration of the $1:Z$ electrolyte. The second term corresponds to an osmotic correction [18]. Without that term and for $h \gg l_{\mathrm{GC}}$, Eq. (5) reduces to $\Pi_{\mathrm{dl}} = \pi kT/(2l_B h^2)$ as initially proposed by Langmuir [19].

The numerically calculated PB pressure profiles are shown in Fig. 1. As the valence Z of the coion is being increased, the profile becomes increasingly nonexponential [Fig. 1(a)]. A decrease of the salt concentration [Fig. 1(b)] has a similar effect. The limiting laws are also illustrated by comparing the exact PB profile with Eq. (5) and Langmuir's relation. The pressure decreases initially slowly but then decays rapidly due to the osmotic contribution in Eq. (5). This rapid decay leads to a well-defined thickness of the diffuse layer. The exponentially decaying Debye-Hückel (DH) limiting law is recovered only at large distances [2]

$$\Pi_{\mathrm{dl}} = 2\varepsilon_0\varepsilon\psi_{\mathrm{eff}}^2\kappa^2 e^{-\kappa h}, \tag{6}$$

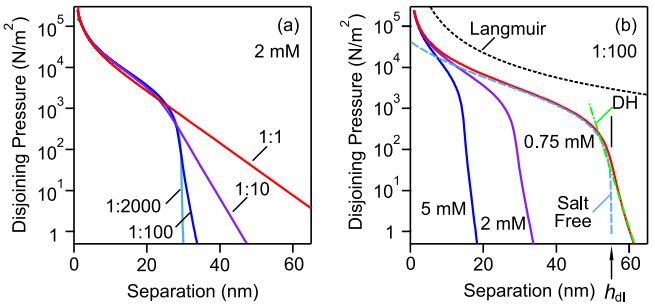

FIG. 1. Disjoining pressure Π_{dl} induced by the electrical double layer versus surface separation h calculated numerically by solving the PB equation for highly asymmetric $1:Z$ electrolytes for a fixed surface change density of -5 mC/m^2 and different concentrations of monovalent ions. Influence of (a) valence Z at a concentration of 2 mM and (b) for a $1:100$ electrolyte of different concentrations. The lowest concentration in (b) also indicates the Langmuir's relationship, approximate salt-free relation Eq. (5), DH limiting law Eq. (6), and the thickness of the diffuse layer h_{dl}. The concentration indicated corresponds to the monovalent counterion concentration.

where ψ_{eff} is the effective potential and κ is the inverse Debye length defined by the relation $\kappa^2 = 4\pi l_B\sum_i z_i^2 c_i$. For such highly asymmetric electrolytes, the respective effective potentials become huge, which simply reflects the fact that the DH limiting law sets in only for $h \gg \kappa^{-1}$. Therefore, the DH approximation cannot be used [10], and the consideration of the PB theory becomes essential.

Very similar features can be observed experimentally. Interaction forces between two silica particles were measured with the colloidal probe technique [20,21]. This technique was implemented with a closed-loop AFM (MFP-3D, Oxford Instruments) mounted on an inverted optical microscope (Olympus, IX 70). Monodisperse silica particles (Bangs Laboratories) were placed to a quartz substrate and glued (Araldite 2000+) to a tipless AFM cantilever (Micromash, CSC37). The particles were heat treated at 1150 °C during 3 h, which results in a solid attachment to the substrate and the cantilever. The heat-treated particles were cleaned in air plasma (PDC-32 G, Harrick) and subsequently washed with ethanol and Milli-Q water (Millipore). The average particle radius is 2.20 μm with a coefficient of variation of 1.2% measured with scanning electron microscopy. The root mean square (rms) roughness of 0.81 ± 0.09 nm was determined by AFM imaging [22]. The attached particles were mounted in the AFM fluid cell, which was filled with a solution of sodium poly(styrene sulfonate) (NaPSS) (Polymer Standards, polydispersity index <1.2) adjusted to pH 4.0 with HCl. The particles were centered by means of the optical microscope with a precision of ~50 nm. Force profiles were extracted from the approach parts of vertical approach-retraction cycles. The contact point was determined from the onset of the constant compliance region with an accuracy of ~0.5 nm. The spring constants

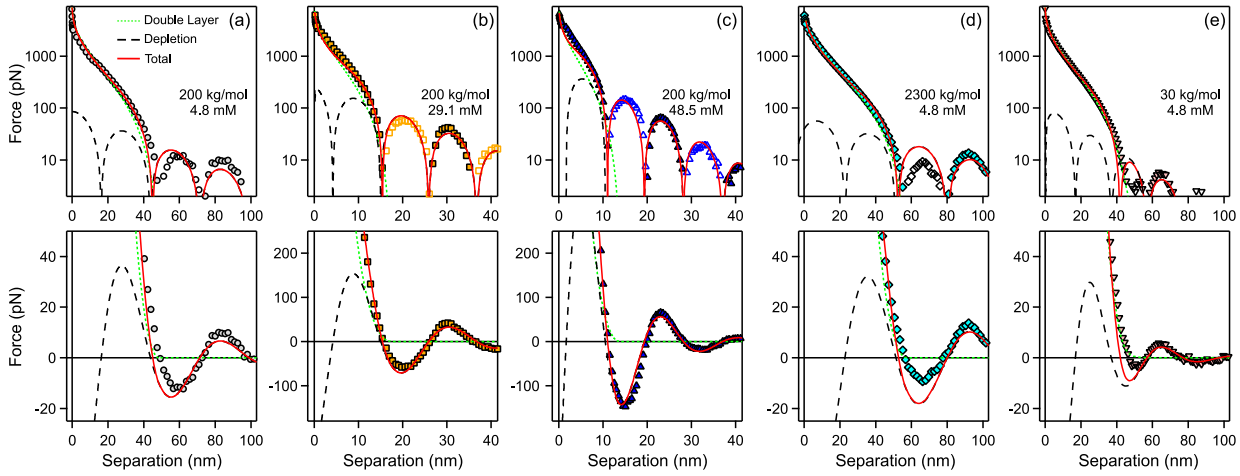

FIG. 2. Forces between silica particles in solutions of NaPSS. Experimental data are compared with calculations based on the PB theory for asymmetric electrolytes and a damped oscillatory depletion force. The concentration indicated corresponds to the monomer concentration. The semilogarithmic representations plot the magnitude of the force. (a)–(c) Variation in concentration and (a),(d),(e) in molecular mass.

of the cantilevers were $\sim 0.3\,\mathrm{N/m}$ as determined by the thermal fluctuation method. By a subsequent averaging of about 100 force profiles, we obtain a force resolution of ~ 2 pN. Force profiles obtained from the approach and retraction traces agreed well for cantilever velocities $<0.5\ \mu\mathrm{m/s}$. The force profiles measured between different pairs of particles were well reproducible at larger distances, while at shorter distances a variation of about 30% was observed. These observations confirm the symmetry of the present measurement geometry, while the lack of this symmetry was considered as a problem in a similar study [10]. Measurements were done also in dialyzed NaPSS solutions, but they were less well reproducible. These measurements showed that a minor changes in the pH and background solution concentration yields very similar results. We have further verified that PSS adsorption on silica is negligible. The fraction of molecular pulling events in the AFM force experiments was $<1\%$ for all PSS samples with molecular mass $>30\,\mathrm{kg/mol}$. PSS adsorption was also measured on oxidized silicon wafers by optical reflectivity with a home-built reflectometer. This fixed-angle reflectometer involves a frequency-modulated polarized diode laser with a wavelength of 533 nm, and an incidence angle of 60° was used [23]. The adsorbed mass of PSS was $<50\ \mu\mathrm{g/m^2}$ in the relevant concentration range.

The force profiles shown in Fig. 2 were quantified by invoking the Derjaguin approximation, which states that the force is given by $F = \pi R W$, where R is the mean particle radius and W is the interaction energy [2]. We approximate this quantity by superposing the contributions from double-layer and depletion forces, namely,

$$W = W_{\mathrm{dl}} + W_{\mathrm{de}}. \tag{7}$$

The depletion contribution is given by Eq. (1), while the double-layer interaction was calculated with the full PB equation assuming a mixture of 0.1 mM monovalent electrolyte and the appropriate concentration of $1{:}Z$ electrolyte. Such results were fitted to the measured force profiles. Thereby, the monomer concentration and the surface charge density σ were fixed. The former was known from the analytical PSS concentration, while the latter value of $-5.0\ \mathrm{mC/m^2}$ was determined by direct force measurements in 10 mM NaCl solution adjusted to pH 4.0. The remaining fitting parameters include the ones of the depletion force, namely, its amplitude A, the correlation length ξ, the wavelength λ, and the phase shift $0 \le \theta < 2\pi$, and the only free parameter entering the double-layer force is the valence. No satisfactory fits could be obtained with the bare valence Z of PSS, which corresponds to the number of charged groups. Therefore, we have introduced an effective valence Z_{eff} as a fitting parameter. The fits systematically yields $Z_{\mathrm{eff}} < Z$, and this difference implies that not all counterions dissociate. This phenomenon is well known as the Manning counterion condensation [24]. The experimental data were compatible with a fixed ratio λ/ξ for each molecular mass. As Fig. 2 illustrates, this model was capable to quantify the experimental force profile very well, typically over 3 orders in magnitude. The resulting parameters are summarized in Figs. 3 and 4. The limiting DH decay is hardly noticeable in the force profiles, as it is hidden by the onset of the depletion force. Van der Waals attraction was not observed either, as it is probably overruled by short-ranged repulsive forces (e.g., hydration and hairy-layer) [20].

Figure 2 illustrates that double-layer forces dominate the force profiles at smaller distances, while depletion forces at larger ones. Because of the rapid decay of the former, both forces contribute simultaneously only in a small distance range. In this range, some deviations from the superposition approximation [Eq. (7)] can be evidenced. However, these deviations are relatively minor, and for this reason we did

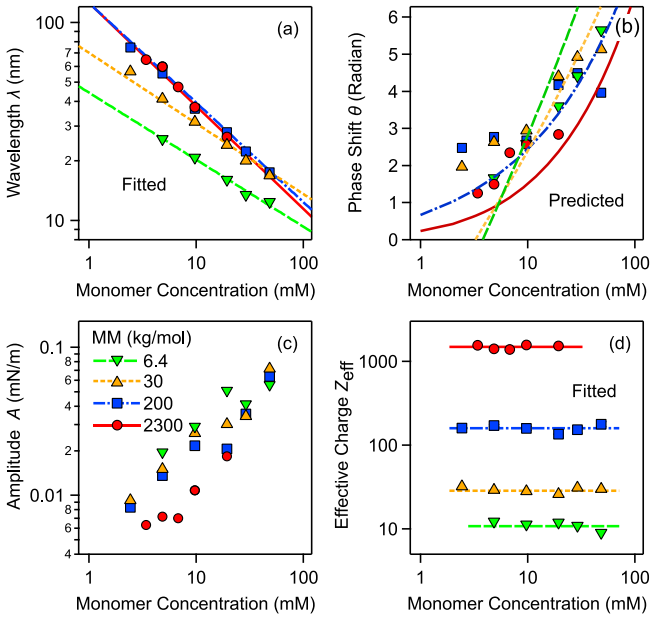

FIG. 3. Fitted parameters extracted from the measured force profiles versus the monomer concentration for NaPSS of different molecular mass (MM). (a) Wavelength λ, (b) phase shift θ, (c) amplitude A, and (d) effective valence Z_{eff}. The solid lines indicate the fitted exponent in the power-law dependence $\lambda \propto c^{-\alpha}$ in (a) and the average value in (d). The solid lines in (b) are model predictions as described in the text.

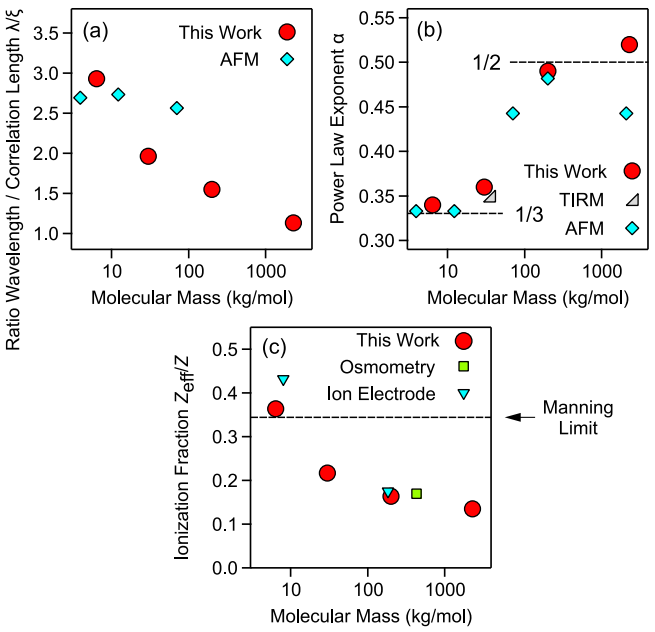

FIG. 4. Dependence of the model parameters in salt-free NaPSS solutions versus the molecular mass. (a) Ratio of the wavelength and correlation length λ/ξ, (b) exponent of the power law $\lambda \propto c^{-\alpha}$, and (c) ionization fraction Z_{eff}/Z. The present data are compared with parameters given in the literature for measured depletion forces in the same system for AFM colloidal probe measurements [13,25] and TIRM [26]. Literature data for the ionization fraction were obtained by osmometry [27] and ion-specific electrodes [28]. The dashed lines indicate the limiting exponents in (b) and the Manning limit in (c).

not attempt to use more detailed models of the depletion force [3,5]. At shorter distances, the depletion force is overwhelmed by the double-layer force by orders of magnitude.

One further observes that the range of the double-layer force increases with increasing molecular mass of the polymer and decreases with increasing concentration. These trends were already suggested by the model calculations with the strongly asymmetric electrolyte presented in Fig. 1. The wavelength of the depletion force also increases with increasing molecular mass of the polymer and decreases with increasing concentration. Such trends were reported by researchers focusing on forces induced by charged depletants earlier [13,25,26].

The dependence of the fitted parameters on the PSS concentration is summarized in Fig. 3. Let us first discuss the parameters describing the depletion force, namely, the wavelength λ, the phase shift θ, and the amplitude A. The wavelength decreases with the concentration following a power law $\lambda \propto c^{-\alpha}$. The phase shift θ and the amplitude A increase with concentration. Figure 4 summarizes the molecular mass dependence of the ratio λ/ξ and the power-law exponent α, and they compare favorably with values obtained from earlier direct force measurements in similar systems [13,25,26]. The fixed ratio λ/ξ decreases with the molecular mass. The power-law exponent α increases from $1/3$ to $1/2$ at a molecular mass of $\sim$100 kg/mol as the solution undergoes a dilute to semidilute transition. For this molecular mass, the crossover concentration is about $\sim$7 mM as can be inferred from the respective gyration radii [29].

The only adjustable parameter characterizing the double-layer force is the effective valence Z_{eff}. This parameter is always lower than the bare valence Z, since some of the counterions are condensed on the polymer and they do not dissociate [24]. The effective valence is concentration independent [Fig. 3(d)] but increases with an increasing molecular mass of PSS. The ratio Z_{eff}/Z decreases initially with the molecular mass but then remains almost constant around 0.15 ± 0.05 [Fig. 4(c)]. The presently measured values are very similar to values found with independent methods earlier [27,28]. The measured values are well comparable to the Manning condensation limit of $Z_{\mathrm{eff}}/Z = a/l_B \simeq 0.35$, where $a \simeq 0.25$ nm is the length of the PSS monomeric unit [24]. The experimentally observed values are somewhat smaller, and this deviation is probably caused by the small amounts of salt present [30]. Indeed, only a minor fraction of the counterions dissociated from the polyelectrolytes contribute to the diffuse layer formed.

This quantitative picture can be used to explore the interplay between depletion and double-layer forces. We now demonstrate that the phase of the depletion force is

determined by the thickness of the diffuse layer. This thickness h_{dl} can be estimated by setting $\Pi_{dl}(h_{dl}) = 0$ in the approximate Eq. (5) as indicated in Fig. 1(b). Once this distance is known, one requires that the argument in Eq. (1) is $2\pi h_{dl}/\lambda + \theta = 5\pi/2$. The physical meaning of this condition is that the depletion force vanishes at the diffuse layer boundary and initially decreases with the distance. A similar condition is approximately valid for hard spheres [3]. From this condition, the phase θ can be calculated, whereby the wavelength λ is obtained from the fitted scaling relations shown in Fig. 3(a). These predictions do not contain any adjustable parameters, and they are plotted as lines in Fig. 3(b). The agreement with the experiment is very good. This finding demonstrates that the onset of the depletion force is related to the thickness of the diffuse part of a polyelectrolyte-free electric double layer.

We conclude by stating that such a consistent description of forces acting on charged surfaces in solutions of like-charged polyelectrolytes by means of a superposition of depletion and double-layer forces has been proposed for the first time. The oscillatory depletion forces dominate at larger distances, whereby the respective wavelength reflects the structure of the polyelectrolyte solution and is in agreement with previous studies. The polyelectrolyte is excluded from the diffuse part of the double layer, and therefore this layer is dominated by monovalent counterions. This structure leads to a highly nonexponential force profile, which can be well rationalized by the PB theory for highly asymmetric electrolytes with monovalent counterions and multivalent polyelectrolyte coions. However, an effective valence must be assigned to the polyelectrolyte, which is typically 2–8 times smaller than its bare value. The effective valence is comparable to the one obtained with independent methods [27,28] and can be relatively well rationalized by counterion condensation [24,30]. The thickness of this diffuse layer further determines the onset of the depletion force and its phase. While a DH regime is also present at large distances and low forces, this regime is typically hidden by the onset of the depletion force.

The present findings will certainly revive experimental and theoretical investigations of the structure of the double layer in strongly asymmetric electrolytes, which include not only polyelectrolyte solutions but also micellar solutions or salt-free suspensions of charged colloidal particles [9–12]. Similar investigations in the latter systems may also shed light on like-charge attraction phenomena [31], which might be related to the interplay of nonexponential force profiles originating from overlapping double layers and oscillatory depletion forces.

This research was supported by the Swiss National Science Foundation (Grant No. 159874) and the University of Geneva.

*Corresponding author.
gregor.trefalt@unige.ch

[1] S. Asakura and F. Oosawa, J. Chem. Phys. **22**, 1255 (1954).
[2] W. B. Russel, D. A. Saville, and W. R. Schowalter, *Colloidal Dispersions* (Cambridge University Press, Cambridge, England, 1989).
[3] A. Trokhymchuk, D. Henderson, A. Nikolov, and D. T. Wasan, Langmuir **17**, 4940 (2001).
[4] K. Binder, P. Virnau, and A. Statt, J. Chem. Phys. **141**, 140901 (2014).
[5] D. Henderson and K.-Y. Chan, Mol. Phys. **98**, 1005 (2000).
[6] A. Milling and S. Biggs, J. Colloid Interface Sci. **170**, 604 (1995).
[7] H. N. W. Lekkerkerker, W. C. K. Poon, P. N. Pusey, A. Stroobants, and P. B. Warren, Europhys. Lett. **20**, 559 (1992).
[8] P. J. Lu, E. Zaccarelli, F. Ciulla, A. B. Schofield, F. Sciortino, and D. A. Weitz, Nature (London) **453**, 499 (2008).
[9] S. H. L. Klapp, Y. Zeng, D. Qu, and R. von Klitzing, Phys. Rev. Lett. **100**, 118303 (2008).
[10] S. Grandner, Y. Zeng, R. von Klitzing, and S. H. L. Klapp, J. Chem. Phys. **131**, 154702 (2009).
[11] P. Richetti and P. Kekicheff, Phys. Rev. Lett. **68**, 1951 (1992).
[12] D. l. Sober and J. Y. Walz, Langmuir **11**, 2352 (1995).
[13] C. Uzum, S. Christau, and R. von Klitzing, Macromolecules **44**, 7782 (2011).
[14] S. Biggs, J. L. Burns, Y. D. Yan, G. J. Jameson, and P. Jenkins, Langmuir **16**, 9242 (2000).
[15] A. J. Milling and K. Kendall, Langmuir **16**, 5106 (2000).
[16] M. M. Hatlo, R. A. Curtis, and L. Lue, J. Chem. Phys. **128**, 164717 (2008).
[17] S. Deshmukh, G. Kamath, S. Ramanathan, and S. K. Sankaranarayanan, Phys. Rev. E **88**, 062119 (2013).
[18] G. Trefalt, Phys. Rev. E **93**, 032612 (2016).
[19] I. Langmuir, J. Chem. Phys. **6**, 873 (1938).
[20] W. A. Ducker, T. J. Senden, and R. M. Pashley, Langmuir **8**, 1831 (1992).
[21] H. J. Butt, B. Cappella, and M. Kappl, Surf. Sci. Rep. **59**, 1 (2005).
[22] V. Valmacco, M. Elzbieciak-Wodka, C. Besnard, P. Maroni, G. Trefalt, and M. Borkovec, Nanoscale Horiz. **1**, 325 (2016).
[23] M. Porus, P. Maroni, and M. Borkovec, Langmuir **28**, 5642 (2012).
[24] G. S. Manning, J. Chem. Phys. **51**, 924 (1969).
[25] A. J. Milling, J. Phys. Chem. **100**, 8986 (1996).
[26] S. Biggs, D. C. Prieve, and R. R. Dagastine, Langmuir **21**, 5421 (2005).
[27] A. Takahashi, N. Kato, and M. Nagasawa, J. Phys. Chem. **74**, 944 (1970).
[28] C. Wandrey, D. Hunkeler, U. Wendler, and W. Jaeger, Macromolecules **33**, 7136 (2000).
[29] J. Yashiro and T. Norisuye, J. Polym. Sci. B **40**, 2728 (2002).
[30] E. Trizac and G. Téllez, Phys. Rev. Lett. **96**, 038302 (2006).
[31] M. Brunner, J. Dobnikar, H. H. von Grunberg, and C. Bechinger, Phys. Rev. Lett. **92**, 078301 (2004).

CHAPTER 6

Depletion and double layer forces acting between charged particles in solutions of like-charged polyelectrolytes and monovalent salt

Moazzami-Gudarzi, M.; Maroni, P.; Borkovec, M.; Trefalt, G., *Soft Matter* **2017**, 13, 3284-3295.

Reproduced with permission

Soft Matter

PAPER

View Article Online
View Journal

Cite this: DOI: 10.1039/c7sm00314e

Depletion and double layer forces acting between charged particles in solutions of like-charged polyelectrolytes and monovalent salts

Mohsen Moazzami-Gudarzi, Plinio Maroni, Michal Borkovec and Gregor Trefalt *

Received 14th February 2017,
Accepted 4th April 2017

DOI: 10.1039/c7sm00314e

rsc.li/soft-matter-journal

Interaction forces between silica particles were measured in aqueous solutions of the sodium salt of poly(styrene sulphonate) (PSS) and NaCl using the colloidal probe technique based on an atomic force microscope (AFM). The observed forces can be rationalized through a superposition of damped oscillatory forces and double layer forces quantitatively. The double layer forces are modeled using Poisson–Boltzmann (PB) theory for a mixture of a monovalent symmetric electrolyte and a highly asymmetric electrolyte, whereby the multivalent coions represent the polyelectrolyte chains. The effective charge of the polyelectrolyte is found to be smaller than the bare number of charged groups residing on one polyelectrolyte molecule. This effect can be explained by counterion condensation. The interplay between depletion and double layer forces can be further used to predict the phase of the depletion force oscillations. However, this picture holds only at not too elevated concentrations of the polyelectrolyte and salt. At higher salt concentrations, attractive van der Waals forces become important, while at higher polyelectrolyte concentrations, the macromolecules adsorb onto the like-charged silica interface.

Introduction

The properties of particle suspensions, such as their stability and rheology, can be tuned by the addition of polyelectrolytes.[1–3] Such effects are being exploited in industrial applications, for example, in papermaking, water treatment, or mineral separation.[4–6] Due to the importance of these applications, interactions between water–solid interfaces in polyelectrolyte solutions have been investigated in substantial detail. Experimental studies often rely on surface force apparatus, total internal reflection microscopy, or the colloidal probe technique, which is based on an atomic force microscope (AFM).[2,3,7] These investigations mainly focused on oppositely charged systems, where the substrate and the polyelectrolytes have the opposite sign of charge. These systems are dominated by polyelectrolyte adsorption and charge reversal, and the resulting interactions can be mostly rationalized by exponential double layer forces.[8–11] Near the charge reversal point, attractive forces are being observed. The strength of this attraction sometimes exceeds the one of the van der Waals force, and this enhancement can be explained by electrostatic attraction between surface charge heterogeneities.[1,9]

Much less attention is focused on like-charged systems, where the substrates and the polyelectrolytes have the same sign of charge. One would naively expect that the polyelectrolyte would not adsorb onto the substrate due to the strong electrostatic repulsion, but that depletion forces could become important. Indeed, several authors reported such forces, and it was demonstrated that these forces become oscillatory.[12–17] Such oscillatory forces could be equally observed to act between other types of surfaces, for example, between polyelectrolyte multilayers or gas bubbles.[18,19] Similar forces could also be induced by other types of charged objects, such as, micelles or nanoparticles.[20–23] The oscillation period of the depletion force was shown to be related to the position of the structural peak observed by small angle scattering.[22] This finding clearly confirms that the oscillatory nature of these forces reflects the structuring of the bulk suspension. These forces thus appear to have a similar origin to the well investigated depletion forces induced by uncharged objects.[24–26] Nevertheless, electrostatic interactions are important in determining these forces, since these forces can be screened away by adding a simple salt to the system.[12,13]

In spite of all the activity on depletion forces in like-charged polyelectrolyte systems, the role of double layer forces is poorly investigated. Typical interfaces considered in such systems are highly charged and should induce strong repulsive double layer forces. While theoretical treatments have stressed the importance of double layer forces in similar systems,[27–31] hardly any

Department of Inorganic and Analytical Chemistry, University of Geneva, Sciences II, 30 Quai Ernest-Ansermet, 1205 Geneva, Switzerland. E-mail: gregor.trefalt@unige.ch; Tel: +41 22 379 6054

experimental information on these forces in systems containing like-charged polyelectrolyte is available.

An exception is our very recent report on force measurements between charged interfaces in salt-free solutions of like-charged polyelectrolytes.[32] This report concludes that double layer forces are indeed important at shorter distances. However, the corresponding profiles are highly non-exponential and they can be only rationalized in terms of Poisson–Boltzmann (PB) theory for a highly asymmetric electrolyte, where the multivalent coions represent the polyelectrolyte chains. The non-exponential nature of the double layer force is due to the presence of a diffuse layer consisting of monovalent counterions only.

The present article extends this approach to systems containing monovalent salts. The double layer forces can be again rationalized in terms of PB theory, but a mixture of a highly asymmetric electrolyte and a monovalent symmetric electrolyte must be explicitly considered. With this modification, one can again use a superposition of depletion and double layer forces to obtain a comprehensive picture of the interaction forces acting in like-charged polyelectrolyte systems even in the presence of salt.

Modeling interaction forces

The force F acting between pairs of colloidal particles was calculated from the interaction energy between two flat surfaces W by means of the Derjaguin approximation

$$F = 2\pi R_{\mathrm{eff}} W \tag{1}$$

where R_{eff} is the effective radius, which is given for two identical spherical particles of radius R by $R_{\mathrm{eff}} = R/2$. In the following, we will always report the normalized force F/R_{eff}.

We assume that the interaction energy can be approximated by a simple superposition of depletion and double layer contributions

$$W = W_{\mathrm{de}} + W_{\mathrm{dl}} \tag{2}$$

Thereby, W_{de} is the contribution due to depletion and W_{dl} the one due to overlap of electric double layers. At larger distances, the dependence of the depletion contribution on the separation distance h is given by an exponentially damped oscillatory function, namely[22,33]

$$W_{\mathrm{de}} = A\,\mathrm{e}^{-h/\xi}\cos(2\pi h/\lambda + \theta) \tag{3}$$

where A is the amplitude, ξ the correlation length characterizing the decay, λ the wavelength of the oscillation, and θ the phase shift.

The double layer force acting between two identically charged plates can be calculated from the PB equation. When the electrolyte solution contains different ions of number concentrations c_i and valence z_i this equation reads[34,35]

$$\frac{\mathrm{d}^2\psi}{\mathrm{d}x^2} = -\frac{q}{\varepsilon_0\varepsilon}\sum_i z_i c_i \mathrm{e}^{-z_i\beta q\psi} \tag{4}$$

where q is the elementary charge, ε_0 is the dielectric permittivity of vacuum, ε is the dielectric constant of water, and β is the inverse thermal energy. The latter parameter is given by $\beta = 1/(kT)$ where T is the absolute temperature and k is the Boltzmann constant. The potential profile is calculated numerically by assuming that the plates are located at $x = \pm h/2$ and by imposing the constant regulation (CR) boundary condition[35]

$$\varepsilon_0\varepsilon\left.\frac{\mathrm{d}\psi}{\mathrm{d}x}\right|_{x=h/2} = \sigma - C_{\mathrm{in}}[\psi(h/2) - \psi_{\mathrm{dl}}] \tag{5}$$

where σ is the surface charge density, ψ_{dl} is the diffuse layer potential, and C_{in} is inner layer capacitance of the isolated surface. The surface charge density and the diffuse layer potential are related through the charge–potential relationship

$$\sigma = \pm\left\{2kT\varepsilon_0\varepsilon\sum_i c_i\left[\mathrm{e}^{-z_i\beta q\psi_{\mathrm{dl}}} - 1\right]\right\}^{1/2} \tag{6}$$

where the + sign applies to a positively charged surface and the − sign to a negatively charged one. Instead of referring to the inner layer capacitance, we use the regulation parameter $p = C_{\mathrm{dl}}/(C_{\mathrm{dl}} + C_{\mathrm{in}})$ where C_{dl} is the diffuse layer capacitance given by $C_{\mathrm{dl}} = \mathrm{d}\sigma/\mathrm{d}\psi_{\mathrm{dl}}$. This parameter has the advantage that it assumes simple values for the classical boundary conditions, namely $p = 1$ for constant charge (CC) and $p = 0$ for constant potential (CP). In the present setting, we solve the PB equation for a negatively charged substrate in contact with a mixture of a monovalent 1 : 1 salt of concentration c_{S} and of a 1 : Z salt with multivalent coions of valence Z and monovalent counterions of concentration c_{M}. The latter asymmetric salt mimics the strong polyelectrolyte. The concentration c_{M} will also be referred to as the monomer concentration, and it provides a more useful parameterization of the problem than the polyelectrolyte concentration, which is given by c_{M}/Z. Thus, the quantities entering the PB equation read $c_1 = c_{\mathrm{S}} + c_{\mathrm{M}}$, $c_2 = c_{\mathrm{S}}$, and $c_3 = c_{\mathrm{M}}/Z$, and accordingly $z_1 = +1$, $z_2 = -1$, and $z_3 = -Z$.

Once the electric potential is known, one can obtain the disjoining pressure from the potential at the mid-plane $\psi_{\mathrm{M}} = \psi(0)$ by means of the relation

$$\Pi_{\mathrm{dl}} = kT\sum_i c_i\left(\mathrm{e}^{-z_i\beta q\psi_{\mathrm{M}}} - 1\right) \tag{7}$$

The interaction energy is then obtained by integration

$$W_{\mathrm{dl}} = \int_h^\infty \Pi_{\mathrm{dl}}(h')\mathrm{d}h' \tag{8}$$

At sufficiently large separation distances, the Debye–Hückel (DH) approximation becomes valid and the interaction energy decays exponentially, namely

$$W_{\mathrm{dl}} = 2\varepsilon_0\varepsilon\kappa\psi_{\mathrm{eff}}{}^2\,\mathrm{e}^{-\kappa h} \tag{9}$$

where ψ_{eff} is an effective potential and κ^{-1} is the Debye screening length defined by

$$\kappa^2 = 8\pi\ell_{\mathrm{B}}I \tag{10}$$

Thereby, I is the ionic strength

$$I = \frac{1}{2}\sum_i z_i^2 c_i \tag{11}$$

and ℓ_B is the Bjerrum length given by

$$\ell_B = \frac{\beta q^2}{4\pi\varepsilon_0\varepsilon} = 0.70 \text{ nm} \quad (12)$$

The numerical value refers to room temperature at T = 298 K and ε = 80 as appropriate for water. The ionic strength is also expressed in terms of the number concentration. The unusual aspect of the highly asymmetric electrolytes with multivalent coions is that this limiting law only sets in at considerably large distances and the effective potential can be substantially larger than the diffuse layer potential in magnitude.[36]

One may question the validity of the superposition approximation given in eqn (2) and particularly the validity of eqn (3) at shorter distances. Based on the studies of hard-sphere fluids, the exponentially damped oscillatory profile is only valid at large distances, and corrections become necessary closer by.[33] At very short distances, the depletion force features an attractive well, which is dominated by the exclusion of the spheres from the gap. In this regime, however, the magnitude of the depletion force is basically negligible with respect to the substantial double layer force in the systems considered here. One can thus use eqn (3) down to contact, and deviations are only expected in the rather narrow transition region between depletion and double layer forces. Nevertheless, a more consistent simultaneous description of depletion and double layer forces would be highly desirable.

Experimental

Materials

Sodium salts of poly(styrene sulfonate) (PSS) with molecular masses near 6.4, 30, 200 and 2100 kg mol^{-1} and polydispersity indices below 1.2 were purchased from Polymer Standards (Germany) and were used as received. Silica microspheres with a diameter of 5.0 μm were obtained from Bangs Laboratories Inc., USA. For all the measurements, PSS was dissolved in pure water overnight and the pH was adjusted to 4.0 with dilute HCl. Such PSS solutions were mixed with NaCl solutions adjusted to pH 4.0. Milli-Q water (Millipore) was used throughout. The measurements were performed at room temperature of 21 ± 3 °C.

Probes and substrates

Forces between pairs of silica particles were measured between particles attached to tip-less AFM cantilevers and quartz slides with deposited colloidal particles. Silica powder was spread on a glass slide and a tiny drop of about 10 μL of an epoxy glue (Araldite 2000+) was placed beside the particles. A tip-less cantilever (MikroMasch, Tallin, Estonia) was cleaned with air plasma (PDC-32G, Harrick, New York) for 10 minutes, and then mounted in the AFM. The cantilever was then dipped into the drop of glue and used to pick up a silica particle from the substrate. Quartz slides (Edmund Optics) were cleaned for 2 hours in a piranha solution, which is a mixture of H_2SO_4 98% and H_2O_2 30% in a volumetric ratio of 3 : 1. The slides were thoroughly washed with water and dried under a stream of nitrogen gas. Small amounts of silica particles were sprinkled over the quartz slide. The cantilevers with the glued silica particles and the quartz substrates were sintered side by side in a furnace for 3 hours at 1150 °C. This procedure resulted in firm attachment of the silica particles to the cantilever and the substrate and complete removal of the glue. Thereby, the silica particles shrink slightly. After shrinking, their mean diameter of 4.4 μm and polydispersity below 2% were determined by scanning electron microscopy. The sintered particles were rather smooth, featuring a root mean square roughness below 1 nm. This procedure results in an almost symmetric system consisting of two silica particles. Further details concerning the attachment procedure can be found elsewhere.[37]

Direct force measurements

The colloidal probe technique was used to measure the forces between pairs of silica particles in PSS solutions and was realized with a closed-loop AFM (MFP-3D, Oxford Instruments) mounted on an inverted optical microscope (Olympus IX73). The cantilever and the substrate were rinsed with pure water and ethanol several times and finally cleaned in a plasma chamber for 10 minutes. The quartz slide with sintered silica particles was glued on the glass plate sealing the AFM cell. The glass plate and cantilever were then mounted in the AFM fluid cell. The fluid cell was thoroughly flushed with polyelectrolyte solution several times and left to equilibrate for at least 20 minutes. The particles on the cantilever were centered above another particle on the substrate by means of an optical microscope with a lateral precision of about 100 nm. The cantilever deflection was acquired with a sampling rate of 5 kHz, a cycle frequency of 0.5 Hz, and an approach velocity of 500 nm s^{-1}. For each pair of particles, about 100 cycles were recorded. The zero separation distance was assumed when the force reached a value of 10 mN m^{-1} for repulsive curves, and 4 mN m^{-1} for the attractive curves. This procedure leads to a precision of 0.3 nm in the determination of the contact point and was used earlier.[38] The force profiles were obtained by applying Hooke's law to convert cantilever deflection to force. The spring constants of the cantilevers were in the range of 0.2–0.4 N m^{-1} as calculated from lateral dimensions of the cantilever and their frequency response as described by Sader *et al.*[39] Individual raw approach–retraction cycles feature a noise level of about 20 pN and they are shown in Fig. 1a. In the absence of a salt, the approach–retraction cycles are fully reversible. In a similar system, non-reversible profiles were reported, but in that case the lack of reversibility was caused by the smaller spring constants of the cantilever and the sphere-plane geometry used.[21] Especially in the presence of NaCl, one frequently observes single-molecule pulling events. These events indicate that PSS adsorbed to the silica surface bridges the two particles. Upon retraction, these bridging polymers are being stretched and finally detached from the probe, leading to typical spikes in the force profile. The force resolution can be substantially improved by averaging the approach profiles from different cycles. By performing such a procedure for about 100 individual profiles, one obtains a force resolution of about 2 pN. This procedure is further illustrated in Fig. 1b. Only such averaged

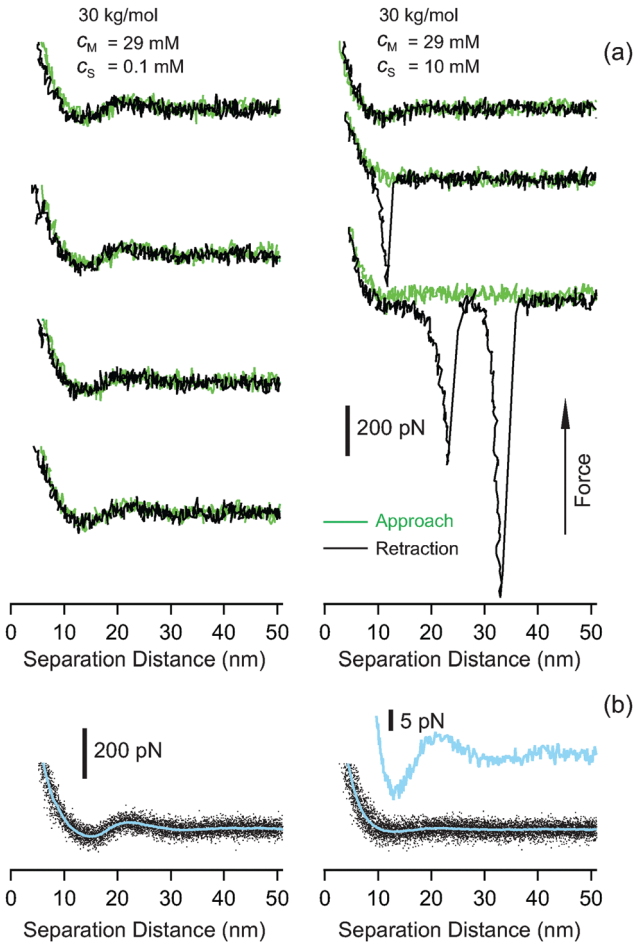

Fig. 1 Raw force profiles recorded with the AFM between silica particles in solutions of sodium PSS of a molecular mass of 30 kg mol^{-1} with a monomer concentration of 29 mM adjusted to pH 4.0. Left column shows data without added NaCl and the right one with a salt concentration of 10 mM. (a) Individual approach–retraction cycles. (b) Raw approach data from about 150 cycles (points) and averaged force profile (solid line). For clarity, only each 10th data point is shown. The inset in (b, right) shows details of the averaged force profile.

force profiles are used in the subsequent analysis and are shown in all the figures except indicated otherwise. Force profiles were determined at least for 3 different pairs of particles for each particular condition.

Results and discussion

Direct force measurements were carried out between pairs of similar silica particles with a diameter of 4.4 μm in solutions of a negatively charged polyelectrolyte and a simple monovalent salt. This system was realized by dissolving sodium PSS salt and NaCl in pure water adjusted to pH 4.0. Already under these mildly acidic conditions, the silica particles acquire a substantial diffuse layer charge.[40,41] We will first focus on the situation of relatively low concentrations of the polyelectrolyte and monovalent salt, where polyelectrolyte adsorption is negligible. In this regime, the forces can be interpreted by superposing damped oscillatory depletion forces and double layer forces, whereby a complete and quantitative picture can be obtained. We will also briefly address the situation for higher concentrations of the polyelectrolyte and/or monovalent salt. This situation is more complex, as the polyelectrolyte adsorbs to the like-charged substrate, and we will only highlight some characteristic phenomena qualitatively.

Calculated double layer force profiles

Let us first illustrate the uncommon aspects of the double layer forces in these systems with model PB calculations in highly asymmetric electrolytes with multivalent coions. Fig. 2 presents the numerical results of the normalized force between two negatively charged surfaces in a mixture of 1 : 1 and 1 : 100 electrolytes. The salt originating from an anionic polyelectrolyte is modeled by the 1 : 100 electrolyte. We assume a surface charge density of −5.0 mC m^{-2} and CC boundary conditions. Fig. 2a illustrates the situation where the monomer concentration c_M is fixed to 1.0 mM. Without addition of any monovalent salt, the force profile is strongly non-exponential, and features a slow decay at intermediate distances. In the semi-logarithmic representation shown, this profile has a typical sigmoidal appearance, which is characteristic of double layer forces in a highly asymmetric electrolyte with multivalent coions. The reason for the slow decay at smaller distances is that the coions are expelled from the gap and the diffuse layer is dominated by the monovalent counterions. This situation resembles a salt-free system, where forces decay slowly as a power-law.[42,43] At larger distances, the pressure decreases rapidly due to the osmotic pressure difference to the electrolyte solution. When a monovalent salt is being added to such a system, the range of the double layer interaction decreases, and the pressure profile approaches the classical DH exponential decay. This decay is indicated as the dotted line in the semi-logarithmic plot shown, see eqn (9). This transition between the salt-free and salt-dominated system is illustrated more clearly in Fig. 2b. In this case, the concentration of the monovalent salt c_S is fixed

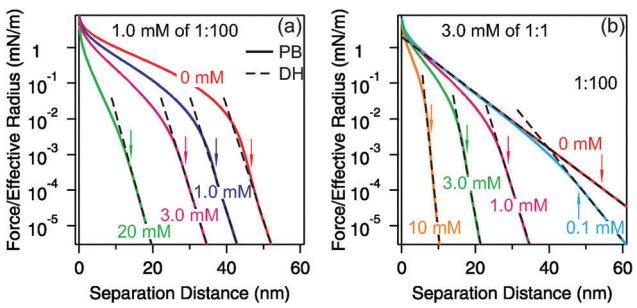

Fig. 2 Double layer forces between surfaces with a charge density of −5.0 mC m^{-2} in a mixture of 1 : 1 and 1 : 100 electrolytes calculated with PB theory. The concentrations refer to the monovalent counterions originating from the respective electrolytes. The dotted lines indicate the DH decay at large distances and the arrow the diffuse layer thickness as defined by eqn (15). (a) Fixed concentration of the 1 : 100 electrolyte and different additions of the monovalent 1 : 1 electrolyte. (b) Fixed concentration of the 1 : 1 electrolyte and different additions of the 1 : 100 electrolyte.

to 3.0 mM. When no polyelectrolyte is present, the force profile decays exponentially. When one starts to add the polyelectrolyte, the force profile becomes progressively sigmoidal, characteristic of a strongly asymmetric electrolyte solution. One should note that charge regulation effects affect these profiles only weakly, and they become only important at short distances, typically below a few nm.

Experimental force profiles and their concentration dependence

Let us now consider the experimentally measured force profiles. These profiles feature the oscillatory depletion force at larger distances and the double layer force at shorter distances. The non-exponential nature of the double layer forces discussed above will be confirmed by these experiments clearly.

Fig. 3 illustrates the situation of the sodium salt of PSS of a molecular mass of 30 kg mol^{-1}. Thereby, the concentration c_M of the PSS monomers is fixed and the concentration c_S of the added monovalent salt is being increased. The top row shows the magnitude of the normalized force in a semi-logarithmic representation, while the bottom row shows the force on a linear scale. The salt-free situation is presented in Fig. 3a. At larger distances, one observes the characteristic oscillations due to structuring of the polyelectrolyte solution. At shorter distances, the strong double layer repulsion sets in. The profile is non-exponential and resembles the one for a strongly asymmetric electrolyte discussed above (see Fig. 2a). The DH decay of the double layer force is not visible in the experimental profiles as it is overruled by the onset of the depletion force. The gyration radius of the PSS chains is about 7 nm and the overlap monomer concentration is around 80 mM under these conditions.[44,45] These numbers confirm that the polymer solution is dilute and that the polymer coils are small with respect to the measured diffuse layer thickness and the wavelength.

Fig. 3b and c illustrate the effect of increasing the concentration of the monovalent salt. One observes a decrease in the amplitude of the oscillation of the depletion force and of the range of the double layer force. At the same time, the double layer force starts to assume the expected exponential dependence. These features are consistent with the fact that the system becomes increasingly dominated by the monovalent salt.

The experimental data were fitted with a superposition of depletion and double layer forces. The depletion forces are modeled with an exponentially damped oscillatory profile and the double layer forces with PB theory for a mixture of 1 : 1 and 1 : Z electrolytes. The details of these calculations are presented in the theory section. The concentrations of the polyelectrolyte monomers and the monovalent salt were set to the known values. The observed force profiles could not be reproduced with the valence Z, which also corresponds to the bare charge of the polyelectrolyte expressed in units of the negative elementary charge $-q$. However, good agreement can be obtained, when this charge was adjusted to an effective value Z_{eff}. In order to retain electroneutrality, the respective concentration of monovalent counterions entering the PB calculations is now given by $c_M Z_{eff}/Z$. The adjustable parameters for the description of the double layer thus were the effective charge Z_{eff}, the charge density of the interface σ, and its regulation parameter p. The parameters describing the depletion interactions are the amplitude A, the wavelength λ, and the correlation length ξ.

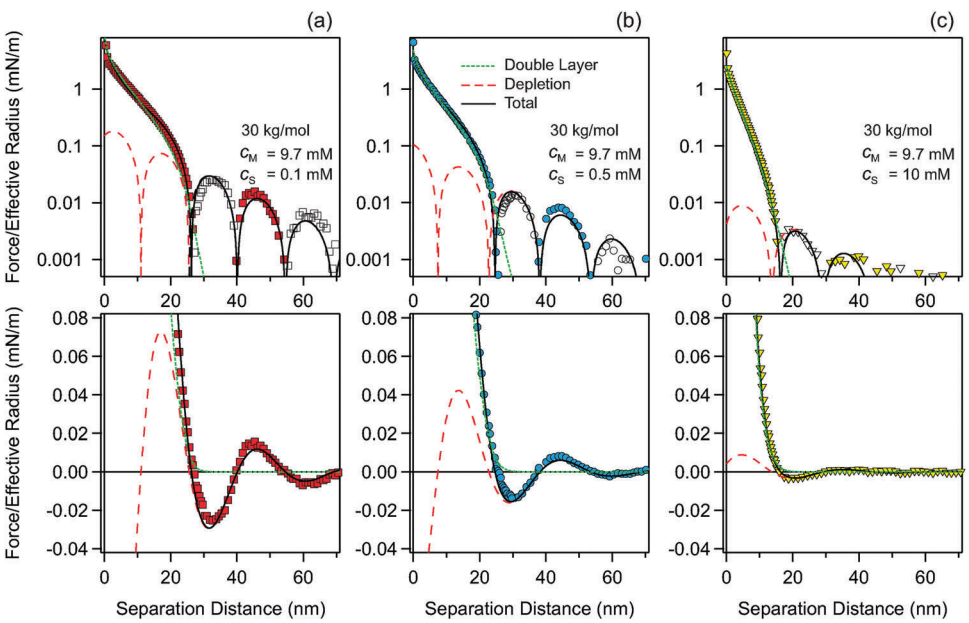

Fig. 3 Effect of addition of salt on forces between silica particles in solutions of sodium PSS with a molecular mass of 30 kg mol^{-1} at pH 4. The magnitude of the force in a semi-logarithmic representation (top) and linear representation of the force (bottom). The PSS monomer concentration is fixed at c_M = 9.7 mM and the NaCl concentration c_S increases from left to right. (a) c_S = 0.1 (no NaCl added), (b) c_S = 0.5 mM, and (c) c_S = 10 mM. Experimental data are compared with calculations based on a superposition of depletion and double layer forces. The individual contributions are also indicated.

For a given molecular mass, the data were consistent with a fixed ratio of the wavelength and the correlation length λ/ξ. In the present case, we find $\lambda/\xi = 1.9 \pm 0.1$. Best fits are indicated in Fig. 3, whereby the separate contributions of the depletion force and the double layer are indicated too. These contributions illustrate that the depletion force given by eqn (3) is indeed negligible with respect to the double layer force at shorter distances. For measurements involving pairs of different silica particles, the typical variation of the fitted parameters is normally below 10%.

The dependence on the concentration c_S of the added monovalent salt was studied at a fixed concentration c_M of PSS monomers. The resulting fitted parameters are summarized in Fig. 4. The lowest concentration of the monovalent salt shown corresponds to 0.1 mM and this condition reflects the addition of HCl for the adjustment of pH to 4.0. However, this value is always substantially smaller than the monomer concentration, and thus the PSS solution can be considered as salt-free under these conditions. The surface charge density and the regulation parameter in PSS-free solutions containing NaCl only are also shown in Fig. 4e and f. Their values are similar to the ones reported earlier.[32,46] Here, the nominal NaCl concentration was used for the PB calculations. If the concentration is adjusted during the PB fit, the difference between the fitted and nominal concentration is less than 10%.

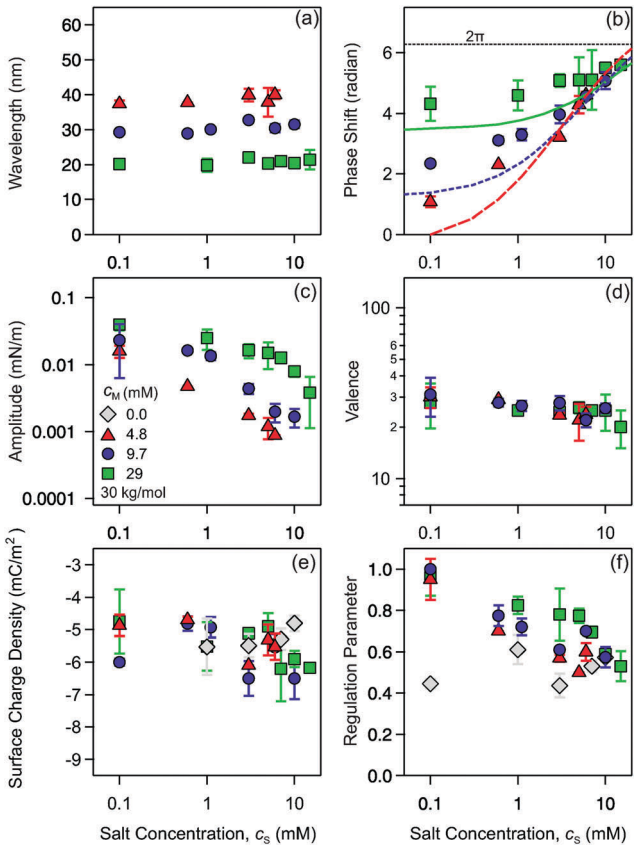

Fig. 4 Dependence of the parameters describing the force profiles on the NaCl concentration c_S obtained by fitting the experimental force profiles in solutions of sodium PSS with a molecular mass of 30 kg mol^{-1} at pH 4.0 and at a fixed monomer concentration c_M indicated. The concentration of c_S = 0.1 mM corresponds to the case of no added NaCl. Parameters describing the depletion force include (a) wavelength λ, (b) phase shift θ, and (c) amplitude A, while those describing the double layer are (d) effective charge Z_{eff} of PSS, (e) surface charge density σ, and (f) regulation parameter p. The correlation length ξ is given through the fixed ratio of λ/ξ = 1.9. The solid lines in (b) are predictions of the phase based on eqn (14) and (15). The error bars refer to standard deviations obtained from the repetition of the same experiment with different pairs of silica particles. In (e) and (f) results for PSS-free solutions, containing only NaCl are shown for comparison.

The parameters describing the depletion force depend on the salt concentration as follows. A crucial aspect is that the wavelength of the oscillation is independent of the concentration of the added monovalent salt as already remarked earlier.[12,13] However, the wavelength decreases with increasing PSS monomer concentration. The phase increases with increasing concentration of the monovalent salt, and with increasing PSS monomer concentration, this dependence becomes less pronounced. The amplitude decreases with increasing monovalent salt concentration.

Let us now focus on the parameters describing the double layer. The effective charge of the PSS decreases slightly with increasing monovalent salt concentration, but otherwise is independent of the PSS monomer concentration. The effective charge Z_{eff} of about 30 is obtained from the fit, and must be compared to the substantially higher bare charge Z of about 140. The effective charge decreases weakly with the salt concentration. The surface charge density scatters around -5.5 mC m^{-2} without featuring any clear trends. This scatter reflects the variability in the surface charge of different silica particles and its modification due to weak adsorption of PSS. Note that the negative sign of the surface charge follows unambiguously from the double layer force profile, as this profile would be completely different if the surface were positively charged. The regulation parameter decreases from about 1.0 in the absence of a salt to about 0.5 in the excess of salt. The latter value is in agreement with the value of p = 0.58, which was obtained by direct force measurements between silica particles in monovalent salt solutions.[46] The high regulation parameter observed in the absence of a monovalent salt is probably related to different behavior of the diffuse layer capacitance for the asymmetric electrolyte with respect to the monovalent one.[47]

Let us now discuss the experimental force profiles for the sodium salt of PSS of a molecular mass of 30 kg mol^{-1} for different PSS monomer concentrations c_M and a fixed concentration c_S of a monovalent salt as shown in Fig. 5. In the absence of PSS, one observes the classical double layer force profile, which is exponential over a wide distance range as reported by various studies earlier.[46,48,49] The minor deviations from the exponential behavior at smaller distances reflect the non-linearities of the PB model, details of the charge regulation conditions, and additional repulsive short-ranged hydration force, which is characteristic of interactions between silica-water interfaces.[46] As the PSS monomer concentration increases, the double layer force profile becomes shorter ranged and non-exponential, and oscillations due to depletion forces set it. The decrease in the range of the

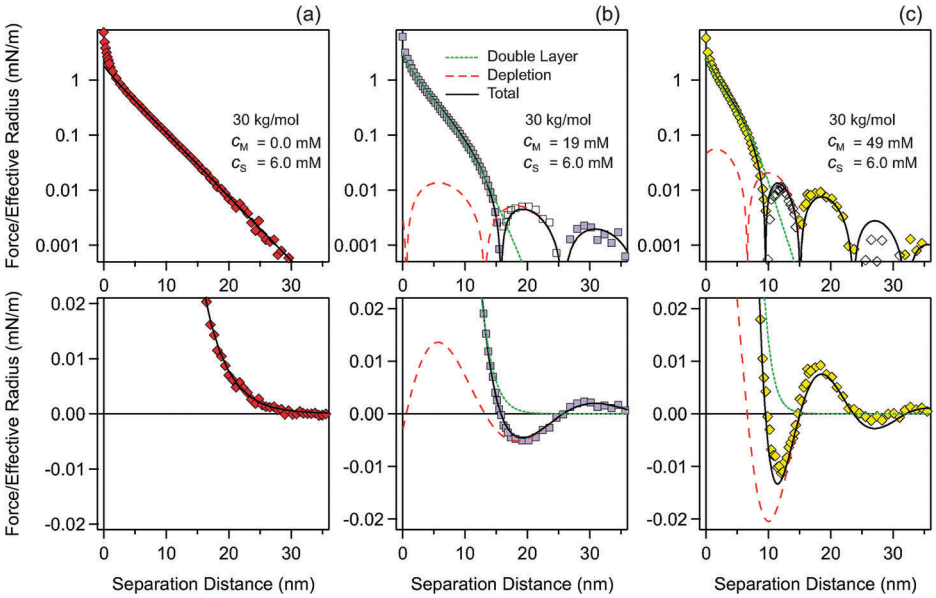

Fig. 5 Effect of addition of polyelectrolyte on forces between silica particles in solutions of sodium PSS with a molecular mass of 30 kg mol^{-1} at pH 4. The magnitude of the force in a semi-logarithmic representation (top) and linear representation of the force (bottom). The NaCl concentration is fixed at c_S = 6.0 mM and the PSS monomer concentration c_M increases from left to right. (a) c_M = 0 (no PSS added), (b) c_M = 19 mM, and (c) c_M = 49 mM. Experimental data are compared with calculations based on a superposition of depletion and double layer forces. The individual contributions are also indicated.

double layer force is similar to the ones reported earlier.[28] The wavelength of these oscillations decreases with increasing PSS monomer concentration. The data were again fitted with the superposition of depletion and double layer forces as described above. The results are also shown in Fig. 5. We also find that the data are consistent with the same value of the ratio between the wavelength and the correlation length as quoted above, namely $\lambda/\xi = 1.9 \pm 0.1$.

Fig. 6 summarizes the fitted parameters *versus* the PSS monomer concentration at various concentrations of a monovalent salt. The wavelength obeys the scaling relation

$$\lambda = Bc_M^{-\alpha} \qquad (13)$$

where $\alpha = 0.33 \pm 0.01$. This dependence was reported for a similar system previously.[17] One again observes that the wavelength remains constant upon addition of a monovalent salt. The value of the exponent reflects the fact that the polymer solution is dilute and that its structuring is due to electrostatic repulsion between the point-like polyelectrolyte chains. Recall that the gyration radius is about 7 nm and the overlap concentration is around 80 mM under these conditions.[44,45]

In the presence of a salt, the plot of the phase *versus* the monomer concentration shows a characteristic minimum. The amplitude increases with increasing polyelectrolyte monomer concentration and this dependence becomes somewhat stronger with increasing concentration of the monovalent salt. The effective charge Z_{eff} is again around 30 and decreases weakly with increasing monomer concentration. This decrease is more pronounced in the presence of a salt, while in the absence of a salt the effective charge remains almost constant.[32] The surface charge density again scatters around -5.5 mC m^{-2}. In the presence of a monovalent salt, weak adsorption of PSS probably causes the observed decrease. The regulation parameter scatters substantially, but increases from about 0.5 to about 1.0. This dependence reflects the same trend as reported in Fig. 4f.

Experimental force profiles and their molecular mass dependence

Let us now address the dependence of these forces on the molecular mass of PSS. Fig. 7 compares forces in sodium PSS for molecular masses of 6.4, 30, and 2100 kg mol^{-1} at a fixed monomer concentration c_M of 4.9 mM and a monovalent salt concentration c_S of 3.0 mM. One observes that the range of the double layer force increases with increasing molecular mass. At the same time, the wavelength of the oscillation increases. The experimental force profiles were fitted to the model used above. The fitted parameters are summarized in Fig. 8 for a fixed concentration of the monovalent salt of 3.0 mM. Again a fixed ratio of the wavelength to the correlation length λ/ξ can be used. However, this ratio must be allowed to vary with the molecular mass, as shown in Fig. 8a. The values for this ratio as expected from a hard-sphere system lie between 1 and 2 for intermediate volume fractions,[33] and thus the presently measured values are comparable but somewhat higher.

Let us now investigate the fitted parameters shown in Fig. 9 in more detail. First, consider the dependence of the wavelength on the polyelectrolyte monomer concentration. This dependence follows a power law given in eqn (13). The data for a lower molecular mass feature the exponent $\alpha = 0.33 \pm 0.01$, but for higher molecular mass this exponent becomes $\alpha = 0.50 \pm 0.01$. This increase is caused by the transition of the polyelectrolyte solution from dilute to semi-dilute.[17] Sodium PSS of a molecular

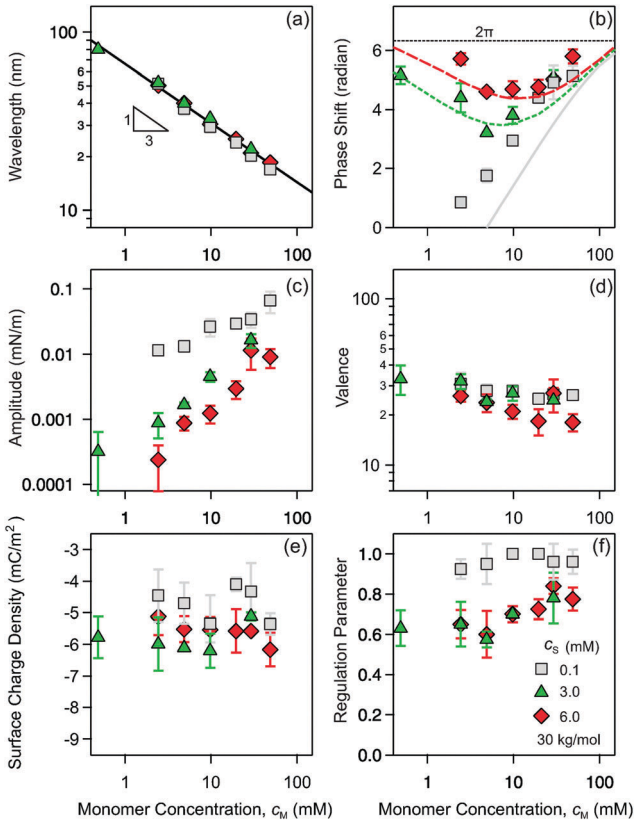

Fig. 6 Dependence of the parameters describing the force profiles on the monomer concentration c_M obtained by fitting the experimental force profiles in solutions of sodium PSS with a molecular mass of 30 kg mol^{-1} at pH 4.0 and a fixed NaCl concentration c_S indicated. The case of c_S = 0.1 mM corresponds to the case of no added NaCl. Parameters describing the depletion force include (a) wavelength λ, (b) phase shift θ, and (c) amplitude A, while those describing the double layer are (d) effective charge Z_{eff} of PSS, (e) surface charge density σ, and (f) regulation parameter p. The correlation length ξ is given through the fixed ratio of λ/ξ = 1.9. The solid line in (a) is the best fit with eqn (13) with α = 0.33 and in (b) the predictions of the phase based on eqn (14) and (15). The error bars refer to standard deviations obtained from the repetition of the same experiment with different pairs of silica particles.

mass of 200 kg mol^{-1} has a gyration radius of about 15 nm and an overlap monomer concentration of around 2 mM.[44,45] These numbers indicate that this system is already situated in the semi-dilute regime.

The phase goes again through a minimum near a monomer concentration of around 10 mM. The amplitude increases monotonously and is rather independent of the molecular mass. The effective charge increases substantially with the molecular mass, since the number of ionizable groups on each polyelectrolyte increases. The effective charge decreases weakly with increasing monomer concentration. This decrease is hardly visible on the scale of Fig. 9d, but can be seen more clearly in Fig. 6d. The surface charge density scatters around -6.5 ± 0.5 mC m^{-2} and the regulation parameter remains approximately constant near 0.6 ± 0.1. The higher magnitudes of the surface charge density are probably due to adsorption of PSS on the particle surface. The adsorption of PSS is probably also the cause of the weak decrease of the surface charge density with increasing monomer concentration, and this effect is most pronounced for the highest molecular mass. Furthermore, the adsorption of PSS might also alter the regulation properties of the interface.

Fig. 8b shows the fitted effective charge of the polyelectrolyte, which is expressed as the fraction Z_{eff}/Z. This fraction can be interpreted as an apparent ionization fraction of the polyelectrolyte. One observes that this number decreases with increasing molecular mass, and converges to a plateau at $Z_{eff}/Z = 0.15 \pm 0.05$ for higher molecular masses. This decrease is the main reason for the increase in the range of the double layer forces shown in Fig. 7. These values are in good agreement with independent experiments based on osmometry or ion selective electrodes.[50,51] While the ionization fraction decreases with an increasing level of monovalent salt, this decrease is weak, and the ionization fraction can be assumed as independent of the solution composition to a good degree of approximation. This assumption was made in our earlier study.[32] A similar salt dependence of the effective charge on the salt concentration was observed with NMR and other techniques.[51,52] The ionization fraction can be estimated through the manning condensation limit $Z_{eff}/Z = a/\ell_B$ where a is the distance between the charged groups and ℓ_B is the Bjerrum length. Taking a = 0.25 nm one obtains Z_{eff}/Z = 0.35. A recent analysis of the ion condensation for a cylinder concludes that the ionization fraction is normally smaller than the Manning value, and decreases further in the presence of a salt.[53] These observations are in line with present experimental data.

Predicting the phase of the depletion force

The phase shift of the depletion force can be obtained by assuming that the depletion force sets in at the outer boundary of the diffuse layer. In particular, the depletion force vanishes at the boundary of the diffuse layer and initially decreases with the distance. The phase θ in eqn (3) is therefore given by the relation

$$2\pi h_{dl}/\lambda + \theta = 5\pi/2 \qquad (14)$$

where h_{dl} is the thickness of the diffuse layer. Eqn (14) was used earlier to predict the phase of salt-free systems.[32] In these systems, the thickness can be easily defined through the vanishing osmotic pressure, since the double layer force decreases at this separation very strongly. In the presence of a monovalent salt, however, the decrease is more gradual and a more elaborate definition of h_{dl} is needed. Here we propose to define this thickness through the electrostatic free energy of the polyelectrolyte. In a slit of thickness h_{dl}, we set this energy to be approximately equal to the thermal energy, namely

$$Z_{eff} q |\psi_M|_{h=h_{dl}} = \gamma kT \qquad (15)$$

where γ is a numerical factor of order unity. In salt-free systems, this definition is equivalent to the one used previously.

The phase of the depletion force can now be predicted as follows. The diffuse layer thickness h_{dl} was obtained from eqn (15) from the known polyelectrolyte and monovalent salt concentrations. For each respective condition, the average values for surface charge density and the effective charge were used.

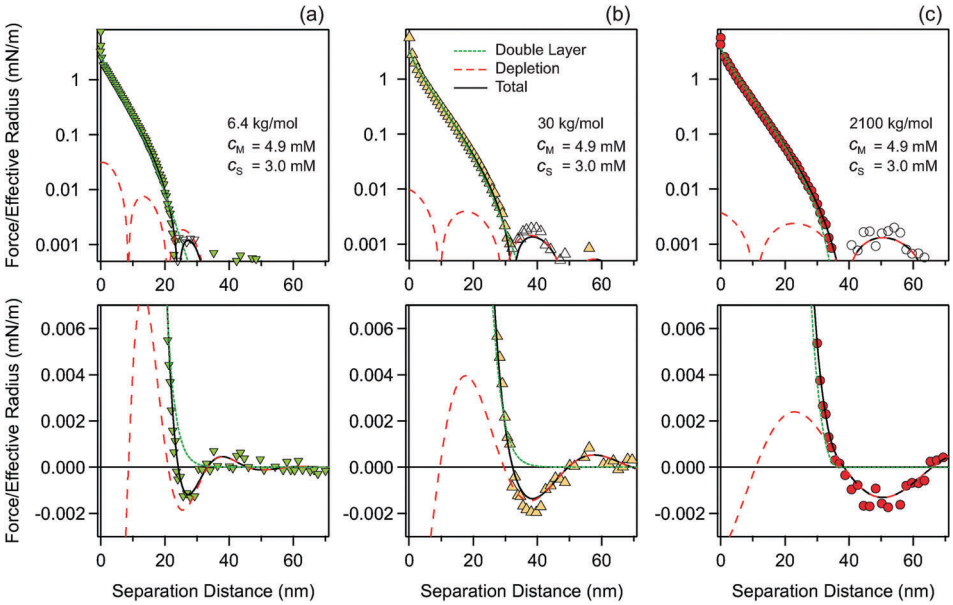

Fig. 7 Forces between silica particles in solutions of sodium PSS of different molecular masses as indicated. The magnitude of the force in a semi-logarithmic representation (top) and linear representation of the force (bottom). The NaCl concentration is fixed at c_S = 3.0 mM and the PSS monomer concentration at c_M = 4.9 mM, pH 4 is used. The molecular mass of sodium PSS increases from left to right. (a) 6.4 kg mol^{-1}, (b) 30 kg mol^{-1}, and (c) 2100 kg mol^{-1}. Experimental data are compared with calculations based on a superposition of depletion and double layer forces. The individual contributions are also indicated.

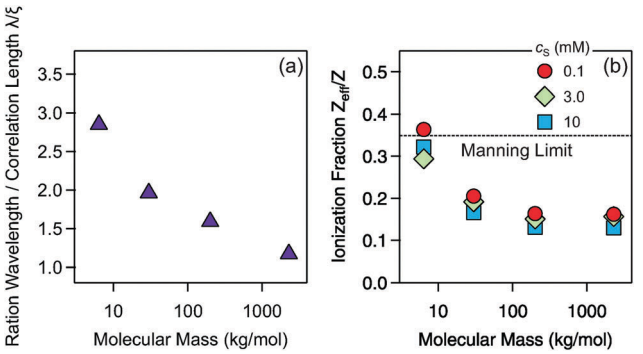

Fig. 8 Molecular mass dependence of the concentration independent parameters used to model the force profiles. (a) Ratio of the wavelength to the correlation length λ/ξ. This ratio is independent of the concentration of monovalent salt added. (b) Ionization fraction Z_{eff}/Z.

Once the thickness h_{dl} is determined, the phase is obtained from eqn (14). In order to do that, the experimental values for the wavelength are interpolated with eqn (13). The adjustable parameter γ is entered into eqn (15). The calculations were carried out for different values of the parameter γ, and we found that γ = 2 gives the best agreement with the experiments. Trefalt proposed the same value in a similar context.[54] Moreover, these results are not too sensitive to this value, provided that this parameter remains of order unity as it should be.

The solid lines in Fig. 4b, 6b and 9b are predictions obtained in this fashion. This calculation captures the experimentally observed phase reasonably well. In particular, the minima that can be seen in Fig. 6b and 9b are predicted satisfactorily. This agreement confirms independently that the presently suggested combined action of depletion and double layer forces is correct.

The observed trends in the phase can be explained as follows. The increase with increasing salt concentration shown in Fig. 4b is due to the decrease of the diffuse layer thickness. Since the wavelength is independent of the salt level, eqn (14) predicts that the phase increases with decreasing thickness of the diffuse layer. The increase with increasing monomer concentration in the absence of a salt shown in Fig. 6b is also related to the decrease of the diffuse layer thickness. This thickness decreases due to the increase of the counterion concentration and this effect is stronger than the one induced by a decrease of the wavelength with monomer concentration. The characteristic minimum shown in Fig. 6b and 9b occurs in the presence of a monovalent salt due to two competing effects. The first is the decrease of the diffuse layer thickness as discussed above, and this effect dominates the phase at high monomer concentrations. At low concentrations, however, the second effect due to the decrease of the wavelength becomes important. At low monomer concentrations, the diffuse layer thickness is approximately constant due to the background monovalent salt, but the decrease in the wavelength also leads to a decrease in the phase as predicted by eqn (14).

In the present system, the typical thickness of the diffuse layer is 10–50 nm, as indicated by the arrows in Fig. 2. This thickness coincides rather closely with the onset of the DH decay. This thickness decreases with increasing concentration of monomer and salt concentration. In the salt-free case, this thickness results from the balance between the positive pressure generated by the diffuse ionic cloud and the negative pressure due to the presence of the multivalent coions.

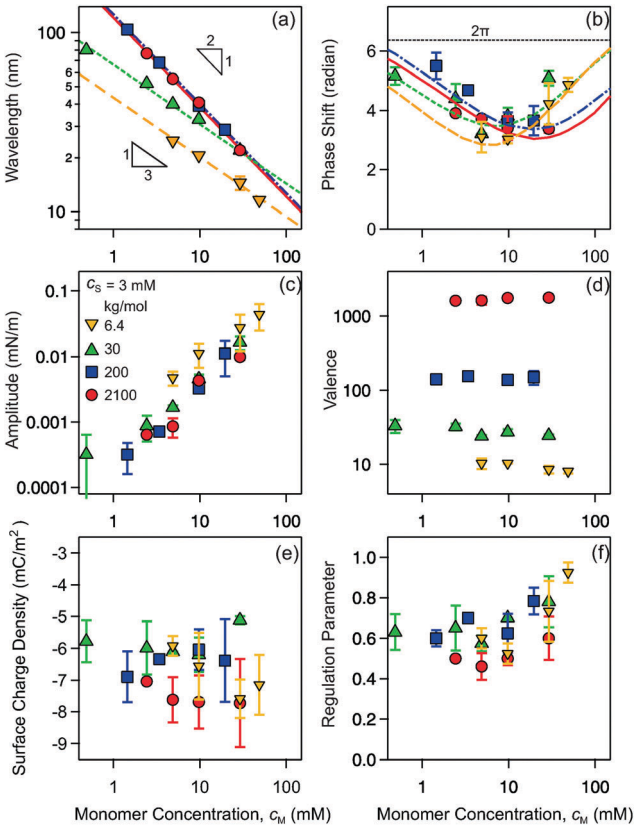

Fig. 9 Dependence of the parameters describing the force profiles on the monomer concentration c_M obtained by fitting the experimental force profiles in PSS solutions at pH 4.0 and a fixed NaCl concentration c_S = 3 mM. Parameters describing the depletion force include (a) wavelength λ, (b) phase shift θ, and (c) amplitude A, while those describing the double layer are (d) effective charge Z_{eff} of PSS, (e) surface charge density σ, and (f) regulation parameter p. The correlation length ξ is given through the fixed ratio of ξ/λ shown in Fig. 8a. The solid lines in (a) are the best fits with eqn (13) with α = 0.33 and in (b) the predictions of the phase based on eqn (14) and (15).

One finds that this thickness is given by eqn (10) that is modified by a numerical factor of order unity and the ionic strength must be replaced by the concentration of the counterions. In this situation, the thickness thus scales as $c_M^{-1/2}$. When the system is dominated by a monovalent salt, this thickness is on the order of a few Debye lengths, and as evident from eqn (10) it scales as $c_S^{-1/2}$.

Further phenomena at high concentrations

So far, we have discussed situations where the concentrations of the polyelectrolyte monomers and of the monovalent salt were not too high, typically below 10 mM. This regime is governed by the combined action of depletion and double layer forces. Thereby, the polyelectrolyte adsorption is negligible, since it is repelled from the like-charged interface strongly. New phenomena occur at higher concentrations.

Let us first focus on the situation of relatively low polyelectrolyte concentrations, but higher monovalent salt concentrations. Under these conditions, the repulsive double layer forces will be screened, and the interactions become dominated by attractive van der Waals forces. This situation is illustrated in Fig. 10a. For illustration, we also report the respective interaction force in a pure NaCl solution of 250 mM. In this experiment, the attractive van der Waals force is evident. This interaction energy can be modeled with the non-retarded expression[34]

$$W = -\frac{H}{12\pi h^2} \qquad (16)$$

where H is the Hamaker constant. When one chooses this constant as 1.5×10^{-21} J the experimental data can be described with this expression rather well. This value is in perfect agreement with the theoretical estimate for silica across water.[55] Very similar force profiles can be observed in the presence of PSS at monomer concentrations typically below 5 mM. The effect of adsorbed polyelectrolytes becomes obvious at even higher levels of monovalent salt, see Fig. 10b. One observes a strong repulsion that sets in at distances of 4–8 nm. In some cases, an attractive well is equally observed. Under these conditions, the force profiles are poorly reproducible, and they can differ in the range of repulsion. This behavior indicates that the polyelectrolyte adsorbs to the silica surface under these conditions. The erratic nature of such force profiles suggests that the adsorbed polyelectrolyte layer is heterogeneous. The present conclusions concerning the existence of adsorption of polyelectrolytes on like-charged substrates are in line with earlier reports.[14,56,57]

Polyelectrolyte adsorption can be much more clearly demonstrated by analyzing the individual retraction force profiles. Exemplary profiles are shown in Fig. 11a and b. The reason for these irregular profiles is that during contact polyelectrolyte chains adsorb onto both particle surfaces, and upon retraction the individual bridging chains are being stretched. Often one observes isolated spikes. These spikes are caused by individual bridging polymer chains, which are firmly attached to both surfaces, and they are being stretched during the retraction of the probe. The force response of a strongly extended polymer chains is non-linear and leads to the curved part on the left-hand side of the spike.[58,59] The right-hand side of the spike originates from the detachment of the bridging chain, and the subsequent part corresponds to the snap-out of the cantilever.

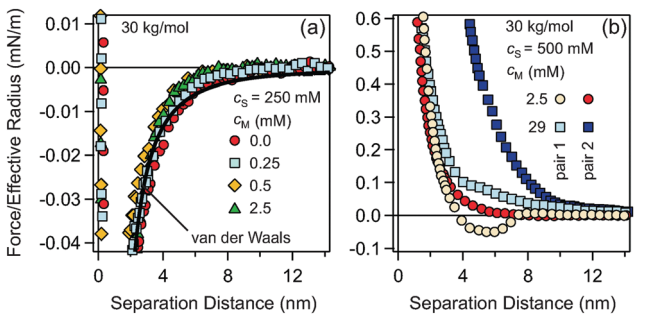

Fig. 10 Typical force profiles at high monovalent salt concentrations. (a) Low PSS monomer concentration reflects the van der Waals force shown as a solid line with a Hamaker constant of H = 1.5 × 10^{-21} J. (b) Erratic force profiles observed at a high PSS monomer concentration.

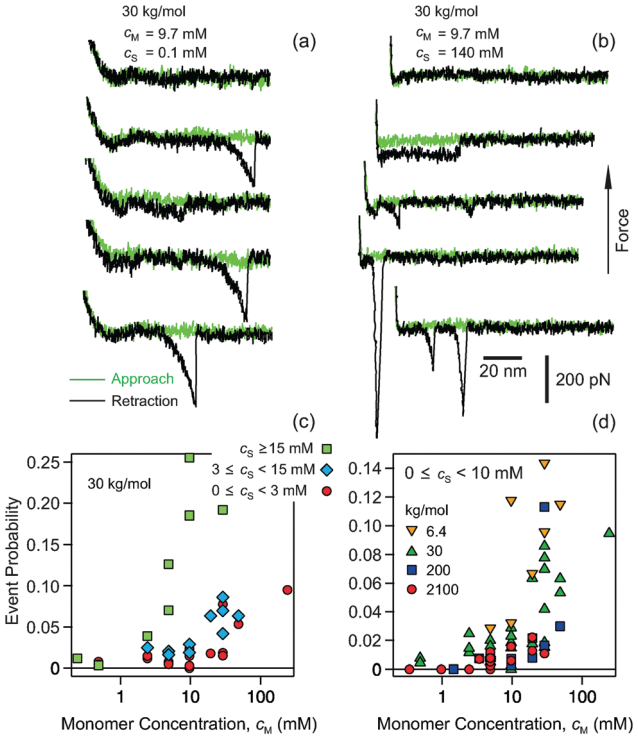

Fig. 11 Single molecule events observed upon retraction of the probe. (a and b) Typical raw individual approach and retraction profiles for sodium PSS of 30 kg mol^{-1} at 9.7 mM PSS monomer concentration. (a) Data without added salt and (b) with a NaCl concentration of 140 mM. The event probabilities are 0.015 in (a) and 0.19 in (b). (c and d) Event probabilities *versus* the PSS monomer concentration. (c) Molecular mass of 30 kg mol^{-1} for three different ranges of salt concentrations. (d) Concentrations of NaCl below 10 mM for different molecular masses. The ranges were chosen to obtain better statistics.

Less frequently, one observes plateau-like events, which result from the peeling of adsorbed polymer chains for which a constant force is necessary.[60,61] Salt-free systems feature a few events and typically they are dominated by pulling of isolated chains. At higher salt levels, one observes more complex retraction profiles that may feature simultaneous stretching of several polymer chains or peeling.

The lower part of Fig. 11 displays the probability of retraction profiles that feature at least one event. The results for the molecular mass of 30 kg mol^{-1} are shown in Fig. 11c. One observes that at low monomer and salt concentrations, such stretching events are very rare, which indicates that the polyelectrolytes hardly adsorb onto the silica surfaces. With increasing monomer and salt concentrations, the probability of such events increases, and it may even exceed 0.2 in favorable situations. Such events clearly indicate that adsorption of the polyelectrolytes occurs on the silica surfaces. The onset of the adsorption occurs at a monomer concentration of about 20 mM in salt-free systems, and this value shifts to a lower monomer concentration as the concentration of the monovalent salt is increased. This onset seems to be governed by the total concentration of the counterions. These counterions are responsible for the screening of the repulsive electrostatic interactions acting between the silica substrate and the like-charged polyelectrolyte, and are thus expected to promote adsorption. The molecular mass dependence on the event probability is weak, as shown in Fig. 11d. One observes a slight tendency that PSS of lower molecular mass is being picked up somewhat more frequently. This trend is probably related to the different lateral heterogeneities of the adsorbed films.

Conclusion

We have investigated interaction forces between silica surfaces in aqueous solutions of like-charged polyelectrolytes and a simple monovalent salt, and find that these forces are dominated by depletion and double layer forces. These forces can be modeled quantitatively through a superposition of exponentially damped oscillatory depletion forces and repulsive double layer forces. However, the double layer forces must be obtained from the full PB equation for a mixture of symmetric monovalent and highly asymmetric electrolytes, whereby the multivalent ions represent coions. The asymmetric electrolyte is used to model the contribution of the polyelectrolyte, whereby an effective charge that is smaller than the bare charge of the polyelectrolyte must be introduced. These smaller effective charges can be explained by Manning's counterion condensation. When the polyelectrolyte is in excess, the resulting double force profiles are strongly non-exponential, and have a characteristic sigmoidal shape in the commonly used semi-logarithmic plot. With increasing concentration of the monovalent salt, the double layer force approaches the classical exponential force law expected from DH theory. Since the depletion force vanishes at the onset of the diffuse layer and initially decreases with the distance, we can successfully predict with this condition the phase of the depletion force. Therefore, the interplay between depletion and double layer force provides a quantitative picture of surface interactions in these systems.

However, this picture only holds up to moderately elevated concentrations of the polyelectrolyte and salt. At higher salt concentrations, attractive van der Waals forces become important. At higher polyelectrolyte concentrations, the anionic polyelectrolytes adsorb onto the like-charged silica interface. This adsorption can be evidenced by a strong modification of the force profiles and the presence of stretching events originating from the presence of individual polyelectrolyte bridging chains. Moreover, polyelectrolyte adsorption is promoted by the presence of a monovalent salt. A detailed investigation of the latter phenomena is outside the scope of this article, and represents a valuable topic for future studies.

Acknowledgements

This research was supported by the Swiss National Science Foundation by the projects No. 150631 and 159874 and the University of Geneva.

References

1 J. Gregory, *J. Colloid Interface Sci.*, 1973, **42**, 448–456.
2 P. M. Claesson, T. Ederth, V. Bergeron and M. W. Rutland, *Adv. Colloid Interface Sci.*, 1996, **67**, 119–183.

3 I. Szilagyi, G. Trefalt, A. Tiraferri and M. Borkovec, *Soft Matter*, 2014, **10**, 2479–2502.
4 B. Bolto and J. Gregory, *Water Res.*, 2007, **41**, 2301–2324.
5 D. Horn and F. Linhart, *Retention aids*, Blackie Academic and Professional, London, 2nd edn, 1996.
6 D. N. H. Tran, C. P. Whitby, D. Fornasiero and J. Ralston, *Int. J. Miner. Process.*, 2010, **94**, 35–42.
7 H. J. Butt, B. Cappella and M. Kappl, *Surf. Sci. Rep.*, 2005, **59**, 1–152.
8 F. Xie, T. Nylander, L. Piculell, S. Utsel, L. Wagberg, T. Akesson and J. Forsman, *Langmuir*, 2013, **29**, 12421–12431.
9 I. Popa, G. Gillies, G. Papastavrou and M. Borkovec, *J. Phys. Chem. B*, 2010, **114**, 3170–3177.
10 M. A. G. Dahlgren, A. Waltermo, E. Blomberg, P. M. Claesson, L. Sjostrom, T. Akesson and B. Jonsson, *J. Phys. Chem.*, 1993, **97**, 11769–11775.
11 E. Poptoshev, M. W. Rutland and P. M. Claesson, *Langmuir*, 1999, **15**, 7789–7794.
12 A. J. Milling, *J. Phys. Chem.*, 1996, **100**, 8986–8993.
13 M. Piech and J. Y. Walz, *J. Phys. Chem. B*, 2004, **108**, 9177–9188.
14 A. J. Milling and K. Kendall, *Langmuir*, 2000, **16**, 5106–5115.
15 S. Biggs, R. R. Dagastine and D. C. Prieve, *J. Phys. Chem. B*, 2002, **106**, 11557–11564.
16 S. Biggs, J. L. Burns, Y. D. Yan, G. J. Jameson and P. Jenkins, *Langmuir*, 2000, **16**, 9242–9248.
17 C. Uzum, S. Christau and R. von Klitzing, *Macromolecules*, 2011, **44**, 7782–7791.
18 Y. Zeng and R. von Klitzing, *Langmuir*, 2012, **28**, 6313–6321.
19 C. Browne, R. F. Tabor, F. Grieser and R. R. Dagastine, *J. Colloid Interface Sci.*, 2015, **449**, 236–245.
20 D. l. Sober and J. Y. Walz, *Langmuir*, 1995, **11**, 2352–2356.
21 N. C. Christov, K. D. Danov, Y. Zeng, P. A. Kralchevsky and R. von Klitzing, *Langmuir*, 2010, **26**, 915–923.
22 S. H. L. Klapp, Y. Zeng, D. Qu and R. von Klitzing, *Phys. Rev. Lett.*, 2008, **100**, 118303.
23 Y. Zeng, S. Schon and R. von Klitzing, *J. Colloid Interface Sci.*, 2015, **449**, 522–529.
24 K. Binder, P. Virnau and A. Statt, *J. Chem. Phys.*, 2014, **141**, 140901.
25 A. Trokhymchuk, D. Henderson, A. D. Nikolov and D. T. Wasan, *Langmuir*, 2004, **20**, 7036–7044.
26 X. C. Xing, L. Hua and T. Ngai, *Curr. Opin. Colloid Interface Sci.*, 2015, **20**, 54–59.
27 J. Y. Walz and A. Sharma, *J. Colloid Interface Sci.*, 1994, **168**, 485–496.
28 R. Tadmor, E. Hernandez-Zapata, N. Chen, P. Pincus and J. N. Israelachvili, *Macromolecules*, 2002, **35**, 2380–2388.
29 B. Jonsson, A. Broukhno, J. Forsman and T. Akesson, *Langmuir*, 2003, **19**, 9914–9922.
30 S. Grandner, Y. Zeng, R. von Klitzing and S. H. L. Klapp, *J. Chem. Phys.*, 2009, **131**, 154702.
31 M. Pelaez-Fernandez, A. Moncho-Jorda and J. Callejas-Fernandez, *J. Chem. Phys.*, 2011, **134**, 054905.
32 M. Moazzami-Gudarzi, T. Kremer, V. Valmacco, P. Maroni, M. Borkovec and G. Trefalt, *Phys. Rev. Lett.*, 2016, **117**, 088001.
33 A. Trokhymchuk, D. Henderson, A. Nikolov and D. T. Wasan, *Langmuir*, 2001, **17**, 4940–4947.
34 W. B. Russel, D. A. Saville and W. R. Schowalter, *Colloidal Dispersions*, Cambridge University Press, Cambridge, 1989.
35 G. Trefalt, I. Szilagyi and M. Borkovec, *J. Colloid Interface Sci.*, 2013, **406**, 111–120.
36 G. Tellez, *Philos. Trans. R. Soc., A*, 2011, **369**, 322–334.
37 V. Valmacco, M. Elzbieciak-Wodka, C. Besnard, P. Maroni, G. Trefalt and M. Borkovec, *Nanoscale Horiz.*, 2016, **1**, 325–330.
38 V. Valmacco, G. Trefalt, P. Maroni and M. Borkovec, *Phys. Chem. Chem. Phys.*, 2015, **17**, 16553–16559.
39 J. E. Sader, J. W. M. Chon and P. Mulvaney, *Rev. Sci. Instrum.*, 1999, **70**, 3967–3969.
40 J. Morag, M. Dishon and U. Sivan, *Langmuir*, 2013, **29**, 6317–6322.
41 F. J. Montes Ruiz-Cabello, M. Moazzami-Gudarzi, M. Elzbieciak-Wodka, P. Maroni, C. Labbez, M. Borkovec and G. Trefalt, *Soft Matter*, 2015, **11**, 1562–1571.
42 I. Langmuir, *J. Chem. Phys.*, 1938, **6**, 873–896.
43 W. H. Briscoe and P. Attard, *J. Chem. Phys.*, 2002, **117**, 5452–5464.
44 J. Yashiro and T. Norisuye, *J. Polym. Sci., Part B: Polym. Phys.*, 2002, **40**, 2728–2735.
45 A. V. Dobrynin, R. H. Colby and M. Rubinstein, *Macromolecules*, 1995, **28**, 1859–1871.
46 V. Valmacco, M. Elzbieciak-Wodka, D. Herman, G. Trefalt, P. Maroni and M. Borkovec, *J. Colloid Interface Sci.*, 2016, **472**, 108–115.
47 G. Trefalt, S. H. Behrens and M. Borkovec, *Langmuir*, 2016, **32**, 380–400.
48 R. M. Pashley, *J. Colloid Interface Sci.*, 1981, **83**, 531–546.
49 M. Borkovec, I. Szilagyi, I. Popa, M. Finessi, P. Sinha, P. Maroni and G. Papastavrou, *Adv. Colloid Interface Sci.*, 2012, **179–182**, 85–98.
50 A. Takahashi, N. Kato and M. Nagasawa, *J. Phys. Chem.*, 1970, **74**, 944–946.
51 C. Wandrey, D. Hunkeler, U. Wendler and W. Jaeger, *Macromolecules*, 2000, **33**, 7136–7143.
52 U. Bohme and U. Scheler, *Adv. Colloid Interface Sci.*, 2010, **158**, 63–67.
53 E. Trizac and G. Tellez, *Phys. Rev. Lett.*, 2006, **96**, 038302.
54 G. Trefalt, *Phys. Rev. E*, 2016, **93**, 032612.
55 H. D. Ackler, R. H. French and Y. M. Chiang, *J. Colloid Interface Sci.*, 1996, **179**, 460–469.
56 P. Maroni, F. J. Montes Ruiz-Cabello and A. Tiraferri, *Soft Matter*, 2014, **10**, 9220–9225.
57 S. X. Ji and J. Y. Walz, *Langmuir*, 2013, **29**, 15159–15167.
58 G. Papastavrou, L. J. Kirwan and M. Borkovec, *Langmuir*, 2006, **22**, 10880–10884.
59 A. Janshoff, M. Neitzert, Y. Oberdorfer and H. Fuchs, *Angew. Chem., Int. Ed.*, 2000, **39**, 3213–3237.
60 C. Friedsam, H. E. Gaub and R. R. Netz, *Europhys. Lett.*, 2005, **72**, 844–850.
61 I. L. Radtchenko, G. Papastavrou and M. Borkovec, *Biomacromolecules*, 2005, **6**, 3057–3066.

CHAPTER 7

Conclusion

This thesis delves into the impact of the multivalent ions and polyelectrolytes on the surface forces between charged interfaces. To answer this question, colloidal probe technique based on atomic force microscopy is used. The acquired force profiles are analyzed by means of mean-field theories, where multivalent ions and polyelectrolytes are considered as point charges. Specifically, the findings of this research emphasize the capability of Poisson-Boltzmann (PB) theory to model the manner of double layer forces in the presence of ions carrying multiple charges. In such cases, the system is very non-linear and linear approximation of PB equation leads to erroneous prediction of forces and full form of equation must be considered.

Other types of forces are identified which their magnitude and range depend on the nature of interfaces and ions in solutions. Among them, van der Waals (vdW) forces are ubiquitous which their range and magnitude are independent of the solution chemistry and are just function of the optical properties of the interacting interfaces and the solution. However, presence of long-ranged forces screens vdW forces and usually at high concentration of ions vdW forces are detected.

Direct force measurements between charged latex particles in the presence of aliphatic oligoamines multivalent ions showed the surface forces are consistent with DLVO theory which states the total interaction is the interplay of vdW and double layer forces. Oligoamines tend to adsorb to the negatively charged particles and this tendency increases with increase of valence and leads to charge inversion of the interface for valences of +3 or more. At short distances, the

measured forces cannot be quantified solely by DLVO forces and additional attractive forces are always present, however with different ranges and magnitudes. In solutions containing multivalent ions, the range of these forces is more than three times higher than the monovalent counterparts and is about one nanometer. Even though exponential force profile can quantitatively describe these non-DLVO forces, the origin and exact force law(s) for these types of interactions remain an open question.

For the cases of multivalent co-ions where they have the same charge as the substrate electrostatic repulsion expels the co-ions from the vicinity of the interface. Depletion of the co-ions as two interfaces approach leaves only monovalent counter-ions between two interfaces. This transition leads to two distinct force regimes as large and small separation distances. This feature is indeed captured within PB theory framework which results in softer forces at smaller distances. In fact, at small separation distances the force profiles agree with the prediction for double layer forces for counter-ion only cases. Experimental data for ranges of interfaces and multivalent ions quantitatively concur with this picture.

Polyelectrolytes also deplete from the like-charged interfaces. However, due to the structuring of polyelectrolyte molecules in solution, long-ranged depletion forces are also observed as two charged interfaces approach. Depletion forces appear in the form of damped oscillatory profiles whereby the wavelength of the oscillation reflects the structure of the polymer solution. At shorter distances, polyelectrolyte molecules expel from the interspace of the interfaces and double layer forces become visible. The double layer forces are highly non-exponential which is uncommon for double layer forces. These non-exponential forces however can be quantified using PB theory for highly asymmetric electrolytes. In this approach, polyelectrolyte molecules are assumed as multivalent co-ions with an effective valence which is always smaller than the

nominal valence of polyelectrolytes. This is consistent with ion condensation of counter-ions on polymer chains. Exclusion of highly charged polyelectrolyte molecules from the vicinity of the surface aids to define a double layer thickness. If one equates this thickness with depletion layer thickness, the phase of oscillatory depletion forces can be predicted. Indeed this prediction matches well with experimental data which implies the double layer and depletion forces are interrelated.

In the mixture of polyelectrolytes and monovalent salt, the total forces acting on the approaching interfaces can be described by depletion and double layer forces, provided that the double layer forces define by PB equation for mixture of asymmetric and monovalent electrolytes. However, at high salt concentrations the double layer and depletion forces vanish and vdW forces dominate the forces. At high salt and polyelectrolyte concentrations, polymer chains adsorb to the like-charged interface and other forces play role.

Acknowledgement

First of all, I would like to express my deep gratitude to my supervisor Professor Michal Borkovec for having me as PhD student in his team and for all thoughtful and countless advices, support and encouragement.

I would like to thank Professor Thomas Bürgi from University of Geneva and Dr. Christophe Labbez from Université de Bourgogne for accepting being member of committee and evaluating my thesis.

Learning AFM was not possible without kind help and advice of Dr. Plinio Maroni. I learnt a lot from all the training and discussion that I had with him during my PhD. I express my gratitude and appreciation to Dr. Gregor Trefalt, not just for all the helps and collaboration but also for being a good friend. His assistance and contribution on writing the codes especially the second part of the thesis was vital. I am very grateful to Dr. Istvan Szilagyi for his enormous advices and helpful opinions, particularly in the first part of the thesis. I would like to thank Dr. Francisco Javier Ruiz Montes-Cabello for his helps and assist, especially when I started working in the lab.

I specially thank Anne-Marie Loup for her passionate help and extraordinary taking care of the bureaucratic issues and on the top of that for her empathy and wholehearted support. I am grateful to Dr. Paul Rouster for his assist for preparing the French version the abstract. I am thankful to Olivier Vassalli for all his help especially TOC measurements.

The majority of experiments and data analysis presented in chapters two, three, five and six were carried out by my contribution. I am very thankful of co-authors of chapter four for their key contribution.

I enjoyed my stay at LCSC group thanks to all the present and former members of the group. I am very thankful to my friends in Geneva which I enjoyed every moment I spent with them.

At the end, I express my deepest gratitude to my family for all support and love. I would like to dedicate this thesis to my parents.